Measurement of $W^{\pm}Z$ production cross sections and gauge boson polarisation in pp collisions at $\sqrt{s}$ = 13 TeV with the ATLAS detector

ATLAS Collaboration

DOI
10.1140/epjc/s10052-019-7027-6

Publication date
2019

Document Version
Final published version

Published in
European Physical Journal C

Eur. Phys. J. C (2019) 79:535
https://doi.org/10.1140/epjc/s10052-019-7027-6

THE EUROPEAN PHYSICAL JOURNAL C

Regular Article - Experimental Physics

Measurement of $W^{\pm}Z$ production cross sections and gauge boson polarisation in pp collisions at $\sqrt{s} = 13$ TeV with the ATLAS detector

ATLAS Collaboration[⋆]

CERN, 1211 Geneva 23, Switzerland

Received: 15 February 2019 / Accepted: 5 June 2019 / Published online: 22 June 2019

Abstract This paper presents measurements of $W^{\pm}Z$ production cross sections in pp collisions at a centre-of-mass energy of 13 TeV. The data were collected in 2015 and 2016 by the ATLAS experiment at the Large Hadron Collider, and correspond to an integrated luminosity of 36.1 fb^{-1}. The $W^{\pm}Z$ candidate events are reconstructed using leptonic decay modes of the gauge bosons into electrons and muons. The measured inclusive cross section in the detector fiducial region for a single leptonic decay mode is $\sigma^{\text{fid.}}_{W^{\pm}Z\to\ell'\nu\ell\ell} = 63.7 \pm 1.0\,(\text{stat.}) \pm 2.3\,(\text{syst.}) \pm 1.4\,(\text{lumi.})$ fb, reproduced by the next-to-next-to-leading-order Standard Model prediction of $61.5^{+1.4}_{-1.3}$ fb. Cross sections for $W^{+}Z$ and $W^{-}Z$ production and their ratio are presented as well as differential cross sections for several kinematic observables. An analysis of angular distributions of leptons from decays of W and Z bosons is performed for the first time in pair-produced events in hadronic collisions, and integrated helicity fractions in the detector fiducial region are measured for the W and Z bosons separately. Of particular interest, the longitudinal helicity fraction of pair-produced vector bosons is also measured.

1 Introduction

The study of $W^{\pm}Z$ diboson production is an important test of the Standard Model (SM) for its sensitivity to gauge boson self-interactions, related to the non-Abelian structure of the electroweak interaction. It provides the means to directly probe the triple gauge boson couplings (TGC), in particular the WWZ gauge coupling. Improved constraints from precise measurements can potentially probe scales of new physics in the multi-TeV range and provide a way to look for signals of new physics in a model-independent way. Previous measurements have concentrated on the inclusive and differential production cross sections. In addition to more precise measurements of these cross sections that include new data, this paper presents measurements of the three helicity fractions of the W and Z bosons. The existence of the third state, the longitudinally polarised state, is a consequence of the non-vanishing mass of the bosons generated by the electroweak symmetry breaking mechanism. The measurement of the polarisation in diboson production therefore tests both the SM innermost gauge symmetry structure, through the existence of the triple gauge coupling, and the particular way this symmetry is spontaneously broken, via the longitudinal helicity state. Angular observables can be used to look for new interactions that can lead to different polarisation behaviour than predicted by the SM, to which the $W^{\pm}Z$ final state would be particularly sensitive [1,2]. Precise calculations, at the next-to-leading order (NLO) in QCD, of SM polarisation observables in $W^{\pm}Z$ production as well as electroweak corrections have recently appeared [3]. Polarisation measurements for each charge of the W boson might be helpful in the investigation of CP violation effects in the interaction between gauge bosons [4,5]. In the longer term, measuring the scattering of longitudinally polarised vector bosons will be a fundamental test of electroweak symmetry breaking [6].

Measurements of the $W^{\pm}Z$ production cross section in proton–antiproton collisions at a centre-of-mass energy of $\sqrt{s} = 1.96$ TeV were published by the CDF and DØ collaborations [7,8] using integrated luminosities of 7.1 fb^{-1} and 8.6 fb^{-1}, respectively. At the Large Hadron Collider (LHC), the most precise measurement of $W^{\pm}Z$ production was reported by the ATLAS Collaboration [9] using 20.1 fb^{-1} of data collected at a centre-of-mass energy of 8 TeV. Measurements of $W^{\pm}Z$ production at $\sqrt{s} = 13$ TeV were reported by the ATLAS [10] and CMS [11] collaborations using integrated luminosities of 3.2 fb^{-1} and 35.9 fb^{-1}, respectively. Other $W^{\pm}Z$ measurements in pp collisions, at centre-of-mass energies of 7 TeV and 8 TeV, were reported previously by ATLAS and CMS [12,13].

⋆ e-mail: atlas.publications@cern.ch

At hadron colliders, the polarisation of the W boson was previously measured in the decay of the top quark by the CDF and DØ [14–16] collaborations and the ATLAS [17] and CMS [18] collaborations, as well as in association with jets by ATLAS [19] and CMS [20]. Polarisation and several other related angular coefficient measurements of a singly produced Z boson were published by the CDF [21], CMS [22] and ATLAS [23] collaborations. The polarisation of W bosons was also measured in ep collisions by the H1 Collaboration [24]. Finally, for dibosons, first measurements of the W polarisation were performed by LEP experiments in W pair production in e^+e^- collisions [25,26] and were used to set limits on anomalous triple gauge couplings (aTGC) in Ref. [27].

This paper presents results obtained using proton–proton (pp) collisions recorded by the ATLAS detector at a centre-of-mass energy of $\sqrt{s} = 13$ TeV in 2015 and 2016, corresponding to an integrated luminosity of 36.1 fb^{-1}. The W and Z bosons are reconstructed using their decay modes into electrons or muons. The production cross section is measured within a fiducial phase space both inclusively and differentially as a function of several individual variables related to the kinematics of the $W^{\pm}Z$ system and to the jet activity in the event. The reported measurements are compared with the SM cross-section predictions at NLO in QCD [28,29] and with the recent calculations at next-to-next-to-leading order (NNLO) in QCD [30,31]. The ratio of the W^+Z cross section to the W^-Z cross section, which is sensitive to the parton distribution functions (PDF) is also measured. Finally, an analysis of angular distributions of leptons from decays of W and Z bosons is performed and integrated helicity fractions in the detector fiducial region are measured for the W and Z bosons separately.

2 ATLAS detector

The ATLAS detector [32–34] is a multipurpose particle detector with a cylindrical geometry[1] and nearly 4π coverage in solid angle. A set of tracking detectors around the collision point (collectively referred to as the inner detector) is located within a superconducting solenoid providing a 2 T axial magnetic field, and is surrounded by a calorimeter system and a muon spectrometer. The inner detector (ID) consists of a silicon pixel detector and a silicon microstrip tracker, together providing precision tracking in the pseudorapidity range $|\eta| < 2.5$, complemented by a straw-tube transition radiation tracker providing tracking and electron identification information for $|\eta| < 2.0$. The electromagnetic calorimeter covers the region $|\eta| < 3.2$ and is based on a lead/liquid-argon (LAr) sampling technology. The hadronic calorimeter uses a steel/scintillator-tile sampling detector in the region $|\eta| < 1.7$ and a copper/LAr detector in the region $1.5 < |\eta| < 3.2$. The most forward region of ATLAS, $3.1 < |\eta| < 4.9$, is equipped with a forward calorimeter, measuring electromagnetic and hadronic energies in copper/LAr and tungsten/LAr modules. The muon spectrometer (MS) comprises separate trigger and high-precision tracking chambers to measure the deflection of muons in a magnetic field generated by three large superconducting toroids with coils arranged with an eightfold azimuthal symmetry around the calorimeters. The high-precision chambers cover the range of $|\eta| < 2.7$ with three layers of monitored drift tubes, complemented by cathode strip chambers in the forward region, where the particle flux is highest. The muon trigger system covers the range $|\eta| < 2.4$ with resistive-plate chambers in the barrel and thin-gap chambers in the endcap regions. A two-level trigger system [35] is used to select events in real time. It consists of a hardware-based first-level trigger that uses a subset of detector information to reduce the event rate to approximately 100 kHz, and a software-based high-level trigger system that reduces the event rate to about 1 kHz. The latter employs algorithms similar to those used offline to identify electrons, muons, photons and jets.

3 Phase space for cross-section measurement

The fiducial $W^{\pm}Z$ cross section is measured in a phase space chosen to follow closely the event selection criteria described in Sect. 5. It is based on the kinematics of particle-level objects as defined in Ref. [36]. These are final-state prompt[2] leptons associated with the W and Z boson decays. Charged leptons after QED final-state radiation are "dressed" by adding to the lepton four-momentum the contributions from photons with an angular distance $\Delta R \equiv \sqrt{(\Delta\eta)^2 + (\Delta\phi)^2} < 0.1$ from the lepton. Dressed leptons, and final-state neutrinos that do not originate from hadron or τ-lepton decays, are matched to the W and Z boson decay products using an algorithm that does not depend on details of the Monte Carlo (MC) generator, called the "resonant shape" algorithm. This algorithm is based on the value of an estimator expressing the product of the nominal lineshapes of the W and Z resonances

[1] ATLAS uses a right-handed coordinate system with its origin at the nominal interaction point (IP) in the centre of the detector and the z-axis along the beam direction. The x-axis points from the IP to the centre of the LHC ring, and the y-axis points upward. Cylindrical coordinates (r, ϕ) are used in the transverse (x, y) plane, ϕ being the azimuthal angle around the beam direction. The pseudorapidity is defined in terms of the polar angle θ as $\eta = -\ln[\tan(\theta/2)]$.

[2] A prompt lepton is a lepton that is not produced in the decay of a hadron, a τ-lepton, or their descendants.

$$P = \left| \frac{1}{m^2_{(\ell^+,\ell^-)} - \left(m_Z^{\mathrm{PDG}}\right)^2 + \mathrm{i}\,\Gamma_Z^{\mathrm{PDG}}\, m_Z^{\mathrm{PDG}}} \right|^2 \times \left| \frac{1}{m^2_{(\ell',\nu_{\ell'})} - \left(m_W^{\mathrm{PDG}}\right)^2 + \mathrm{i}\,\Gamma_W^{\mathrm{PDG}}\, m_W^{\mathrm{PDG}}} \right|^2 ,$$

where m_Z^{PDG} (m_W^{PDG}) and Γ_Z^{PDG} (Γ_W^{PDG}) are the world average mass and total width of the Z (W) boson, respectively, as reported by the Particle Data Group [37]. The input to the estimator is the invariant mass m of all possible pairs (ℓ^+, ℓ^-) and $(\ell', \nu_{\ell'})$ satisfying the fiducial selection requirements defined in the next paragraph. The final choice of which leptons are assigned to the W or Z bosons corresponds to the configuration exhibiting the largest value of the estimator. Using this specific association algorithm, the gauge boson kinematics can be computed using the kinematics of the associated leptons independently of any internal MC generator details.

The reported cross sections are measured in a fiducial phase space defined at particle level as follows. The dressed leptons from Z and W boson decay must have $|\eta| < 2.5$ and transverse momentum p_{T} above 15 GeV and 20 GeV, respectively; the invariant mass of the two leptons from the Z boson decay differs by at most 10 GeV from the world average value of the Z boson mass m_Z^{PDG}. The W transverse mass, defined as $m_{\mathrm{T}}^W = \sqrt{2 \cdot p_{\mathrm{T}}^{\nu} \cdot p_{\mathrm{T}}^{\ell} \cdot [1 - \cos\Delta\phi(\ell, \nu)]}$, where $\Delta\phi(\ell, \nu)$ is the angle between the lepton and the neutrino in the transverse plane, and p_{T}^{ℓ} and p_{T}^{ν} are the transverse momenta of the lepton from W boson decay and of the neutrino, respectively, must be greater than 30 GeV. In addition, it is required that the angular distance ΔR between the charged leptons from the W and Z decay is larger than 0.3, and that ΔR between the two leptons from the Z decay is larger than 0.2. A requirement that the transverse momentum of the leading lepton be above 27 GeV reduces the acceptance of the fiducial phase space by less than 0.5%. This criterion is therefore not added to the definition of the fiducial phase space, while it is present in the selection at the detector level.

The fiducial cross section is extrapolated to the total phase space and corrected for the leptonic branching fractions of the W and Z bosons, $(10.86 \pm 0.09)\%$ and $(3.3658 \pm 0.0023)\%$ [37], respectively. The total phase space is defined by requiring the invariant mass of the lepton pair associated with the Z boson to be in the range $66 < m_{\ell\ell} < 116$ GeV.

For the differential measurements related to jets, particle-level jets are reconstructed from stable particles with a lifetime of $\tau > 30$ ps in the simulation. Stable particles are taken after parton showering, hadronisation, and the decay of particles with $\tau < 30$ ps. Muons, electrons, neutrinos and photons associated with W and Z decays are excluded from the jet collection. The particle-level jets are reconstructed with the anti-k_t algorithm [38] with a radius parameter $R = 0.4$ and are required to have a p_{T} above 25 GeV and an absolute value of pseudorapidity below 4.5.

4 Signal and background simulation

A sample of simulated $W^{\pm}Z$ events is used to correct the signal yield for detector effects, to extrapolate from the fiducial to the total phase space, and to compare the measurements with the theoretical predictions. The production of $W^{\pm}Z$ pairs and the subsequent leptonic decays of the vector bosons were simulated at NLO in QCD using the Powheg-Box v2 [39–42] generator, interfaced to Pythia 8.210 [43] for simulation of parton showering, hadronisation and the underlying event. Final-state radiation resulting from QED interactions is simulated using Pythia 8.210 and the AZNLO [44] set of tuned parameters. The CT10 [45] PDF set was used for the hard-scattering process, while the CTEQ6L1 [46] PDF set was used for the parton shower. The sample was generated with dynamic renormalisation and factorisation QCD scales, μ_{R} and μ_{F}, equal to $m_{WZ}/2$, where m_{WZ} is the invariant mass of the WZ system. An additional $W^{\pm}Z$ sample was generated by interfacing Powheg-Box v2 matrix elements to the Herwig++ 2.7.1 [47] fragmentation model and is used to estimate the uncertainty due to the fragmentation modelling. Also for this sample, the CT10 and CTEQ6L1 PDF sets are used for the matrix elements and the parton showers, respectively, while QED final-state radiation is internally modelled in Herwig. An alternative signal sample was generated at NLO QCD using the Sherpa 2.2.2 generator [48]. Matrix elements contain all diagrams with four electroweak vertices. They were calculated for up to one parton at NLO and up to three partons at LO using Comix [49] and OpenLoops [50], and merged with the Sherpa parton shower [51] according to the ME+PS@NLO prescription [52]. The NNPDF3.0nnlo [53] PDF set was used in conjunction with the dedicated parton shower tuning developed by the Sherpa authors. A calculation using Sherpa 2.1 with one to three partons at LO is also used for comparisons to measured jet observables. Finally, the NLO QCD predictions from the MC@NLO v4.0 [54] MC generator interfaced to the Herwig fragmentation model, using the CT10 PDF set, are also used to estimate signal modelling uncertainties.

NNLO QCD cross sections for $W^{\pm}Z$ production in the fiducial and total phase spaces are provided by the MATRIX computational framework [30,31,50,55–59]. The calculation includes contributions from off-shell electroweak bosons and all relevant interference effects. The renormalisation and factorisation scales were fixed to $(m_Z + m_W)/2$, chosen following Ref. [30], and the NNPDF3.0nnlo PDF set was used. The predictions from the Powheg+Pythia sample

were rescaled by a global factor of 1.18 to match the NNLO cross section predicted by MATRIX.

The background sources in this analysis include processes with two or more electroweak gauge bosons, namely ZZ, WW and VVV ($V = W, Z$); processes with top quarks, such as $t\bar{t}$ and $t\bar{t}V$, single top and tZ; and processes with gauge bosons associated with jets or photons ($Z + j$ and $Z\gamma$). MC simulation is used to estimate the contribution from background processes with three or more prompt leptons. Background processes with at least one misidentified lepton are evaluated using data-driven techniques and simulated events are used to assess the systematic uncertainties of these backgrounds (see Sect. 6).

The SHERPA 2.2.2 event generator was used to simulate $q\bar{q}$-initiated ZZ processes with up to one parton at NLO and up to three partons at LO and using the NNPDF3.0nnlo PDF set. A SHERPA 2.1.1 ZZ sample was generated with the loop-induced gg-initiated process simulated at LO using the CT10 PDF, with up to one additional parton. A K-factor of 1.67 ± 0.25 was applied to the cross section of the loop-induced gg-initiated process to account for the NLO corrections [60]. Triboson events were simulated at LO with the SHERPA 2.1.1 generator using the CT10 PDF set. The $t\bar{t}V$ processes were generated at NLO with the MADGRAPH5_AMC@NLO [61] MC generator using the NNPDF3.0nlo PDF set interfaced to the PYTHIA 8.186 [62] parton shower model. Finally, the tZ events were generated at LO with the MADGRAPH5_AMC@NLO using the NNPDF2.3lo [63] PDF set interfaced with PYTHIA 6.428 [64].

All generated MC events were passed through the ATLAS detector simulation [65], based on GEANT4 [66], and processed using the same reconstruction software as used for the data. The event samples include the simulation of additional proton–proton interactions (pile-up) generated with PYTHIA 8.186 using the MSTW2008LO [67] PDF set and the A2 [68] set of tuned parameters for the underlying event and parton fragmentation. Simulated events were reweighted to match the pile-up conditions observed in the data. Scale factors are applied to simulated events to correct for small differences in the efficiencies observed in data and predicted by MC simulation for the trigger, reconstruction, identification, isolation and impact parameter requirements of electrons and muons [69,70]. Furthermore, the electron energy and muon momentum in simulated events are smeared to account for small differences in resolution between data and MC events [70,71].

5 Event selection

Only data recorded with stable beam conditions and with all relevant detector subsystems operational are considered. Candidate events are selected using triggers [35] that require at least one electron or muon. The transverse momentum threshold applied to leptons by the triggers in 2015 was 24 GeV for electrons and 20 GeV for muons satisfying a loose isolation requirement based only on ID track information. Due to the higher instantaneous luminosity in 2016 the trigger threshold was increased to 26 GeV for both the electrons and muons. Furthermore, tighter lepton isolation and tighter electron identification requirements were applied in 2016. Possible inefficiencies for leptons with large transverse momentum are reduced by using additional triggers with tighter thresholds, $p_{\mathrm{T}} = 60$ GeV and 50 GeV for electrons and muons respectively, and no isolation requirements. Finally, a single-electron trigger requiring $p_{\mathrm{T}} > 120$ GeV (in 2015) and $p_{\mathrm{T}} > 140$ GeV (in 2016) with less restrictive electron identification criteria was used to increase the selection efficiency for high-p_{T} electrons. The combined efficiency of these triggers is close to 100% for $W^{\pm}Z$ events passing the offline selection criteria.

Events are required to have a primary vertex compatible with the luminous region of the LHC. The primary vertex is defined as the reconstructed vertex with at least two charged particle tracks, that has the largest sum of the p_{T}^2 for the associated tracks.

All final states with three charged leptons (electrons e or muons μ) and missing transverse momentum ($E_{\mathrm{T}}^{\mathrm{miss}}$) from $W^{\pm}Z$ leptonic decays are considered. In the following, the different final states are referred to as $\mu^{\pm}\mu^{+}\mu^{-}$, $e^{\pm}\mu^{+}\mu^{-}$, $\mu^{\pm}e^{+}e^{-}$ and $e^{\pm}e^{+}e^{-}$, where the first label is from the charged lepton of the W decay, and the last two labels are for the Z decay. No requirement on the number of jets is applied.

Muon candidates are identified by tracks reconstructed in the muon spectrometer (MS) and matched to tracks reconstructed in the inner detector (ID). Muons are required to pass a "medium" identification selection, which is based on requirements on the number of hits in the ID and the MS [70]. The efficiency of this selection averaged over p_{T} and η is larger than 98%. The muon momentum is calculated by combining the MS measurement, corrected for the energy deposited in the calorimeters, and the ID measurement. The p_{T} of the muon must be greater than 15 GeV and its pseudorapidity must satisfy $|\eta| < 2.5$.

Electron candidates are reconstructed from energy clusters in the electromagnetic calorimeter matched to ID tracks. Electrons are identified using a discriminant that is the value of a likelihood function constructed with information about the shape of the electromagnetic showers in the calorimeter, the track properties, and the quality of the track-to-cluster matching for the candidate [69]. Electrons must satisfy a "medium" likelihood requirement, which provides an overall identification efficiency of 90%. The electron momentum is computed from the cluster energy and the direction of the track. The p_{T} of the electron must be greater than 15 GeV and the pseudorapidity of the cluster must satisfy $|\eta| < 1.37$

or $1.52 < |\eta| < 2.47$ to be within the tracking system, excluding the transition region between the barrel and endcap sections of the electromagnetic calorimeter.

Electron and muon candidates are required to originate from the primary vertex. Thus, the significance of the track's transverse impact parameter calculated relative to the beam line, $|d_0/\sigma_{d_0}|$, must be smaller than 3.0 for muons and less than 5.0 for electrons. Furthermore, the longitudinal impact parameter, z_0 (the difference between the value of z of the point on the track at which d_0 is defined and the longitudinal position of the primary vertex), is required to satisfy $|z_0 \cdot \sin(\theta)| < 0.5$ mm.

Electrons and muons are required to be isolated from other particles using both calorimeter-cluster and ID-track information. The isolation requirement for electrons is tuned for an efficiency of at least 90% for $p_{\mathrm{T}} > 25$ GeV and at least 99% for $p_{\mathrm{T}} > 60$ GeV [69], while fixed requirements on the isolation variables are used for muons, providing an efficiency above 90% for $p_{\mathrm{T}} > 15$ GeV and at least 99% for $p_{\mathrm{T}} > 60$ GeV [70].

Jets are reconstructed from clusters of energy deposition in the calorimeter [72] using the anti-k_t algorithm [38] with a radius parameter $R = 0.4$. The energy of jets is calibrated using a jet energy correction derived from both simulation and *in situ* methods using data [73]. Jets with p_{T} below 60 GeV and with $|\eta| < 2.4$ have to pass a requirement on the *jet vertex tagger* [74], a likelihood discriminant that uses a combination of track and vertex information to suppress jets originating from pile-up activity. All jets must have $p_{\mathrm{T}} > 25$ GeV and be reconstructed in the pseudorapidity range $|\eta| < 4.5$. Jets in the ID acceptance containing a b-hadron are identified with a multivariate algorithm [75,76] that uses the impact parameter and reconstructed secondary vertex information of the tracks contained in the jets. Jets initiated by b-quarks are selected by setting the algorithm's output threshold such that a 70% b-jet selection efficiency is achieved in simulated $t\bar{t}$ events. The corresponding light-flavour (u,d,s-quark and gluon) and c-jet misidentification efficiencies are 0.3% and 8.2%, respectively. Corrections to the flavour-tagging efficiencies are based on data-driven calibration analyses.

The transverse momentum of the neutrino is estimated from the missing transverse momentum in the event, $E_{\mathrm{T}}^{\mathrm{miss}}$, calculated as the negative vector sum of the transverse momentum of all identified hard physics objects (electrons, muons, jets), with a contribution from an additional soft term. This soft term is calculated from ID tracks matched to the primary vertex and not assigned to any of the hard objects (electrons, muons and jets) [77].

To avoid cases where the detector response to a single physical object is reconstructed as two different final-state objects, e.g. an electron reconstructed as both an electron and a jet, several steps are followed to remove such overlaps, as described in Ref. [78].

Events are required to contain exactly three lepton candidates satisfying the selection criteria described above. To ensure that the trigger efficiency is well determined, at least one of the candidate leptons is required to have $p_{\mathrm{T}} > 25$ GeV for 2015 and $p_{\mathrm{T}} > 27$ GeV for 2016 data, as well as being geometrically matched to a lepton that was selected by the trigger.

To suppress background processes with at least four prompt leptons, events with a fourth lepton candidate satisfying looser selection criteria are rejected. For this looser selection, the lepton p_{T} requirement is lowered to $p_{\mathrm{T}} > 5$ GeV, electrons are allowed to be reconstructed in the barrel-endcap calorimeter gap ($1.37 < |\eta| < 1.52$), and "loose" identification requirements [69,70] are used for both the electrons and muons. A less stringent requirement is applied for electron isolation and is based only on ID track information.

Candidate events are required to have at least one pair of leptons with the same flavour and opposite charge, with an invariant mass that is consistent with the nominal Z boson mass [37] to within 10 GeV. This pair is considered to be the Z boson candidate. If more than one pair can be formed, the pair whose invariant mass is closest to the nominal Z boson mass is taken as the Z boson candidate. The remaining third lepton is assigned to the W boson decay. The transverse mass of the W candidate, computed using $E_{\mathrm{T}}^{\mathrm{miss}}$ and the p_{T} of the associated lepton, is required to be greater than 30 GeV.

Backgrounds originating from misidentified leptons are suppressed by requiring the lepton associated with the W boson to satisfy more stringent selection criteria. Thus, the transverse momentum of these leptons is required to be greater than 20 GeV. Furthermore, charged leptons associated with the W boson decay are required to pass the "tight" identification requirements, which results in an efficiency between 90% and 98% for muons and an overall efficiency of 85% for electrons. Finally, muons associated to the W boson must also pass a tighter isolation requirement, tuned for an efficiency of at least 90% (99%) for $p_{\mathrm{T}} > 25$ (60) GeV.

6 Background estimation

The background sources are classified into two groups: events where at least one of the candidate leptons is not a prompt lepton (reducible background) and events where all candidates are prompt leptons or are produced in the decay of a τ-lepton (irreducible background). Candidates that are not prompt leptons are also called "misidentified" or "fake" leptons.

Events in the first group originate from $Z + j$, $Z\gamma$, $t\bar{t}$, and WW production processes and constitute about 40% of the total backgrounds. This reducible background is esti-

mated with a data-driven method based on the inversion of a matrix containing the efficiencies and the misidentification probabilities for prompt and fake leptons [9,79]. The method exploits the classification of the leptons as loose or tight candidates and the probability that a fake lepton is misidentified as a loose or tight lepton. Tight leptons are signal leptons as defined in Sect. 5. Loose leptons are leptons that do not meet the isolation and identification criteria of signal leptons but satisfy only looser criteria. The misidentification probabilities for fake leptons are determined from data using dedicated control samples enriched in misidentified leptons from light- or heavy-flavour jets and from photon conversions. The lepton efficiencies and misidentification probabilities are combined with event rates in data samples of $W^{\pm}Z$ candidate events where at least one and up to three of the leptons are loose. Then, solving the system of linear equations, the number of events with at least one misidentified lepton, which represents the amount of reducible background in the $W^{\pm}Z$ sample, is obtained. About 2% of this background contribution arises from events with two fake leptons. The background from events with three fake leptons, e.g., from multijet processes, is negligible. The method allows the shape of any kinematic distribution of reducible background events to be estimated. Another independent method to assess the reducible background was also considered. This method estimates the amount of reducible background using MC simulations scaled to data by process-dependent factors determined from the data-to-MC comparison in dedicated control regions. Good agreement with the matrix method estimate is obtained at the level of 4% in the yield and 40% in the shape of the distributions of irreducible background events.

The events contributing to the second group of background processes originate from ZZ, $t\bar{t}+V$, VVV (where $V = Z$ or W) and $tZ(j)$ events. The amount of irreducible background is estimated using MC simulations because processes with a small cross section and signal leptons can be simulated with a better statistical accuracy than an estimate obtained with data-driven methods. Events from VH production processes with leptonic decays of the bosons can also contribute. This contribution was estimated using MC simulations to be of the order of 0.1% and was therefore neglected. The dominant contribution in this second group is from ZZ production, where one of the leptons from the ZZ decay falls outside the detector acceptance. It represents about 70% of the irreducible background. The MC-based estimates of the ZZ and $t\bar{t}+V$ backgrounds are validated by comparing the MC expectations with the event yield and several kinematic distributions of a data sample enriched in ZZ and $t\bar{t}+V$ events, respectively.

The ZZ control sample is selected by requiring a Z candidate that meets all the analysis selection criteria and is accompanied by two additional leptons, satisfying the lepton criteria described in Sect. 5. The ZZ MC expectation needs to be rescaled by a factor of 1.12 in order to match the observed event yield of data in this control region. This scaling factor relative to SHERPA predictions is in agreement with the ZZ cross-section measurements performed at $\sqrt{s} = 13$ TeV [80]. The shapes of distributions of the main kinematic variables are found to be well described by the MC predictions.

The $t\bar{t}+V$ control sample is selected by requiring $W^{\pm}Z$ events to have at least two reconstructed b-jets. The $t\bar{t}+V$ MC calculation needs to be rescaled by a factor of 1.3 in order to match the observed event yield in data. This scaling factor relative to predictions is in line with the $t\bar{t}V$ cross-section measurements performed at $\sqrt{s} = 13$ TeV [81]. Here again, the distributions of the main kinematic variables are found to be well described by the MC predictions.

7 Detector-level results

Table 1 summarises the predicted and observed numbers of events together with the estimated background contributions. Only statistical uncertainties are quoted. Figure 1 shows the measured distributions of the transverse momentum and the invariant mass of the Z candidate, the transverse mass of the W candidate, and for the WZ system the variable m_{T}^{WZ}, defined as follows:

$$m_{\mathrm{T}}^{WZ} = \sqrt{\left(\sum_{\ell=1}^{3} p_{\mathrm{T}}^{\ell} + E_{\mathrm{T}}^{\mathrm{miss}}\right)^2 - \left[\left(\sum_{\ell=1}^{3} p_x^{\ell} + E_x^{\mathrm{miss}}\right)^2 + \left(\sum_{\ell=1}^{3} p_y^{\ell} + E_y^{\mathrm{miss}}\right)^2\right]}.$$

The POWHEG+PYTHIA MC prediction is used for the $W^{\pm}Z$ signal contribution. Figure 1 indicates that the MC predictions provide a fair description of the shapes of the data distributions.

8 Corrections for detector effects and acceptance

For a given channel $W^{\pm}Z \to \ell'^{\pm}\nu\ell^{+}\ell^{-}$, where ℓ and ℓ' indicates each type of lepton (e or μ), the integrated fiducial cross section that includes the leptonic branching fractions of the W and Z bosons is calculated as

$$\sigma^{\mathrm{fid.}}_{W^{\pm}Z\to\ell'\nu\ell\ell} = \frac{N_{\mathrm{data}} - N_{\mathrm{bkg}}}{\mathcal{L}\cdot C_{WZ}} \times \left(1 - \frac{N_{\tau}}{N_{\mathrm{all}}}\right),$$

where N_{data} and N_{bkg} are the number of observed events and the estimated number of background events, respectively, $\mathcal{L}$ is the integrated luminosity, and C_{WZ}, obtained from simulation, is the ratio of the number of selected signal events at detector level to the number of events at particle level in the fiducial phase space. This factor corrects for detector efficiencies and for QED final-state radiation

Table 1 Observed and expected numbers of events after the $W^{\pm}Z$ inclusive selection described in Sect. 5 in each of the considered channels and for the sum of all channels. The expected number of $W^{\pm}Z$ events from POWHEG+PYTHIA and the estimated number of background events from other processes are detailed. The POWHEG+PYTHIA MC prediction is scaled by a global factor of 1.18 to match the NNLO cross section predicted by MATRIX. The sum of background events containing misidentified leptons is labelled "Misid. leptons". Only statistical uncertainties are reported

Channel	eee		μee		$e\mu\mu$		$\mu\mu\mu$		All	
Data	1279		1281		1671		1929		6160	
Total expected	1221	7	1281	6	1653	8	1830	7	5986	14
WZ	922	5	1077	6	1256	6	1523	7	4778	12
Misid. leptons	138	5	34	2	193	5	71	2	436	8
ZZ	86	1	89	1	117	1	135	1	426	3
$t\bar{t}$+V	50.0	0.7	54.0	0.7	56.1	0.7	63.8	0.8	225	1
tZ	23.1	0.4	24.8	0.4	28.8	0.4	33.5	0.5	110	1
VVV	2.5	0.1	2.8	0.1	3.2	0.1	3.6	0.1	12.0	0.2

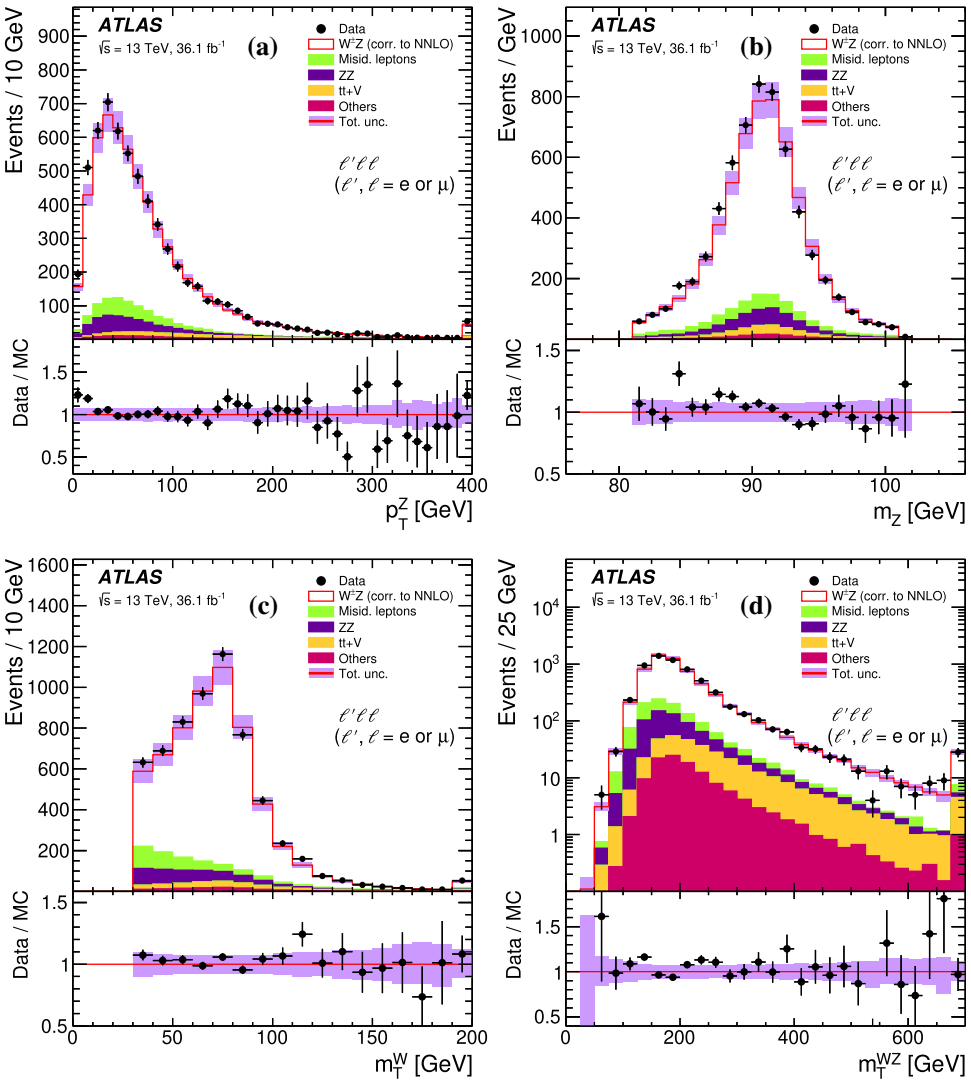

Fig. 1 The distributions, for the sum of all channels, of the kinematic variables **a** p_{T}^{Z}, **b** m_Z, **c** m_{T}^{W} and **d** m_{T}^{WZ}. The points correspond to the data with the error bars representing the statistical uncertainties, and the histograms correspond to the predictions of the various SM processes. The sum of the background processes with misidentified leptons is labelled "Misid. leptons". The POWHEG+PYTHIA MC prediction is used for the $W^{\pm}Z$ signal contribution. It is scaled by a global factor of 1.18 to match the NNLO cross section predicted by MATRIX. The open red histogram shows the total prediction; the shaded violet band is the total uncertainty of this prediction. The last bin contains the overflow. The lower panels in each figure show the ratio of the data points to the open red histogram with their respective uncertainties

effects. The contribution from τ-lepton decays, amounting approximately to 4%, is removed from the cross-section definition by introducing the term in parentheses. This term is computed using simulation, where N_τ is the number of selected events at detector level in which at least one of the bosons decays into a τ-lepton and N_{all} is the

Table 2 The C_{WZ} factors for each of the eee, μee, $e\mu\mu$, and $\mu\mu\mu$ inclusive channels. The POWHEG+PYTHIA MC event sample with the "resonant shape" lepton assignment algorithm at particle level is used. Only statistical uncertainties are reported

Channel	C_{W^-Z}	C_{W^+Z}	$C_{W^\pm Z}$
eee	0.399 ± 0.003	0.394 ± 0.003	0.396 ± 0.002
μee	0.470 ± 0.004	0.469 ± 0.003	0.469 ± 0.002
$e\mu\mu$	0.548 ± 0.004	0.541 ± 0.003	0.544 ± 0.003
$\mu\mu\mu$	0.660 ± 0.005	0.663 ± 0.004	0.662 ± 0.003

number of selected WZ events with decays into any lepton.

The C_{WZ} factors for W^-Z, W^+Z, and $W^\pm Z$ inclusive processes computed with POWHEG+PYTHIA for each of the four leptonic channels are shown in Table 2.

The total cross section is calculated as

$$\sigma^{\text{tot.}}_{W^\pm Z} = \frac{\sigma^{\text{fid.}}_{W^\pm Z \to \ell' \nu \ell \ell}}{\mathcal{B}_W \, \mathcal{B}_Z \, A_{WZ}},$$

where $\mathcal{B}_W = (10.86 \pm 0.09)\%$ and $\mathcal{B}_Z = (3.3658 \pm 0.0023)\%$ are the W and Z leptonic branching fractions [37], respectively, and A_{WZ} is the acceptance factor calculated at particle level as the ratio of the number of events in the fiducial phase space to the number of events in the total phase space as defined in Sect. 3.

A single acceptance factor of $A_{WZ} = 0.343 \pm 0.002$ (stat.), obtained by averaging the acceptance factors computed in the μee and $e\mu\mu$ channels, is used since it was verified for the fiducial phase space used that interference effects related to the presence of identical leptons in the final state, as in the eee and $\mu\mu\mu$ channels, are below 1% of the cross section. The use of only the μee and $e\mu\mu$ channels for the computation of A_{WZ} avoids the ambiguity arising from the assignment of particle-level final-state leptons to the W and Z bosons.

The differential detector-level distributions within the fiducial phase space are corrected for detector resolution and for QED final-state radiation effects using simulated signal events and an iterative Bayesian unfolding method [82], as implemented in the RooUnfold toolkit [83]. The number of iterations used ranges from two to four, depending on the resolution in the unfolded variable. The width of the bins in each distribution is chosen according to the experimental resolution and to the statistical significance of the expected number of events in each bin. The fraction of signal MC events generated in a bin that are reconstructed in the same bin is around 70% on average and always greater than 50%, except for the jet multiplicity distribution, where it can decrease to 40% for $N_{\text{jets}} = 4$.

In the inclusive measurements, the POWHEG+PYTHIA signal sample is used for unfolding since it provides a fair description of the data distributions. For differential measurements with jets, the SHERPA 2.2.2 signal sample is used for the computation of the response matrix since this sample includes up to three partons in the matrix element calculation and therefore better describes the jet multiplicity in data.

9 Systematic uncertainties

The systematic uncertainties in the measured cross sections are due to uncertainties of experimental and theoretical nature in the acceptance, in the correction procedure for detector effects, in the background estimate and in the luminosity.

The theoretical modelling systematic uncertainties in the A_{WZ} and C_{WZ} factors are due to the choice of PDF set, QCD renormalisation μ_R and factorisation μ_F scales, and the parton showering simulation. The uncertainties due to the choice of PDF are computed using the CT10 eigenvectors and the envelope of the differences between the CT10 and CT14 [84], MMHT2014 [85] and NNPDF 3.0 [53] PDF sets, according to the PDF4LHC recommendations [86]. The effects of QCD scale uncertainties are estimated by varying μ_R and μ_F by factors of two around the nominal scale $m_{WZ}/2$ with the constraint $0.5 \leq \mu_R/\mu_F \leq 2$, where m_{WZ} is the invariant mass of the WZ system. Uncertainties arising from the choice of parton shower model are estimated by interfacing POWHEG with PYTHIA or HERWIG and comparing the results. Among these three sources of theoretical uncertainty, only the choice of parton shower model has an effect on the C_{WZ} factors, of 0.5%. The uncertainty of the acceptance factor A_{WZ} is less than 0.5% due to the PDF choice, less than 0.7% due to the QCD scale choice, and about 0.5% for the choice of parton shower model.

Uncertainties in the unfolding from detector to particle level due to imperfect description of the data by the MC simulation are evaluated using a data-driven method [87]. The MC differential distribution is corrected to match the data distribution and the resulting weighted MC distribution at detector level is unfolded with the response matrix used in the actual data unfolding. The new unfolded distribution is compared with the weighted MC distribution at particle level and the difference is taken as the systematic uncertainty. Uncertainties in the unfolding are typically of the order of 2% but can vary from 0.1% to 10% depending on the considered observable and bin. For the inclusive measurements, differences in the unfolded results if the POWHEG+PYTHIA or SHERPA 2.2.2 MC signal samples are used for the unfolding are found to be covered by these unfolding uncertainties.

The experimental systematic uncertainty on the C_{WZ} factors and on the unfolding procedure includes uncertainties on the scale and resolution of the electron energy, muon momentum, jet energy and $E_{\text{T}}^{\text{miss}}$, as well as uncertainties on the scale factors applied to the simulation in order to repro-

duce the trigger, reconstruction, identification and isolation efficiencies measured in data. The systematic uncertainties on the measured cross sections are determined by repeating the analysis after applying appropriate variations for each source of systematic uncertainty to the simulated samples. The uncertainties on the jet energy scale and resolution are based on their respective measurements in data [73]. The uncertainty on $E_{\mathrm{T}}^{\mathrm{miss}}$ is estimated by propagating the uncertainties on the transverse momenta of reconstructed objects and by applying momentum scale and resolution uncertainties to the track-based soft term [77]. A variation in the pileup reweighting of the MC is included to cover the uncertainty on the ratio between the predicted and measured inelastic cross-section in the fiducial volume defined by $M_X > 13$ GeV where M_X is the mass of the hadronic system [88]. For the measurements of the W charge-dependent cross sections, an uncertainty arising from the charge misidentification of leptons is also considered. It affects only electrons and leads to an uncertainty of less than 0.15% in the ratio of W^+Z to W^-Z integrated cross sections determined by combining the four decay channels.

The dominant contribution among the experimental systematic uncertainties in the eee and μee channels is due to the uncertainty on the electron identification efficiency, contributing at most a 2.8% uncertainty to the integrated cross section, while in the $e\mu\mu$ and $\mu\mu\mu$ channels it originates from the muon reconstruction efficiency and is at most 2.8%.

The uncertainty on the amount of background from misidentified leptons takes into account the limited number of events in the control regions as well as differences in background composition between the control region used to determine the lepton misidentification rate and the control regions used to estimate the yield in the signal region. This results in a total uncertainty of 30% on the misidentified-leptons background yield for the integrated cross-section measurements and of 40% when the shape of the differential distributions of the reducible background events is also considered.

A global uncertainty of $\pm 12\%$ is assigned to the amount of ZZ background predicted by the MC simulation, based on the comparison with data in the ZZ control region. Similarly, a global uncertainty of $\pm 30\%$ is assigned to the $t\bar{t}+V$ background.

The uncertainty due to other irreducible background sources is evaluated by propagating the uncertainty in their MC cross sections. These are 20% for VVV [89] and 15% for tZ [9].

The uncertainty on the combined 2015+2016 integrated luminosity is 2.1%. It is derived from a calibration of the luminosity scale using x–y beam-separation scans, following a methodology similar to that detailed in Ref. [90], and using the LUCID-2 detector for the baseline luminosity measurements [91]. It is applied to the signal normalisation as well as to all background contributions that are estimated using only MC simulations and has an effect of 2.4% on the measured cross sections.

Table 3 Summary of the relative uncertainties on the measured fiducial cross section $\sigma^{\mathrm{fid.}}_{W^\pm Z}$ for each channel and for their combination. The uncertainties are reported as percentages. The first rows indicate the main sources of systematic uncertainty for each channel and their combination, which are treated as correlated between channels. A row with uncorrelated uncertainties follows, which comprise all uncertainties of statistical origin including MC statistics as well as statistical uncertainties in the fake-factors calculation, which are uncorrelated between channels

	eee	μee	$e\mu\mu$	$\mu\mu\mu$	Combined
Relative uncertainties [%]					
e energy scale	0.2	0.1	0.1	< 0.1	0.1
e id. efficiency	2.8	1.8	1.0	< 0.1	1.1
μ momentum scale	< 0.1	< 0.1	< 0.1	< 0.1	< 0.1
μ id. efficiency	< 0.1	1.3	1.6	2.8	1.5
$E_{\mathrm{T}}^{\mathrm{miss}}$ and jets	0.2	0.2	0.3	0.5	0.3
Trigger	< 0.1	< 0.1	0.2	0.3	0.2
Pile-up	1.0	1.5	1.2	1.5	1.3
Misid. leptons background	4.7	1.1	4.5	1.6	1.9
ZZ background	1.0	1.0	1.1	1.0	1.0
Other backgrounds	1.6	1.5	1.4	1.2	1.4
Uncorrelated	0.7	0.6	0.7	0.5	0.3
Total systematic uncertainty	6.0	3.5	5.4	4.1	3.6
Luminosity	2.2	2.2	2.2	2.2	2.2
Theoretical modelling	0.5	0.5	0.5	0.5	0.5
Statistics	3.6	3.3	3.2	2.7	1.6
Total	7.3	5.3	6.6	5.3	4.5

The total systematic uncertainty on the $W^\pm Z$ fiducial cross section, excluding the luminosity uncertainty, varies between 4 and 6% for the four different measurement channels, and is dominated by the uncertainty on the reducible background estimate. Table 3 shows the statistical uncertainty and the main sources of systematic uncertainty on the $W^\pm Z$ fiducial cross section for each of the four channels and for their combination. The modelling uncertainty on the measurements is dominated by the modelling of the fragmentation.

10 Cross-section measurements

10.1 Integrated cross sections

The measured fiducial cross sections for the four channels are combined using a χ^2 minimisation method that accounts for correlations between the sources of systematic uncertainty affecting each channel [92–94]. The combination of the $W^\pm Z$ cross sections in the fiducial phase space for the four channels yields a χ^2 per degree of freedom (dof) of

$\chi^2/n_{\text{dof}} = 3.3/3$. The combinations of the W^+Z and W^-Z cross sections separately yield $\chi^2/n_{\text{dof}} = 3.7/3$ and $1.5/3$, respectively.

The $W^\pm Z$ production cross section in the fiducial phase space resulting from the combination of the four channels including the W and Z branching ratio in a single leptonic channel with muons or electrons is

$$\sigma^{\text{fid.}}_{W^\pm Z\to\ell'\nu\ell\ell} = 63.7 \pm 1.0\,(\text{stat.}) \pm 2.3\,(\text{exp. syst.}) \pm 0.3(\text{mod. syst}) \pm 1.4\,(\text{lumi.})\ \text{fb},$$

where the uncertainties correspond to statistical, experimental systematic, modelling systematic and luminosity uncertainties, respectively. The corresponding SM NNLO QCD prediction from MATRIX is $61.5^{+1.4}_{-1.3}$ fb, where the uncertainty corresponds to the QCD scale uncertainty estimated conventionally by varying the scales μ_R and μ_F by factors of two around the nominal value of $(m_W + m_Z)/2$ with the constraint $0.5 \le \mu_R/\mu_F \le 2$. This prediction is obtained by correcting the result in Ref. [31] for Born level leptons to dressed leptons by a factor of 0.96, which is estimated in the fiducial phase space using POWHEG+PYTHIA. Changing the PDF set used from NNPDF3.0nnlo to MMHT2014 or CT14 affects the MATRIX prediction by +2% and +1%, respectively. The uncertainty due to varying the α_S coupling constant value used in the PDF determination is 0.6% and 1.0% for W^+Z and W^-Z production, respectively. The measured $W^\pm Z$ production cross sections are compared with the SM NNLO prediction from MATRIX using three different PDF sets, NNDPF3.0nnlo, MMHT2014 and CT14, as well as with NLO predictions from SHERPA 2.2.2 in Fig. 2. All results for $W^\pm Z$, W^+Z and W^-Z final states are reported in Table 4. The NNLO SM calculations reproduce the measured cross sections well. The production of $W^\pm Z$ in association with two jets produced as a result of electroweak processes is not included in the NNLO SM prediction and amounts to 1.2% of the measured cross section, as estimated using SHERPA 2.2.2.

The ratio of the W^+Z to W^-Z production cross sections is

$$\frac{\sigma^{\text{fid.}}_{W^+Z\to\ell'\nu\ell\ell}}{\sigma^{\text{fid.}}_{W^-Z\to\ell'\nu\ell\ell}} = 1.47 \pm 0.05\,(\text{stat.}) \pm 0.02\,(\text{syst.}).$$

Most of the systematic uncertainties, especially the luminosity uncertainty, almost cancel out in the ratio, so that the measurement is dominated by the statistical uncertainty. The measured cross-section ratios, for each channel and for their combination, are compared in Fig. 3 with the SM prediction of $1.44^{+0.03}_{-0.06}$, calculated with MATRIX [31] and the NNDPF3.0nnlo PDF set. The uncertainties correspond to PDF uncertainties estimated at NLO with POWHEG+PYTHIA using the CT10 eigenvectors and the envelope of the differences between the CT10 and CT14, MMHT2014 and NNPDF 3.0nnlo PDF sets. The effects of QCD scale uncertainties on the predicted cross-section ratio are negligible. The cross-section ratio is also calculated with MATRIX using the MMHT2014 and CT14 PDF sets, yielding values of 1.42 and 1.44, respectively, as shown in Fig. 3.

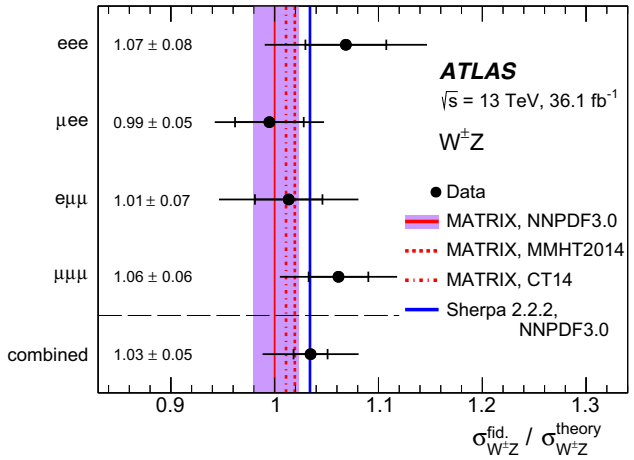

Fig. 2 Ratio of the measured $W^\pm Z$ integrated cross sections in the fiducial phase space to the NNLO SM prediction from MATRIX in each of the four channels and for their combination. The inner and outer error bars on the data points represent the statistical and total uncertainties, respectively. The NNLO SM prediction from MATRIX using the NNPDF3.0nnlo PDF set is shown as the red line; the shaded violet band shows the effect of QCD scale uncertainties on this prediction. The prediction from MATRIX using the MMHT2014 and CT14 PDF sets and the NLO prediction from SHERPA 2.2.2 are also displayed as dashed-red, dotted-dashed-red and blue lines, respectively

The combined fiducial cross section is extrapolated to the total phase space. The result is

$$\sigma^{\text{tot.}}_{W^\pm Z} = 51.0 \pm 0.8\,(\text{stat.}) \pm 1.8\,(\text{exp. syst.}) \pm 0.9\,(\text{mod. syst.}) \pm 1.1\,(\text{lumi.})\ \text{pb},$$

where the modelling uncertainty accounts for the uncertainties in the A_{WZ} factor due to the choice of PDF set, QCD scales and the fragmentation model. The NNLO SM prediction calculated with MATRIX [30] is $49.1^{+1.1}_{-1.0}\,(\text{scale})$ pb, which is in good agreement with the present measurement. As the MATRIX calculation does not include effects of QED final-state radiation, a correction factor of 0.99, as estimated from POWHEG+PYTHIA in the total phase space, is applied to it to obtain the above prediction.

10.2 Differential cross sections

For the measurements of the differential distributions, all four decay channels, eee, $e\mu\mu$, μee, and $\mu\mu\mu$, are added together. The resulting distributions are unfolded with a response matrix computed using a POWHEG+PYTHIA MC signal sample that includes all four topologies and is divided by four,

Table 4 Fiducial integrated cross section in fb, for $W^{\pm}Z$, $W^{+}Z$ and $W^{-}Z$ production, measured in each of the channels eee, μee, $e\mu\mu$, and $\mu\mu\mu$ and for all four channels combined. The statistical ($\delta_{\text{stat.}}$), experimental systematic ($\delta_{\text{exp. syst.}}$), modelling systematic ($\delta_{\text{mod. syst.}}$), luminosity ($\delta_{\text{lumi.}}$) and total ($\delta_{\text{tot.}}$) uncertainties are given in percent. The NNLO SM predictions from MATRIX using the NNDPF3.0nnlo set are also reported

Channel	$\sigma^{\text{fid.}}$ (fb) $\sigma^{\text{fid.}}_{W^{\pm}Z\to\ell'\nu\ell\ell}$	$\delta_{\text{stat.}}$ (%)	$\delta_{\text{exp. syst.}}$ (%)	$\delta_{\text{mod. syst.}}$ (%)	$\delta_{\text{lumi.}}$ (%)	$\delta_{\text{tot.}}$ (%)
$e^{\pm}ee$	65.8	3.6	6.0	0.5	2.2	7.3
$\mu^{\pm}ee$	61.2	3.3	3.5	0.5	2.2	5.3
$e^{\pm}\mu\mu$	62.4	3.2	5.4	0.5	2.2	6.6
$\mu^{\pm}\mu\mu$	65.3	2.7	4.1	0.5	2.2	5.3
Combined	63.7	1.6	3.6	0.5	2.2	4.5
SM prediction	61.5	–	–	–	–	$^{2.3}_{2.1}$
	$\sigma^{\text{fid.}}_{W^{+}Z\to\ell'\nu\ell\ell}$					
$e^{+}ee$	40.8	4.6	5.4	0.5	2.2	7.4
$\mu^{+}ee$	36.5	4.3	3.3	0.5	2.2	5.8
$e^{+}\mu\mu$	36.7	4.1	5.0	0.5	2.2	6.8
$\mu^{+}\mu\mu$	38.2	3.5	4.0	0.5	2.2	5.7
Combined	37.9	2.0	3.4	0.5	2.2	4.5
SM prediction	36.3	—	—	—	—	$^{2.2}_{2.0}$
	$\sigma^{\text{fid.}}_{W^{-}Z\to\ell'\nu\ell\ell}$					
$e^{-}ee$	24.9	6.1	7.1	0.5	2.2	9.6
$\mu^{-}ee$	24.8	5.3	4.0	0.5	2.2	7.0
$e^{-}\mu\mu$	25.7	5.1	6.2	0.5	2.2	8.3
$\mu^{-}\mu\mu$	27.1	4.3	4.3	0.5	2.2	6.4
Combined	25.9	8.1	4.0	0.5	2.2	5.2
SM prediction	25.2	—	—	—	—	$^{2.3}_{2.1}$

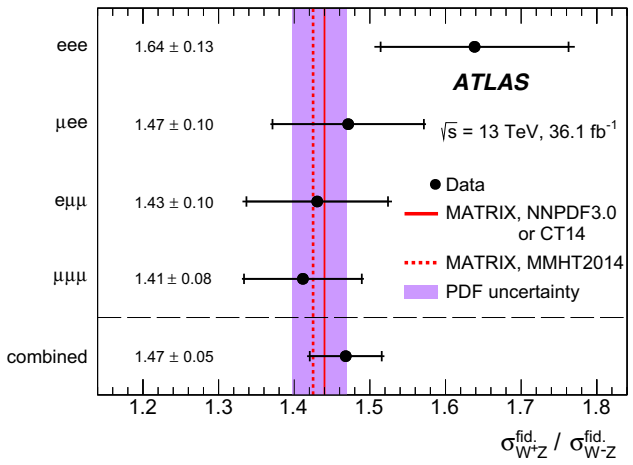

Fig. 3 Measured ratio $\sigma^{\text{fid.}}_{W^{+}Z}/\sigma^{\text{fid.}}_{W^{-}Z}$ of $W^{+}Z$ and $W^{-}Z$ integrated cross sections in the fiducial phase space in each of the four channels and for their combination. The error bars on the data points represent the total uncertainties, which are dominated by the statistical uncertainties. The NNLO SM predictions from MATRIX using the NNPDF3.0nnlo or CT14 PDF sets are equal and represented as a single red line. The shaded violet band represents the effect of PDF uncertainties estimated using the POWHEG+PYTHIA NLO calculation using the CT10 eigenvectors and the envelope of the differences between the CT10 and CT14, MMHT2014 and NNPDF 3.0nnlo PDF sets. The MATRIX prediction using the MMHT2014 PDF set is also displayed as the dashed-red line

such that cross sections refer to final states where the W and Z bosons decay in a single leptonic channel with muons or electrons.

The $W^{\pm}Z$ production cross section is measured as a function of several variables: the transverse momenta of the Z and W bosons, p_{T}^{Z} and p_{T}^{W}, the transverse mass of the $W^{\pm}Z$ system m_{T}^{WZ} and the azimuthal angle between the W and Z bosons in Fig. 4; as a function of the p_{T} of the neutrino associated with the decay of the W boson, p_{T}^{ν}, and the absolute difference between the rapidities of the Z boson and the charged lepton from the decay of the W boson, $|y_Z - y_{\ell,W}|$ in Fig. 5.

In order to derive p_{T}^{W} and p_{T}^{ν} from data events, it is assumed that the whole $E_{\text{T}}^{\text{miss}}$ of each event arises from the neutrino of the W boson decay. The validity of this assumption was verified for SM WZ events using MC samples at the level of precision of the present results.

The measured differential cross sections in Figs. 4 and 5 are compared with the predictions at NNLO in QCD from the MATRIX computational framework. The predictions from MATRIX are corrected from Born-level leptons to dressed leptons using binned correction factors determined using POWHEG+PYTHIA. The correction factors are found to be mostly constant over the ranges of all differential distribu-

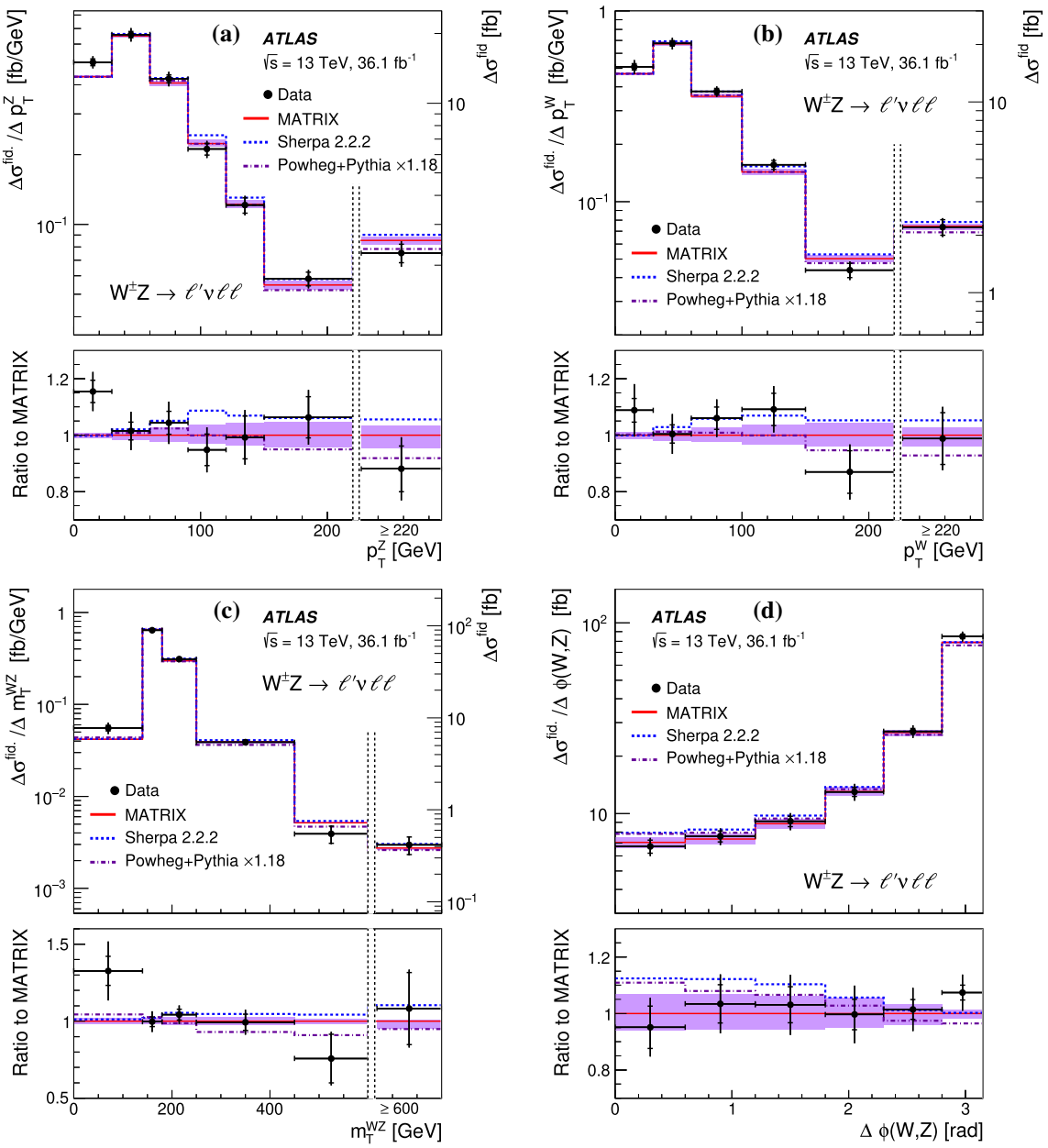

Fig. 4 The measured $W^{\pm}Z$ differential cross section in the fiducial phase space as a function of **a** p_{T}^{Z}, **b** p_{T}^{W}, **c** m_{T}^{WZ} and **d** $\Delta\phi(W, Z)$. The inner and outer error bars on the data points represent the statistical and total uncertainties, respectively. The measurements are compared with the NNLO prediction from MATRIX (red line, see text for details). The violet band shows how the QCD scale uncertainties affect the NNLO predictions. The predictions from the POWHEG+PYTHIA and SHERPA MC generators are also indicated by dotted-dashed and dashed lines, respectively. In **a**–**c**, the right vertical axis refers to the last cross-section point, separated from the others by vertical dashed lines, as this last bin is integrated up to the maximum value reached in the phase space and the cross section is not divided by the bin width

tions, with a mean value of 0.96. The predicted and measured cross sections are in good agreement. The measurements are also compared with NLO MC predictions from POWHEG+PYTHIA, after a rescaling of its predicted integrated fiducial cross section to the NNLO cross section, and to SHERPA 2.2.2 without rescaling its prediction. Good agreement of the shapes of the measured distributions with the predictions of POWHEG+PYTHIA and SHERPA 2.2.2 is observed. The $\Delta\phi(W, Z)$ distribution, which is sensitive to QCD higher-order perturbative effects, is better described by MATRIX than by POWHEG+PYTHIA or SHERPA 2.2.2.

As shown in previous publications, the high energy tails of the p_{T}^{Z} [12] and m_{T}^{WZ} [9] observables are sensitive to aTGC, p_{T}^{Z} having the disadvantage of being more subject to higher-

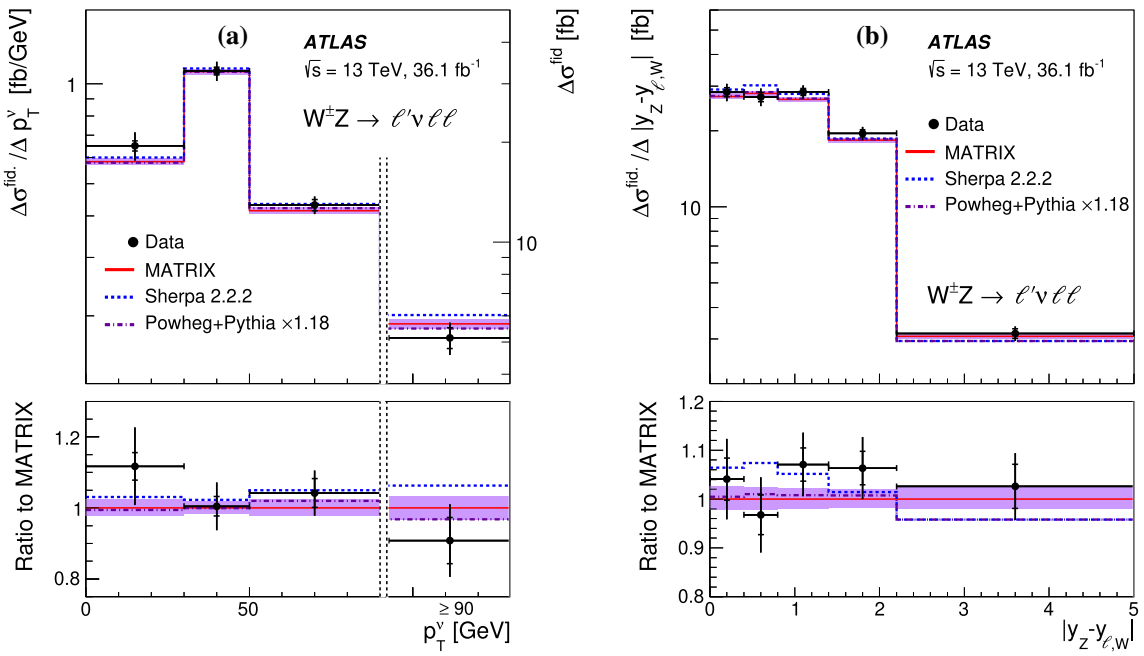

Fig. 5 The measured $W^{\pm}Z$ differential cross section in the fiducial phase space as a function of **a** p_{T}^{ν} and **b** $|y_Z - y_{\ell,W}|$. The inner and outer error bars on the data points represent the statistical and total uncertainties, respectively. The measurements are compared with the NNLO prediction from MATRIX (red line, see text for details). The violet band shows how the QCD scale uncertainties affect the NNLO predictions. The predictions from the POWHEG+PYTHIA and SHERPA MC generators are also indicated by dotted-dashed and dashed lines, respectively. In **a**, the right vertical axis refers to the last cross-section point, separated from the others by vertical dashed lines, as this last bin is integrated up to the maximum value reached in the phase space and the cross section is not divided by the bin width

order perturbative effects in QCD [95] and electroweak theory [96]. This is seen also here with larger NNLO QCD scale uncertainties predicted by MATRIX for p_{T}^{Z} than for m_{T}^{WZ}. No excess of data events in the tails of these distributions is observed.

The exclusive multiplicity of jets above a p_{T} threshold of 25 GeV unfolded at particle level is presented in Fig. 6a. The measurements are compared with predictions from SHERPA 2.2.2, SHERPA 2.1 and POWHEG+PYTHIA. The SHERPA predictions provide a better description of the ratio of 0-jet to 1-jet event cross sections than POWHEG+PYTHIA. However, the SHERPA 2.2.2 prediction, which models up to one parton at NLO, tends to overestimate the cross section of events with two or more jets, while SHERPA 2.1 agrees better with data for N_{jets} up to three. Yields of events with higher jet multiplicities are described by the parton shower modelling of the POWHEG+PYTHIA MC. Finally, the measured $W^{\pm}Z$ differential cross section as a function of the invariant mass, m_{jj}, of the two leading jets with $p_{\mathrm{T}} > 25$ GeV is presented in Fig. 6b. The measurement is better described by the SHERPA predictions. The production of $W^{\pm}Z$ in association with two jets produced as a result of electroweak processes is not included in the SM predictions presented in the figure. In the last m_{jj} bin it amounts to 17% of the measured cross section, as estimated using SHERPA 2.2.2.

11 Polarisation measurement

11.1 Formalism and analysis principle

The polarisation of a gauge boson can be determined from the angular distribution of its decay products. At the Born level, the expected angular distribution for massless fermions in the rest frame of the parent W boson is given in terms of the diagonal elements f_0, f_{L} and f_{R} of the spin density matrix [97–100] by

$$\frac{1}{\sigma_{W^{\pm}Z}}\frac{\mathrm{d}\sigma_{W^{\pm}Z}}{\mathrm{d}\cos\theta_{\ell,W}} = \frac{3}{8}f_{\mathrm{L}}[(1\mp\cos\theta_{\ell,W})^2] + \frac{3}{8}f_{\mathrm{R}}[(1\pm\cos\theta_{\ell,W})^2] + \frac{3}{4}f_0\sin^2\theta_{\ell,W}, \quad (1)$$

where $\theta_{\ell,W}$ is defined using the helicity frame, as the decay angle of the charged lepton in the W rest frame relative to the W direction in the WZ centre-of-mass frame, as shown in Fig. 7. The terms f_0, f_{L} and f_{R} refer to the longitudinal, transverse left-handed and transverse right-handed helicity fractions, respectively, and the normalisation is chosen such that $f_0 + f_{\mathrm{L}} + f_{\mathrm{R}} = 1$. In the equation, the upper and lower signs correspond to W^+ and W^- bosons, respectively. All dependencies on the azimuthal angle are integrated over.

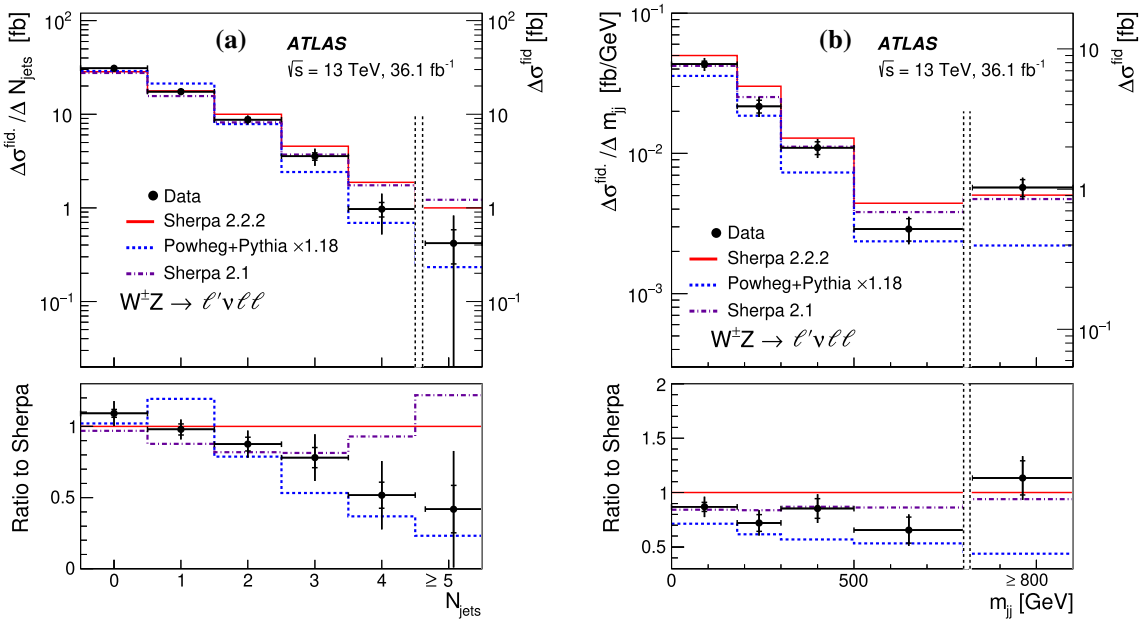

Fig. 6 The measured $W^{\pm}Z$ differential cross section in the fiducial phase space as a function of the exclusive multiplicity of jets with $p_{\mathrm{T}} > 25$ GeV (**a**) and of the invariant mass of the two leading jets with $p_{\mathrm{T}} > 25$ GeV (**b**). The inner and outer error bars on the data points represent the statistical and total uncertainties, respectively. The measurements are compared with the predictions from SHERPA 2.2.2 (red line), POWHEG+PYTHIA (dashed blue line) and SHERPA 2.1 (dotted-dashed violet line). The right vertical axis refers to the last cross-section point, separated from the others by vertical dashed lines, as this last bin is integrated up to the maximum value reached in the phase space and the cross section is not divided by the bin width

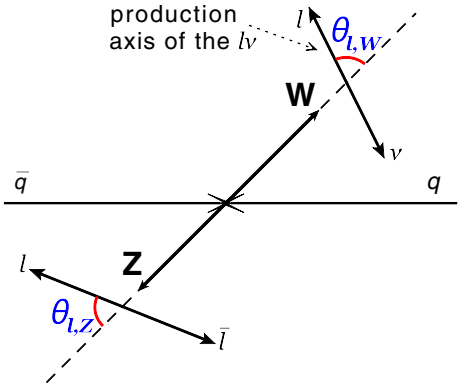

Fig. 7 The decay angle $\theta_{\ell,W(Z)}$ is defined as the angle between the negatively (positively for W^{+}) charged lepton produced in the decay of the W (Z) boson as seen in the W (Z) rest frame and the direction of the W (Z) which is given in the WZ centre-of-mass frame

The expected angular distribution of the lepton decay products of the Z boson is described by the generalisation of Equation (1) [97–99]:

$$\frac{1}{\sigma_{W^{\pm}Z}}\frac{\mathrm{d}\sigma_{W^{\pm}Z}}{\mathrm{d}\cos\theta_{\ell,Z}} = \frac{3}{8}f_{\mathrm{L}}(1+2\alpha\cos\theta_{\ell,Z}+\cos^2\theta_{\ell,Z}) + \frac{3}{8}f_{\mathrm{R}}(1+\cos^2\theta_{\ell,Z}-2\alpha\cos\theta_{\ell,Z}) + \frac{3}{4}f_0\sin^2\theta_{\ell,Z}\,, \quad (2)$$

where $\theta_{\ell,Z}$ is defined using the helicity frame, as the decay angle of the negatively charged lepton in the Z rest frame relative to the Z direction in the WZ centre-of-mass frame. The parameter $\alpha = (2c_v c_a)/(c_v^2+c_a^2)$ is expressed in terms of the vector $c_v = -\frac{1}{2}+2\sin^2\theta_{\mathrm{W}}^{\mathrm{eff}}$ and axial-vector $c_a = -\frac{1}{2}$ couplings of the Z boson to leptons, respectively, where the effective value of the Weinberg angle $\sin^2\theta_{\mathrm{W}}^{\mathrm{eff}} = 0.23152$ [37] is used. Equation (2) also holds for the contribution from γ^* and its interference with the Z boson, with appropriate c_v and c_a coefficients. The tight invariant mass window of ± 10 GeV around the nominal Z boson mass minimises the contribution from γ^*, although all the helicity fractions presented here are effective fractions, containing the small contribution from γ^*.

Equations (1) and (2) are valid only when the full phase space of the leptonic decays of the gauge bosons is accessible. Restrictions on the p_{T} and η values of the charged decay lepton or of the neutrino suppress events at $|\cos\theta_{\ell,W(Z)}| \sim 1$, as shown in Fig. 8, and the analytic expressions of Eqs. (1) and (2) cannot be used to extract the helicity fractions. Simulated templates therefore must be used.

Another major difficulty arises for the W boson from incomplete knowledge of the neutrino momentum. The large angular coverage of the ATLAS detector enables measurement of the missing transverse momentum, which can be identified as the transverse momentum of the neutrino. The

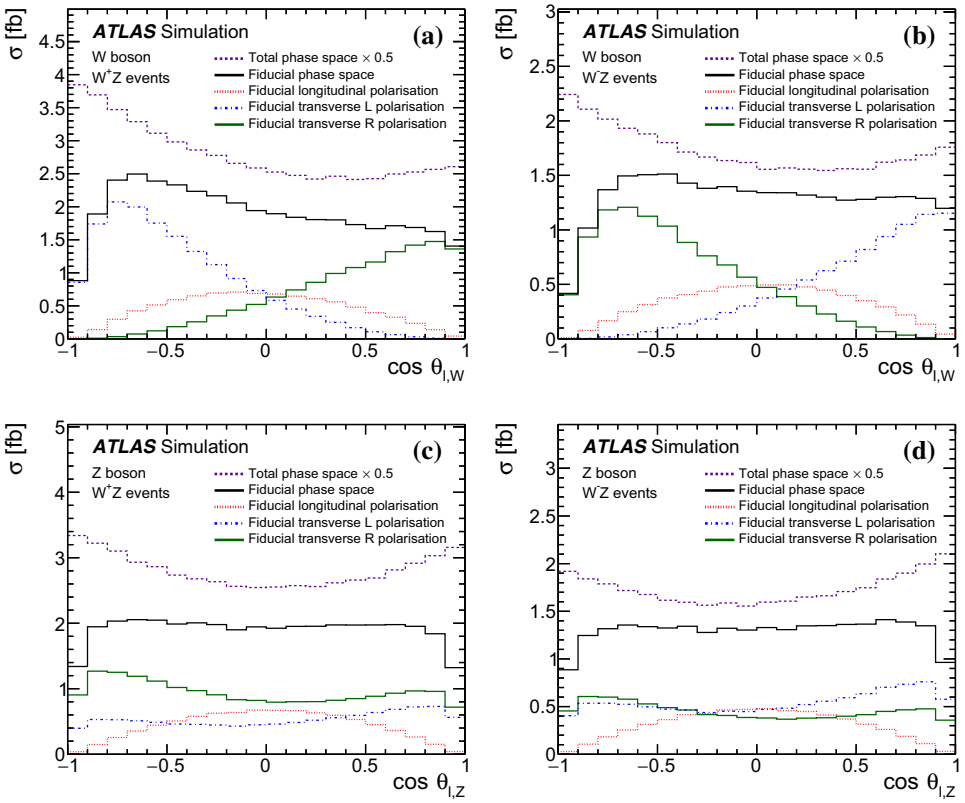

Fig. 8 Distributions in the total and fiducial phase space at particle level of the variables **a**, **b** $\cos\theta_{\ell,W}$ and **c**, **d** $\cos\theta_{\ell,Z}$ for **a**, **c** W^+Z and **b**, **d** W^-Z events. The black line corresponds to the sum of all helicity states. The red, blue and green lines correspond to the purely longitudinal, transverse left-handed and transverse right-handed helicity components, respectively. The distributions are obtained using the POWHEG+PYTHIA MC. All four decay channels, eee, $e\mu\mu$, μee, and $\mu\mu\mu$, are added together

neutrino longitudinal momentum p_z^ν is obtained using the W mass constraint. Solving the corresponding equation leads to a twofold ambiguity, which is resolved by choosing the solution with the smaller $|p_z^\nu|$. If the measured transverse mass is larger than the nominal W mass, no real solutions exist for p_z^ν. The most likely cause is that the measured $E_{\mathrm{T}}^{\mathrm{miss}}$ is larger than the actual neutrino p_{T}. In this case, the best estimate is obtained by choosing the real part of the complex solutions. As an alternative to the $\cos\theta_{\ell,W}$ observable using this reconstruction of the neutrino momentum, a "transverse helicity" observable introduced in Ref. [19] was tested, but a similar or lower sensitivity for the measurement of the f_0 helicity fraction for W bosons was obtained, so it was not pursued further.

For the polarisation measurements, all four decay channels, eee, $e\mu\mu$, μee, and $\mu\mu\mu$, are added together. The measurements of W and Z boson polarisation are performed separately for W^+Z, W^-Z and $W^\pm Z$ events. To allow the datasets of both W boson charges to be combined for the measurement in $W^\pm Z$ events, $\cos\theta_{\ell,W}$ is multiplied by the sign of the lepton charge q_ℓ. Figure 9a, b present the reconstructed distributions for $W^\pm Z$ events of $q_\ell \cdot \cos\theta_{\ell,W}$ for the W bosons and of $\cos\theta_{\ell,Z}$ for Z bosons. The MC predictions provide a good description of the shapes of the data distributions.

The helicity parameters f_0 and $f_{\mathrm{L}} - f_{\mathrm{R}}$ are measured in $W^\pm Z$ events separately for W and Z bosons using a binned profile-likelihood fit [101] of templates of the three helicity states to the $q_\ell \cdot \cos\theta_{\ell,W}$ and $\cos\theta_{\ell,Z}$ distributions. The equation $f_0 + f_{\mathrm{R}} + f_{\mathrm{L}} = 1$ is used to constrain the independent parameters of the fit to f_0, $f_{\mathrm{L}} - f_{\mathrm{R}}$ and the integrated fiducial cross section. The templates of $q_\ell \cdot \cos\theta_{\ell,W}$ and $\cos\theta_{\ell,Z}$ distributions for each of the three helicity states of the W and Z bosons are extracted from the POWHEG+PYTHIA MC sample [19]. For each of the gauge bosons, generically denoted as V, the predicted helicity fractions of POWHEG+PYTHIA MC events are determined as a function of p_{T}^V and y_V by fitting the analytic functions of Eqs. (1) and (2) to the predicted $\cos\theta_{\ell,V}$ distributions in the total phase space. Two dimensional bins as a function of p_{T}^V and y_V are used. The bin boundaries are optimised such that possible bias on the evolution of the extracted helicity fractions is minimised. The MC templates at detector level representing longitudinal, left- and right-handed states of the W boson are then obtained by reweighting of POWHEG+PYTHIA MC events according to

$$\frac{\frac{1}{\sigma_{W^\pm Z}}\frac{\mathrm{d}\sigma_{W^\pm Z}}{\mathrm{d}\cos\theta_{\ell,W}}\Big|_{\mathrm{L/0/R}}}{\frac{3}{8}f_{\mathrm{L}}^{\mathrm{gen.}}(1\mp\cos\theta_{\ell,W})^2 + \frac{3}{8}f_{\mathrm{R}}^{\mathrm{gen.}}(1\pm\cos\theta_{\ell,W})^2 + \frac{3}{4}f_0^{\mathrm{gen.}}\sin^2\theta_{\ell,W}},$$

where

$$\frac{1}{\sigma_{W^\pm Z}}\frac{\mathrm{d}\sigma_{W^\pm Z}}{\mathrm{d}\cos\theta_{\ell,W}}\Bigg|_{\mathrm{R}}^{\mathrm{L}}_{0} = \frac{3}{8}\begin{cases}(1\mp\cos\theta_{\ell,W})^2\\ 2\sin^2\theta_{\ell,W}\\ (1\pm\cos\theta_{\ell,W})^2\end{cases},$$

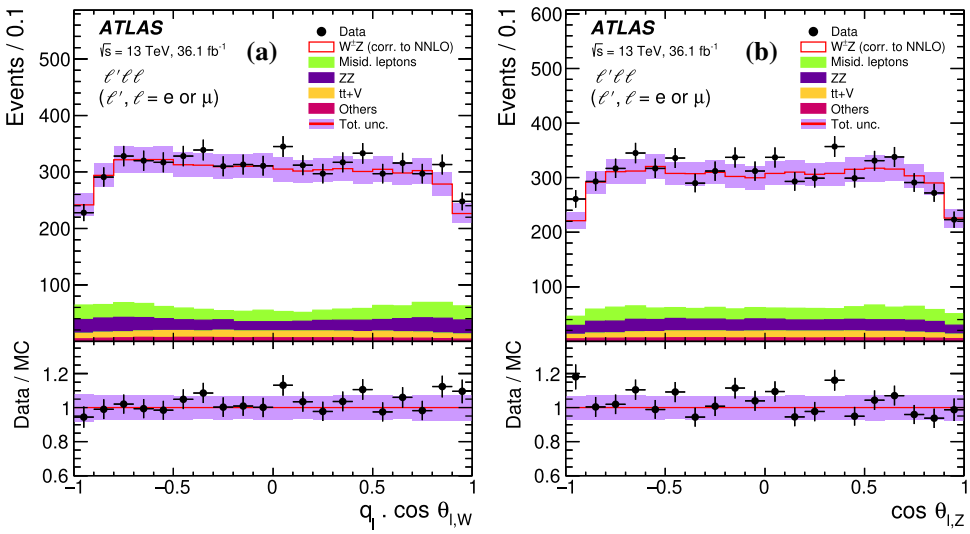

Fig. 9 The detector-level distributions for the sum of all channels of the variables **a** $q_\ell \cdot \cos\theta_{\ell,W}$ and **b** $\cos\theta_{\ell,Z}$. The points correspond to the data with the error bars representing the statistical uncertainties, and the histograms correspond to the predictions of the different SM processes. The sum of the background processes with misidentified leptons is labelled "Misid. leptons". The POWHEG+PYTHIA MC prediction is used for the $W^{\pm}Z$ signal contribution. It is scaled by a global factor of 1.18 to match the NNLO cross section predicted by MATRIX. The open red histogram shows the total prediction; the shaded violet band is the total uncertainty of this prediction. The lower panels in each figure show the ratio of the data points to the open red histogram with their respective uncertainties

and where $f_{\mathrm{L/0/R}}^{\mathrm{gen.}}$ are the helicity fractions at generator level, extracted by the fit, of POWHEG+PYTHIA MC events. Similar equations hold for the polarisation of the Z boson. The procedural uncertainty of the reweighting method for the generation of MC templates was estimated to be below 0.5%. Helicity fractions are extracted by the template fit at detector level. To be expressed in a fiducial phase space at particle level, each helicity fraction is then corrected independently for detector efficiencies and QED final-state radiation effects using factors obtained from the simulation. Measured helicity fractions are thus reported at particle level for a fiducial phase space which follows the definition of Sect. 3 with the difference that leptons with kinematics defined before QED final state radiation ("Born leptons") are used instead of dressed leptons. Experimental systematic uncertainties detailed in Sect. 9 are considered and treated as nuisance parameters with an assumed Gaussian distribution. Theoretical systematic uncertainties due to the modelling in the event generator used to evaluate the helicity templates are considered. The effects of PDF and QCD scale uncertainties are estimated as detailed in Sect. 9. An additional modelling uncertainty is considered and estimated by comparing predictions from the POWHEG+PYTHIA and MC@NLO MC event generators for the shape of helicity template distributions.

11.2 Results

The measurements of f_0 and $f_{\mathrm{L}} - f_{\mathrm{R}}$ are summarised in Table 5, where they are compared with the predictions from POWHEG+PYTHIA. The POWHEG+PYTHIA MC sample was generated at LO in the electroweak formalism using the G_μ scheme with $\sin^2\theta_{\mathrm{W}} = 0.2229$. This choice impacts the predicted $f_{\mathrm{L}} - f_{\mathrm{R}}$ values which depend on the chosen value of the Weinberg angle via the angular coefficient A_4 [97,102]. The impact of the value of $\sin^2\theta_{\mathrm{W}}$ on $f_{\mathrm{L}} - f_{\mathrm{R}}$ is estimated using MCFM [103–105] calculations with two electroweak schemes, the G_μ scheme and a scheme where the value $\sin^2\theta_{\mathrm{W}}^{\mathrm{eff}} = 0.23152$ is imposed. The difference between the two calculations is used to correct the $f_{\mathrm{L}} - f_{\mathrm{R}}$ values predicted by POWHEG+PYTHIA.

The longitudinal helicity fraction f_0 of the Z boson is measured with an observed significance of $6.5\,\sigma$, compared to $6.1\,\sigma$ expected. The longitudinal helicity fraction f_0 of the W boson is more difficult to extract than for the Z boson and has a larger uncertainty. This measurement establishes the presence of longitudinally polarised W bosons with an observed significance of $4.2\,\sigma$, compared to $3.8\,\sigma$ expected. Table 6 shows the main sources of uncertainty in the measurement of the helicity fractions. The measurements are dominated by statistical uncertainties. Good agreement of the measured helicity fractions of both the W and Z bosons with the predictions from POWHEG+PYTHIA and MATRIX is observed. Measured f_0 values agree within 1σ with the prediction, while $f_{\mathrm{L}} - f_{\mathrm{R}}$ values agree within $2\,\sigma$. The POWHEG+PYTHIA and MATRIX predictions are only at NLO and NNLO in QCD, respectively, but, more importantly for polarisation, both calculations use only LO electroweak matrix elements. Therefore, and also because of the still large statistical uncer-

Table 5 Measured helicity fractions in the fiducial phase space with Born-level leptons, for $W^{\pm}Z$ $W^{+}Z$ and $W^{-}Z$ events. The total uncertainties in the measurements are reported. The measurements are compared with predictions at electroweak LO from POWHEG+PYTHIA and MATRIX corrected to $\sin^2\theta_{\mathrm{W}}^{\mathrm{eff}} = 0.23152$. The uncertainties on the POWHEG+PYTHIA prediction include QCD scale and PDF uncertainties; the uncertainties in the MATRIX prediction include QCD scale uncertainties

	f_0						$f_{\mathrm{L}} - f_{\mathrm{R}}$					
	Data		POWHEG+PYTHIA		MATRIX		Data		POWHEG+PYTHIA		MATRIX	
W^{+} in $W^{+}Z$	0.26	0.08	0.233	0.004	0.2448	0.0010	−0.02	0.04	0.091	0.004	0.0868	0.0014
W^{-} in $W^{-}Z$	0.32	0.09	0.245	0.005	0.2651	0.0015	−0.05	0.05	−0.063	0.006	−0.034	0.004
$W^{\pm}$ in $W^{\pm}Z$	0.26	0.06	0.2376	0.0031	0.2506	0.0006	−0.024	0.033	0.0289	0.0022	0.0375	0.0011
Z in $W^{+}Z$	0.27	0.05	0.225	0.004	0.2401	0.0014	−0.32	0.21	−0.297	0.021	−0.262	0.009
Z in $W^{-}Z$	0.21	0.06	0.235	0.005	0.2389	0.0015	−0.46	0.25	0.052	0.023	0.0468	0.0034
Z in $W^{\pm}Z$	0.24	0.04	0.2294	0.0033	0.2398	0.0014	−0.39	0.16	−0.156	0.016	−0.135	0.006

Table 6 Summary of the absolute uncertainties in the helicity fractions f_0 and $f_{\mathrm{L}} - f_{\mathrm{R}}$ measured in $W^{\pm}Z$ events for W and Z bosons

	$W^{\pm}$ in $W^{\pm}Z$		Z in $W^{\pm}Z$	
	f_0	$f_{\mathrm{L}} - f_{\mathrm{R}}$	f_0	$f_{\mathrm{L}} - f_{\mathrm{R}}$
e energy scale and id. efficiency	0.0024	0.0004	0.005	0.0021
μ momentum scale and id. efficiency	0.0013	0.0027	0.0018	0.008
$E_{\mathrm{T}}^{\mathrm{miss}}$ and jets	0.0024	0.0010	0.0017	0.005
Pile-up	0.005	0.00009	0.0014	0.005
Misid. lepton background	0.031	< 0.001	0.007	0.019
ZZ background	0.009	0.0004	0.0007	0.0012
Other backgrounds	0.0012	0.0005	0.0018	0.005
QCD scale	0.0008	0.0013	0.0004	0.008
PDF	0.0011	0.0009	0.00004	< 0.00001
Modelling	0.004	0.007	0.0015	0.0028
Total systematic uncertainty	0.033	0.008	0.009	0.024
Luminosity	0.0015	< 0.0001	< 0.0001	0.0008
Statistics	0.06	0.032	0.04	0.15
Total	0.06	0.033	0.04	0.16

tainties in the measurements, no stringent constraints nor clear inconsistencies between measurements and predictions can be deduced. The values of f_0 and $f_{\mathrm{L}} - f_{\mathrm{R}}$ measured in $W^{\pm}Z$ events are shown in Fig. 10 for the W and Z bosons, respectively.

12 Conclusion

Measurements of $W^{\pm}Z$ production cross sections in $\sqrt{s} = 13$ TeV pp collisions at the LHC are presented. The data analysed were collected with the ATLAS detector in 2015 and 2016 and correspond to an integrated luminosity of 36.1 fb^{-1}. The measurements use leptonic decay modes of the gauge bosons to electrons or muons and are performed in a fiducial phase space closely matching the detector acceptance. The measured inclusive cross section in the fiducial region for leptonic decay modes (electrons or muons) is $\sigma^{\mathrm{fid.}}_{W^{\pm}Z\to\ell'\nu\ell\ell} = 63.7 \pm 1.0\,(\mathrm{stat.}) \pm 2.3\,(\mathrm{syst.}) \pm 1.4\,(\mathrm{lumi.})$ fb, in agreement with the NNLO Standard Model expectation of $61.5^{+1.4}_{-1.3}$ fb. The ratio of the cross sections for $W^{+}Z$ and $W^{-}Z$ production is also measured. The $W^{\pm}Z$ production cross section is measured as a function of several kinematic variables and compared with SM predictions at NNLO from the MATRIX calculation and at NLO from the POWHEG+PYTHIA and SHERPA MC event generators. The differential cross-section distributions are fairly well described by the theory predictions, with the exception of the jet multiplicity. The MATRIX calculations show the best agreement with the data.

Furthermore, an analysis of angular distributions of leptons from decays of W and Z bosons has been performed. Helicity fractions of pair-produced vector bosons are measured for the first time in hadronic collisions. Integrated over the fiducial region, the longitudinal polarisation fractions of the W and Z bosons in $W^{\pm}Z$ events are measured to be $f_0^W = 0.26 \pm 0.06$ and $f_0^Z = 0.24 \pm 0.04$, respectively, in agreement with the SM predictions at NLO in QCD and

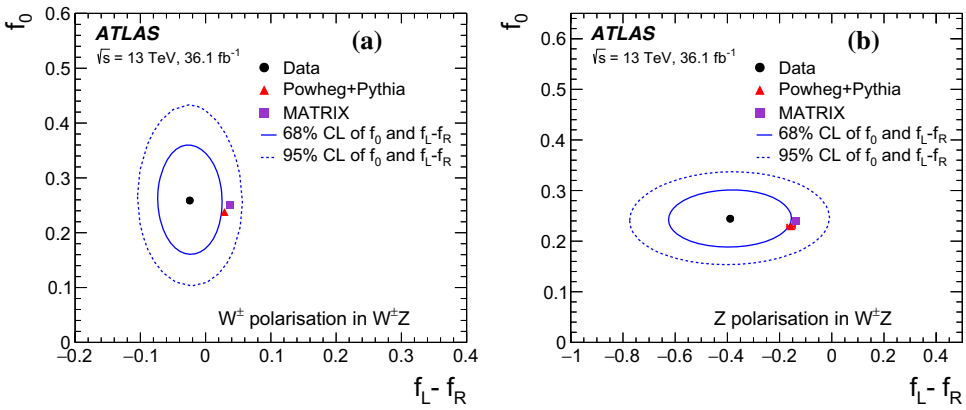

Fig. 10 Measured helicity fractions f_0 and $f_L - f_R$ for **a** the W and **b** Z bosons in $W^{\pm}Z$ events, compared with predictions at LO for the electroweak interaction and with $\sin^2\theta_W = 0.23152$ from POWHEG+PYTHIA (red triangle) and MATRIX (purple square). The effect of PDF and QCD scale uncertainties on the POWHEG+PYTHIA prediction and the effect of QCD scale uncertainties on the MATRIX prediction are of the same size as the triangle marker. The full and dashed ellipses around the data points correspond to one and two standard deviations, respectively

at LO for electroweak corrections, of 0.238 ± 0.003 and 0.230 ± 0.003, respectively. The differences of the left and right transverse polarisations are also measured. The measured values agree with the SM predictions within less than one and two standard deviations of their uncertainties for f_0 and $f_L - f_R$, respectively.

These polarisation measurements represent a step towards further new constraints on the electroweak symmetry breaking mechanism of the Standard Model, in particular by polarisation measurements in vector boson scattering.

Acknowledgements We thank CERN for the very successful operation of the LHC, as well as the support staff from our institutions without whom ATLAS could not be operated efficiently. We acknowledge the support of ANPCyT, Argentina; YerPhI, Armenia; ARC, Australia; BMWFW and FWF, Austria; ANAS, Azerbaijan; SSTC, Belarus; CNPq and FAPESP, Brazil; NSERC, NRC and CFI, Canada; CERN; CONICYT, Chile; CAS, MOST and NSFC, China; COLCIENCIAS, Colombia; MSMT CR, MPO CR and VSC CR, Czech Republic; DNRF and DNSRC, Denmark; IN2P3-CNRS, CEA-DRF/IRFU, France; SRNSFG, Georgia; BMBF, HGF, and MPG, Germany; GSRT, Greece; RGC, Hong Kong SAR, China; ISF and Benoziyo Center, Israel; INFN, Italy; MEXT and JSPS, Japan; CNRST, Morocco; NWO, Netherlands; RCN, Norway; MNiSW and NCN, Poland; FCT, Portugal; MNE/IFA, Romania; MES of Russia and NRC KI, Russian Federation; JINR; MESTD, Serbia; MSSR, Slovakia; ARRS and MIZŠ, Slovenia; DST/NRF, South Africa; MINECO, Spain; SRC and Wallenberg Foundation, Sweden; SERI, SNSF and Cantons of Bern and Geneva, Switzerland; MOST, Taiwan; TAEK, Turkey; STFC, UK; DOE and NSF, USA. In addition, individual groups and members have received support from BCKDF, CANARIE, CRC and Compute Canada, Canada; COST, ERC, ERDF, Horizon 2020, and Marie Skłodowska-Curie Actions, European Union; Investissements d' Avenir Labex and Idex, ANR, France; DFG and AvH Foundation, Germany; Herakleitos, Thales and Aristeia programmes co-financed by EU-ESF and the Greek NSRF, Greece; BSF-NSF and GIF, Israel; CERCA Programme Generalitat de Catalunya, Spain; The Royal Society and Leverhulme Trust, UK. The crucial computing support from all WLCG partners is acknowledged gratefully, in particular from CERN, the ATLAS Tier-1 facilities at TRIUMF (Canada), NDGF (Denmark, Norway, Sweden), CC-IN2P3 (France), KIT/GridKA (Germany), INFN-CNAF (Italy), NL-T1 (Netherlands), PIC (Spain), ASGC (Taiwan), RAL (UK) and BNL (USA), the Tier-2 facilities worldwide and large non-WLCG resource providers. Major contributors of computing resources are listed in Ref. [106].

Data Availability Statement This manuscript has no associated data or the data will not be deposited. [Authors' comment: All ATLAS scientific output is published in journals, and preliminary results are made available in Conference Notes. All are openly available, without restriction on use by external parties beyond copyright law and the standard conditions agreed by CERN. Data associated with journal publications are also made available: tables and data from plots (e.g. cross section values, likelihood profiles, selection efficiencies, cross section limits, ...) are stored in appropriate repositories such as HEPDATA (http://hepdata.cedar.ac.uk/). ATLAS also strives to make additional material related to the paper available that allows a reinterpretation of the data in the context of new theoretical models. For example, an extended encapsulation of the analysis is often provided for measurements in the framework of RIVET (http://rivet.hepforge.org/). This information is taken from the ATLAS Data Access Policy, which is a public document that can be downloaded from http://opendata.cern.ch/record/413[opendata.cern.ch].]

Funded by SCOAP[3].

References

1. A. Azatov, J. Elias-Miro, Y. Reyimuaji, E. Venturini, Novel measurements of anomalous triple gauge couplings for the LHC. JHEP **10**, 027 (2017). arXiv:1707.08060 [hep-ph]
2. G. Panico, F. Riva, A. Wulzer, Diboson interference resurrection. Phys. Lett. B **776**, 473 (2018). arXiv:1708.07823 [hep-ph]

3. J. Baglio, L.D. Ninh, Fiducial polarization observables in hadronic WZ production: a next-to-leading order QCD + EW study. JHEP **04**, 065 (2019). https://doi.org/10.1007/JHEP04(2019)065
4. G. Gounaris, D. Schildknecht, F.M. Renard, Genuine tests of CP invariance in e+ e− → W+ W−. Phys. Lett. B **263**, 291–297 (1991)
5. J. Kumar, A. Rajaraman, J.D. Wells, Probing CP-violation at colliders through interference effects in diboson production and decay. Phys. Rev. D **78**, 035014 (2008). arXiv:0801.2891 [hep-ph]
6. A. Ballestrero, E. Maina, G. Pelliccioli, W boson polarization in vector boson scattering at the LHC. JHEP **03**, 170 (2018). arXiv:1710.09339 [hep-ph]
7. CDF Collaboration, Measurement of the WZ cross section and triple gauge couplings in $p\bar{p}$ collisions at $\sqrt{s} = 1.96$ TeV. Phys. Rev. D **86**, 031104 (2012). arXiv:1202.6629 [hep-ph]
8. D0 Collaboration, Measurement of the WZ and ZZ production cross sections using leptonic final states in 8.6fb^{-1} of $p\bar{p}$ collisions. Phys. Rev. D **85**, 112005 (2012). arXiv:1201.5652 [hep-ph]
9. ATLAS Collaboration, Measurements of $W^{\pm}Z$ production cross sections in pp collisions at $\sqrt{s} = 8$ TeV with the ATLAS detector and limits on anomalous gauge boson self-couplings. Phys. Rev. D **93**, 092004 (2016). arXiv:1603.02151 [hep-ph]
10. ATLAS Collaboration, Measurement of the $W^{\pm}Z$ boson pair-production cross section in pp collisions at $\sqrt{s} = 13$ TeV with the ATLAS Detector. Phys. Lett. B **762**, 1 (2016). arXiv:1606.04017 [hep-ph]
11. CMS Collaboration, Measurements of the pp → WZ inclusive and differential production cross section and constraints on charged anomalous triple gauge couplings at $\sqrt{s} = 13$ TeV (2019). arXiv:1901.03428 [hep-ex]
12. ATLAS Collaboration, Measurement of $W^{\pm}Z$ production in proton–proton collisions at $\sqrt{s} = 7$ TeV with the ATLAS detector. Eur. Phys. J. C **72**, 2173 (2012). arXiv:1208.1390 [hep-ex]
13. CMS Collaboration, Measurement of the WZ production cross section in pp collisions at $\sqrt{s} = 7$ and 8 TeV and search for anomalous triple gauge couplings at $\sqrt{s} = 8$ TeV. Eur. Phys. J. C **77**, 236 (2017). arXiv:1609.05721 [hep-ex]
14. CDF and D0 Collaborations, Combination of CDF and D0 measurements of the W boson helicity in top quark decays. Phys. Rev. D **85**, 071106 (2012). arXiv:1202.5272 [hep-ex]
15. CDF Collaboration, Measurement of W-boson polarization in top-quark decay in $p\bar{p}$ Collisions at $\sqrt{s} = 1.96$ TeV. Phys. Rev. Lett. **105**, 042002 (2010). arXiv:1003.0224 [hep-ex]
16. D0 Collaboration, Measurement of the W boson helicity in top quark decays using 5.4 fb^{-1} of $p\bar{p}$ collision data. Phys. Rev. D **83**, 032009 (2011). arXiv:1011.6549 [hep-ex]
17. ATLAS Collaboration, Measurement of the W boson polarization in top quark decays with the ATLAS detector. JHEP **06**, 088 (2012). arXiv:1205.2484 [hep-ex]
18. CMS Collaboration, Measurement of the W boson helicity fractions in the decays of top quark pairs to lepton + jets final states produced in pp collisions at $\sqrt{s} = 8$ TeV. Phys. Lett. B **762**, 512 (2016). arXiv:1605.09047 [hep-ex]
19. ATLAS Collaboration, Measurement of the polarisation of W bosons produced with large transverse momentum in pp collisions at $\sqrt{s} = 7$ TeV with the ATLAS experiment. Eur. Phys. J. C **72**, 2001 (2012). arXiv:1203.2165 [hep-ex]
20. CMS Collaboration, Measurement of the polarization of W bosons with large transverse momenta in W+jets events at the LHC. Phys. Rev. Lett. **107**, 021802 (2011). arXiv:1104.3829 [hep-ex]
21. CDF Collaboration, First measurement of the angular coefficients of Drell–Yan e^+e^- pairs in the Z mass region from $p\bar{p}$ collisions at $\sqrt{s} = 1.96$ TeV. Phys. Rev. Lett. **106**, 241801 (2011). arXiv:1103.5699 [hep-ex]
22. CMS Collaboration, Angular coefficients of Z bosons produced in pp collisions at $\sqrt{s} = 8$ TeV and decaying to $\mu^+\mu^-$ as a function of transverse momentum and rapidity. Phys. Lett. B **750**, 154 (2015). arXiv:1504.03512 [hep-ex]
23. ATLAS Collaboration, Measurement of the angular coefficients in Z-boson events using electron and muon pairs from data taken at $\sqrt{s} = 8$ TeV with the ATLAS detector. JHEP **08**, 159 (2016). arXiv:1606.00689 [hep-ex]
24. H1 Collaboration, Events with isolated leptons and missing transverse momentum and measurement of W production at HERA. Eur. Phys. J. C **64**, 251 (2009). arXiv:0901.0488 [hep-ex]
25. L3 Collaboration, Measurement of W polarisation at LEP. Phys. Lett. B **557**, 147 (2003). arXiv:hep-ex/0301027 [hep-ex]
26. OPAL Collaboration, W boson polarization at LEP2. Phys. Lett. B **585**, 223 (2004). arXiv:hep-ex/0312047 [hep-ex]
27. DELPHI Collaboration, Study of W-boson polarisations and triple gauge boson couplings in the reaction e+e- → W+W- at LEP 2. Eur. Phys. J. C **54**, 345 (2008). arXiv:0801.1235 [hep-ex]
28. J. Ohnemus, Order-α_s calculation of hadronic $W^{\pm}Z$ production. Phys. Rev. D **44**, 3477 (1991)
29. S. Frixione, P. Nason, G. Ridolfi, Strong corrections to W Z production at hadron colliders. Nucl. Phys. B **383**, 3 (1992)
30. M. Grazzini, S. Kallweit, D. Rathlev, M. Wiesemann, $W^{\pm}Z$ production at hadron colliders in NNLO QCD. Phys. Lett. B **761**, 179–183 (2016). arXiv:1604.08576 [hep-ph]
31. M. Grazzini, S. Kallweit, D. Rathlev, M. Wiesemann, $W^{\pm}Z$ production at the LHC: fiducial cross sections and distributions in NNLO QCD. JHEP **05**, 139 (2017). arXiv:1703.09065 [hep-ph]
32. ATLAS Collaboration, The ATLAS experiment at the CERN large hadron collider. JINST **3**, S08003 (2008)
33. ATLAS Collaboration, ATLAS insertable B-layer technical design report. CERN-LHCC-2010-013. ATLAS-TDR-19, CERN (2010). http://cds.cern.ch/record/1291633
34. B. Abbott et al., Production and integration of the ATLAS insertable B-layer. JINST **13**, T05008 (2018). arXiv:1803.00844 [hep-ex]
35. ATLAS Collaboration, Performance of the ATLAS trigger system in 2015. Eur. Phys. J. C **77**, 317 (2017). arXiv:1611.09661 [hep-ex]
36. ATLAS Collaboration, Proposal for particle-level object and observable definitions or use in physics measurements at the LHC. Technical report. ATL-PHYS-PUB-2015-013, CERN (2015). http://cds.cern.ch/record/2022743
37. M. Tanabashi et al., Review of particle physics. Phys. Rev. D **98**, 030001 (2018)
38. M. Cacciari, G.P. Salam, G. Soyez, The anti-k_t jet clustering algorithm. JHEP **04**, 063 (2008). arXiv:0802.1189 [hep-ph]
39. P. Nason, A new method for combining NLO QCD with shower Monte Carlo algorithms. JHEP **11**, 040 (2004). arXiv:hep-ph/0409146
40. S. Frixione, P. Nason, C. Oleari, Matching NLO QCD computations with parton shower simulations: the POWHEG method. JHEP **11**, 070 (2007). arXiv:0709.2092 [hep-ph]
41. S. Alioli, P. Nason, C. Oleari, E. Re, A general framework for implementing NLO calculations in shower Monte Carlo programs: the POWHEG BOX. JHEP **06**, 043 (2010). arXiv:1002.2581 [hep-ph]
42. T. Melia, P. Nason, R. Röntsch, G. Zanderighi, W^+W^-, WZ and ZZ production in the POWHEG BOX. JHEP **11**, 078 (2011). arXiv:1107.5051 [hep-ph]
43. T. Sjöstrand, S. Ask, J.R. Christiansen, R. Corke, N. Desai, P. Ilten, S. Mrenna, S. Prestel, C.O. Rasmussen, P.Z. Skands, An introduction to PYTHIA 8.2. Comput. Phys. Commun. **191**, 159 (2015). arXiv:1410.3012 [hep-ph]
44. ATLAS Collaboration, Measurement of the Z/γ^* boson transverse momentum distribution in pp collisions at $\sqrt{s} = 7$ TeV with the ATLAS detector. JHEP **09**, 145 (2014). arXiv:1406.3660 [hep-ex]

45. H.-L. Lai, M. Guzzi, J. Huston, Z. Li, P.M. Nadolsky, J. Pumplin, C.P. Yuan, New parton distributions for collider physics. Phys. Rev. D **82**, 074024 (2010). arXiv:1007.2241 [hep-ex]
46. J. Pumplin, D.R. Stump, J. Huston, H.L. Lai, P.M. Nadolsky, W.K. Tung, New generation of parton distributions with uncertainties from global QCD analysis. JHEP **07**, 012 (2002). arXiv:hep-ph/0201195
47. M. Bähr et al., Herwig++ physics and manual. Eur. Phys. J. C **58**, 639 (2008). arXiv:0803.0883 [hep-ph]
48. T. Gleisberg, S. Hoeche, F. Krauss, M. Schonherr, S. Schumann, F. Siegert, J. Winter, Event generation with SHERPA 1.1. JHEP **02**, 007 (2009). arXiv:0811.4622 [hep-ph]
49. T. Gleisberg, S. Höche, Comix, a new matrix element generator. JHEP **12**, 039 (2008). arXiv:0808.3674 [hep-ph]
50. F. Cascioli, P. Maierhöfer, S. Pozzorini, Scattering amplitudes with open loops. Phys. Rev. Lett. **108**, 111601 (2012). arXiv:1111.5206 [hep-ph]
51. S. Schumann, F. Krauss, A parton shower algorithm based on Catani–Seymour dipole factorisation. JHEP **03**, 038 (2008). arXiv:0709.1027 [hep-ph]
52. S. Höche, F. Krauss, M. Schönherr, F. Siegert, QCD matrix elements + parton showers: the NLO case. JHEP **04**, 027 (2013). arXiv:1207.5030 [hep-ph]
53. NNPDF Collaboration, R.D. Ball et al., Parton distributions for the LHC run II. JHEP **04**, 040 (2015). arXiv:1410.8849 [hep-ph]
54. S. Frixione, B.R. Webber, Matching NLO QCD computations and parton shower simulations. JHEP **06**, 029 (2002). arXiv:hep-ph/0204244
55. M. Grazzini, S. Kallweit, M. Wiesemann, Fully differential NNLO computations with MATRIX. Eur. Phys. J. C **78**, 537 (2018). arXiv:1711.06631 [hep-ph]
56. A. Denner, S. Dittmaier, L. Hofer, Collier: a fortran-based complex one-loop library in extended regularizations. Comput. Phys. Commun. **212**, 220 (2017). arXiv:1604.06792 [hep-ph]
57. T. Gehrmann, A. von Manteuffel, L. Tancredi, The two-loop helicity amplitudes for $q\bar{q}' \to V_1V_2 \to 4$ leptons. JHEP **09**, 128 (2015). arXiv:1503.04812 [hep-ph]
58. S. Catani, L. Cieri, D. de Florian, G. Ferrera, M. Grazzini, Vector-boson production at hadron colliders: hard-collinear coefficients at the NNLO. Eur. Phys. J. C **72**, 2195 (2012). arXiv:1209.0158 [hep-ph]
59. S. Catani, M. Grazzini, Next-to-next-to-leading-order subtraction formalism in hadron collisions and its application to Higgs-boson production at the large hadron collider. Phys. Rev. Lett. **98**, 222002 (2007). arXiv:hep-ph/0703012
60. F. Caola, K. Melnikov, R. Röntsch, L. Tancredi, QCD corrections to ZZ production in gluon fusion at the LHC. Phys. Rev. D **92**(9), 094028 (2015). arXiv:1509.06734
61. J. Alwall, R. Frederix, S. Frixione, V. Hirschi, F. Maltoni, O. Mattelaer, H.S. Shao, T. Stelzer, P. Torrielli, M. Zaro, The automated computation of tree-level and next-to-leading order differential cross sections, and their matching to parton shower simulations. JHEP **07**, 079 (2014). arXiv:1405.0301 [hep-ph]
62. T. Sjöstrand, S. Mrenna, P. Skands, A brief introduction to PYTHIA 8.1. Comput. Phys. Commun. **178**, 852 (2008). arXiv:0710.3820 [hep-ph]
63. NNPDF Collaboration, R.D. Ball et al., Parton distributions with LHC data. Nucl. Phys. B **867**, 244 (2013). arXiv:1207.1303 [hep-ph]
64. T. Sjöstrand, S. Mrenna, P. Skands, PYTHIA 6.4 physics and manual. JHEP **0605**, 026 (2006). arXiv:hep-ph/0603175
65. ATLAS Collaboration, The ATLAS simulation infrastructure. Eur. Phys. J. C **70**, 823 (2010). arXiv:1005.4568
66. S. Agostinelli et al., GEANT4—a simulation toolkit. Nucl. Instrum. Methods A **506**, 250 (2003)
67. A.D. Martin, W.J. Stirling, R.S. Thorne, G. Watt, Parton distributions for the LHC. Eur. Phys. J. C **63**, 189 (2009). arXiv:0901.0002 [hep-ph]
68. ATLAS Collaboration, Summary of ATLAS Pythia 8 tunes. ATL-PHYS-PUB-2012-003, CERN, (2012). http://cds.cern.ch/record/1474107
69. ATLAS Collaboration, Electron efficiency measurements with the ATLAS detector using the 2015 LHC proton–proton collision data. Technical report. ATLAS-CONF-2016-024, CERN (2016). http://cds.cern.ch/record/2157687
70. ATLAS Collaboration, Muon reconstruction performance of the ATLAS detector in proton–proton collision data at $\sqrt{s} = 13$ TeV. Eur. Phys. J. C **76**, 292 (2016). arXiv:1603.05598 [hep-ex]
71. ATLAS Collaboration, Electron and photon energy calibration with the ATLAS detector using 2015–2016 LHC proton–proton collision data (2018). arXiv:1812.03848 [hep-ex]
72. ATLAS Collaboration, Topological cell clustering in the ATLAS calorimeters and its performance in LHC Run 1. Eur. Phys. J. C **77**, 490 (2017). arXiv:1603.02934 [hep-ex]
73. ATLAS Collaboration, Jet energy scale measurements and their systematic uncertainties in proton–proton collisions at $\sqrt{s} = 13$ TeV with the ATLAS detector. Phys. Rev. D **96**, 072002 (2017). arXiv:1703.09665 [hep-ex]
74. ATLAS Collaboration, Performance of pile-up mitigation techniques for jets in pp collisions at $\sqrt{s} = 8$ TeV using the ATLAS detector. Eur. Phys. J. C **76**, 581 (2016). arXiv:1510.03823 [hep-ex]
75. ATLAS Collaboration, Performance of b-jet identification in the ATLAS experiment. JINST **11**, P04008 (2016). arXiv:1512.01094 [hep-ex]
76. ATLAS Collaboration, Optimisation of the ATLAS b-tagging performance for the 2016 LHC Run. ATL-PHYS-PUB-2016-012 (2016). https://cds.cern.ch/record/2160731
77. ATLAS Collaboration, Performance of missing transverse momentum reconstruction with the ATLAS detector using proton–proton collisions at $\sqrt{s} = 13$ TeV. Eur. Phys. J. C **78**, 903 (2018). arXiv:1802.08168 [hep-ex]
78. ATLAS Collaboration, Measurement of the cross-section for producing a W boson in association with a single top quark in pp collisions at $\sqrt{s} = 13$ TeV with ATLAS. JHEP **01**, 063 (2018). arXiv:1612.07231 [hep-ex]
79. ATLAS Collaboration, Search for supersymmetry at $\sqrt{s} = 8$ TeV in final states with jets and two same-sign leptons or three leptons with the ATLAS detector. JHEP **06**, 035 (2014). arXiv:1404.2500 [hep-ex]
80. ATLAS Collaboration, $ZZ \to \ell^+\ell^-\ell'^+\ell'^-$ cross-section measurements and search for anomalous triple gauge couplings in 13 TeV pp collisions with the ATLAS detector. Phys. Rev. D **97**(3), 032005 (2018). arXiv:1709.07703 [hep-ex]
81. ATLAS Collaboration, Measurement of the $t\bar{t}Z$ and $t\bar{t}W$ production cross sections in multilepton final states using 3.2fb^{-1} of pp collisions at $\sqrt{s} = 13$ TeV with the ATLAS detector. Eur. Phys. J. C **77**, 40 (2017). arXiv:1609.01599 [hep-ex]
82. G. D'Agostini, A multidimensional unfolding method based on Bayes' theorem. Nucl. Instrum. Methods A **362**, 487 (1995)
83. T. Adye, Unfolding algorithms and tests using RooUnfold, in *Proceedings of the PHYSTAT 2011 Workshop, CERN, Geneva, Switzerland* (2011), p. 313. arXiv:1105.1160
84. S. Dulat, T.-J. Hou, J. Gao, M. Guzzi, J. Huston, P. Nadolsky, J. Pumplin, C. Schmidt, D. Stump, C.P. Yuan, New parton distribution functions from a global analysis of quantum chromodynamics. Phys. Rev. D **93**, 033006 (2016). arXiv:1506.07443 [hep-ph]
85. L.A. Harland-Lang, A.D. Martin, P. Motylinski, R.S. Thorne, Parton distributions in the LHC era: MMHT 2014 PDFs. Eur. Phys. J. C **75**, 204 (2015). arXiv:1412.3989 [hep-ex]

90. ATLAS Collaboration, Luminosity determination in pp collisions at $\sqrt{s} = 8$ TeV using the ATLAS detector at the LHC. Eur. Phys. J. C **76**, 653 (2016). arXiv:1608.03953 [hep-ex]
91. G. Avoni et al., The new LUCID-2 detector for luminosity measurement and monitoring in ATLAS. JINST **13**, P07017 (2018)
92. A. Glazov, Averaging of DIS cross section data. AIP Conf. Proc. **792**, 237 (2005)
93. H1 Collaboration, Measurement of the inclusive *ep* scattering cross section at low Q^2 and x at HERA. Eur. Phys. J. C **63**, 625 (2009). arXiv:0904.0929 [hep-ex]
94. H1 and ZEUS Collaborations, Combined measurement and QCD analysis of the inclusive $e^{\pm}p$ scattering cross sections at HERA. JHEP **01**, 109 (2010). arXiv:0911.0884 [hep-ex]
95. F. Campanario, S. Sapeta, WZ production beyond NLO for high-p_T observables. Phys. Lett. B **718**, 100 (2012). arXiv:1209.4595 [hep-ph]
96. B. Biedermann, A. Denner, L. Hofer, Next-to-leading-order electroweak corrections to the production of three charged leptons plus missing energy at the LHC. JHEP **10**, 043 (2017). arXiv:1708.06938 [hep-ph]
97. E. Mirkes, J. Ohnemus, W and Z polarization effects in hadronic collisions. Phys. Rev. D **50**, 5692 (1994). arXiv:hep-ph/9406381
98. S. Groote, J.G. Korner, P. Tuvike, $O(\alpha_s)$ corrections to the decays of polarized $W^{\pm}$ and Z bosons into massive quark pairs. Eur. Phys. J. C **72**, 2177 (2012). arXiv:1204.5295 [hep-ph]
99. W.J. Stirling, E. Vryonidou, Electroweak gauge boson polarisation at the LHC. JHEP **07**, 124 (2012). arXiv:1204.6427 [hep-ph]
100. G. Gounaris, J. Layssac, G. Moultaka, F.M. Renard, Analytic expressions of cross-sections, asymmetries and W density matrices for e+ e− → W+ W− with general three boson couplings. Int. J. Mod. Phys. A **8**, 3285 (1993)
101. G. Cowan, K. Cranmer, E. Gross, O. Vitells, Asymptotic formulae for likelihood-based tests of new physics. Eur. Phys. J. C **71**, 1554 (2011). arXiv: 1007.1727 [physics.data-an] [Erratum: Eur. Phys. J. C **73**, 2501 (2013)]
102. J.C. Collins, D.E. Soper, Angular distribution of dileptons in high-energy hadron collisions. Phys. Rev. D **6**, 2219 (1977)
103. J.M. Campbell, R.K. Ellis, Update on vector boson pair production at hadron colliders. Phys. Rev. D **60**, 113006 (1999). arXiv:hep-ph/9905386
104. J.M. Campbell, R.K. Ellis, C. Williams, Vector boson pair production at the LHC. JHEP **07**, 018 (2011). arXiv:1105.0020 [hep-ph]
105. J.M. Campbell, R.K. Ellis, W.T. Giele, A multi-threaded version of MCFM. Eur. Phys. J. C **75**, 246 (2015). arXiv:1503.06182 [physics.comp-ph]
106. ATLAS Collaboration, ATLAS computing acknowledgements. ATL-GEN-PUB-2016-002. https://cds.cern.ch/record/2202407

ATLAS Collaboration

M. Aaboud[35d], G. Aad[100], B. Abbott[127], O. Abdinov[13,*], B. Abeloos[131], D. K. Abhayasinghe[92], S. H. Abidi[166], O. S. AbouZeid[40], N. L. Abraham[155], H. Abramowicz[160], H. Abreu[159], Y. Abulaiti[6], B. S. Acharya[65a,65b,n], S. Adachi[162], L. Adam[98], C. Adam Bourdarios[131], L. Adamczyk[82a], J. Adelman[120], M. Adersberger[113], A. Adiguzel[12c], T. Adye[143], A. A. Affolder[145], Y. Afik[159], C. Agheorghiesei[27c], J. A. Aguilar-Saavedra[139a,139f], F. Ahmadov[78,ac], G. Aielli[72a,72b], S. Akatsuka[84], T. P. A. Åkesson[95], E. Akilli[53], A. V. Akimov[109], G. L. Alberghi[23a,23b], J. Albert[175], P. Albicocco[50], M. J. Alconada Verzini[87], S. Alderweireldt[118], M. Aleksa[36], I. N. Aleksandrov[78], C. Alexa[27b], T. Alexopoulos[10], M. Alhroob[127], B. Ali[141], G. Alimonti[67a], J. Alison[37], S. P. Alkire[147], C. Allaire[131], B. M. M. Allbrooke[155], B. W. Allen[130], P. P. Allport[21], A. Aloisio[68a,68b], A. Alonso[40], F. Alonso[87], C. Alpigiani[147], A. A. Alshehri[56], M. I. Alstaty[100], B. Alvarez Gonzalez[36], D. Álvarez Piqueras[173], M. G. Alviggi[68a,68b], B. T. Amadio[18], Y. Amaral Coutinho[79b], A. Ambler[102], L. Ambroz[134], C. Amelung[26], D. Amidei[104], S. P. Amor Dos Santos[139a,139c], S. Amoroso[45], C. S. Amrouche[53], C. Anastopoulos[148], L. S. Ancu[53], N. Andari[144], T. Andeen[11], C. F. Anders[60b], J. K. Anders[20], K. J. Anderson[37], A. Andreazza[67a,67b], V. Andrei[60a], C. R. Anelli[175], S. Angelidakis[38], I. Angelozzi[119], A. Angerami[39], A. V. Anisenkov[121a,121b], A. Annovi[70a], C. Antel[60a], M. T. Anthony[148], M. Antonelli[50], D. J. A. Antrim[170], F. Anulli[71a], M. Aoki[80], J. A. Aparisi Pozo[173], L. Aperio Bella[36], G. Arabidze[105], J. P. Araque[139a], V. Araujo Ferraz[79b], R. Araujo Pereira[79b], A. T. H. Arce[48], R. E. Ardell[92], F. A. Arduh[87], J-F. Arguin[108], S. Argyropoulos[76], A. J. Armbruster[36], L. J. Armitage[91], A. Armstrong[170], O. Arnaez[166], H. Arnold[119], M. Arratia[32], O. Arslan[24], A. Artamonov[110,*], G. Artoni[134], S. Artz[98], S. Asai[162], N. Asbah[58], E. M. Asimakopoulou[171], L. Asquith[155], K. Assamagan[29], R. Astalos[28a], R. J. Atkin[33a], M. Atkinson[172], N. B. Atlay[150], K. Augsten[141], G. Avolio[36], R. Avramidou[59a], M. K. Ayoub[15a], A. M. Azoulay[167b], G. Azuelos[108,aq], A. E. Baas[60a], M. J. Baca[21], H. Bachacou[144], K. Bachas[66a,66b], M. Backes[134], P. Bagnaia[71a,71b], M. Bahmani[83], H. Bahrasemani[151], A. J. Bailey[173], J. T. Baines[143], M. Bajic[40], C. Bakalis[10], O. K. Baker[182], P. J. Bakker[119], D. Bakshi Gupta[8], S. Balaji[156], E. M. Baldin[121a,121b], P. Balek[179], F. Balli[144], W. K. Balunas[136], J. Balz[98], E. Banas[83], A. Bandyopadhyay[24], Sw. Banerjee[180,i], A. A. E. Bannoura[181], L. Barak[160], W. M. Barbe[38], E. L. Barberio[103], D. Barberis[54a,54b], M. Barbero[100], T. Barillari[114], M-S. Barisits[36], J. Barkeloo[130], T. Barklow[152], R. Barnea[159], S. L. Barnes[59c], B. M. Barnett[143], R. M. Barnett[18], Z. Barnovska-Blenessy[59a], A. Baroncelli[73a], G. Barone[29], A. J. Barr[134], L. Barranco Navarro[173], F. Barreiro[97], J. Barreiro Guimarães da Costa[15a], R. Bartoldus[152], A. E. Barton[88], P. Bartos[28a], A. Basalaev[137], A. Bassalat[131,ak], R. L. Bates[56], S. J. Batista[166], S. Batlamous[35e], J. R. Batley[32], M. Battaglia[145], M. Bauce[71a,71b], F. Bauer[144], K. T. Bauer[170], H. S. Bawa[31,l], J. B. Beacham[125], T. Beau[135], P. H. Beauchemin[169], P. Bechtle[24], H. C. Beck[52], H. P. Beck[20,p], K. Becker[51], M. Becker[98], C. Becot[45], A. Beddall[12d],

A. J. Beddall[12a], V. A. Bednyakov[78], M. Bedognetti[119], C. P. Bee[154], T. A. Beermann[75], M. Begalli[79b], M. Begel[29], A. Behera[154], J. K. Behr[45], A. S. Bell[93], G. Bella[160], L. Bellagamba[23b], A. Bellerive[34], M. Bellomo[159], P. Bellos[9], K. Belotskiy[111], N. L. Belyaev[111], O. Benary[160,*], D. Benchekroun[35a], M. Bender[113], N. Benekos[10], Y. Benhammou[160], E. Benhar Noccioli[182], J. Benitez[76], D. P. Benjamin[48], M. Benoit[53], J. R. Bensinger[26], S. Bentvelsen[119], L. Beresford[134], M. Beretta[50], D. Berge[45], E. Bergeaas Kuutmann[171], N. Berger[5], B. Bergmann[141], L. J. Bergsten[26], J. Beringer[18], S. Berlendis[7], N. R. Bernard[101], G. Bernardi[135], C. Bernius[152], F. U. Bernlochner[24], T. Berry[92], P. Berta[98], C. Bertella[15a], G. Bertoli[44a,44b], I. A. Bertram[88], G. J. Besjes[40], O. Bessidskaia Bylund[181], M. Bessner[45], N. Besson[144], A. Bethani[99], S. Bethke[114], A. Betti[24], A. J. Bevan[91], J. Beyer[114], R. Bi[138], R. M. Bianchi[138], O. Biebel[113], D. Biedermann[19], R. Bielski[36], K. Bierwagen[98], N. V. Biesuz[70a,70b], M. Biglietti[73a], T. R. V. Billoud[108], M. Bindi[52], A. Bingul[12d], C. Bini[71a,71b], S. Biondi[23a,23b], M. Birman[179], T. Bisanz[52], J. P. Biswal[160], C. Bittrich[47], D. M. Bjergaard[48], J. E. Black[152], K. M. Black[25], T. Blazek[28a], I. Bloch[45], C. Blocker[26], A. Blue[56], U. Blumenschein[91], S. Blunier[146a], G. J. Bobbink[119], V. S. Bobrovnikov[121a,121b], S. S. Bocchetta[95], A. Bocci[48], D. Boerner[181], D. Bogavac[113], A. G. Bogdanchikov[121a,121b], C. Bohm[44a], V. Boisvert[92], P. Bokan[52,171], T. Bold[82a], A. S. Boldyrev[112], A. E. Bolz[60b], M. Bomben[135], M. Bona[91], J. S. Bonilla[130], M. Boonekamp[144], A. Borisov[122], G. Borissov[88], J. Bortfeldt[36], D. Bortoletto[134], V. Bortolotto[72a,72b], D. Boscherini[23b], M. Bosman[14], J. D. Bossio Sola[30], K. Bouaouda[35a], J. Boudreau[138], E. V. Bouhova-Thacker[88], D. Boumediene[38], S. K. Boutle[56], A. Boveia[125], J. Boyd[36], D. Boye[33b], I. R. Boyko[78], A. J. Bozson[92], J. Bracinik[21], N. Brahimi[100], A. Brandt[8], G. Brandt[181], O. Brandt[60a], F. Braren[45], U. Bratzler[163], B. Brau[101], J. E. Brau[130], W. D. Breaden Madden[56], K. Brendlinger[45], L. Brenner[45], R. Brenner[171], S. Bressler[179], B. Brickwedde[98], D. L. Briglin[21], D. Britton[56], D. Britzger[114], I. Brock[24], R. Brock[105], G. Brooijmans[39], T. Brooks[92], W. K. Brooks[146b], E. Brost[120], J. H. Broughton[21], P. A. Bruckman de Renstrom[83], D. Bruncko[28b], A. Bruni[23b], G. Bruni[23b], L. S. Bruni[119], S. Bruno[72a,72b], B. H. Brunt[32], M. Bruschi[23b], N. Bruscino[138], P. Bryant[37], L. Bryngemark[45], T. Buanes[17], Q. Buat[36], P. Buchholz[150], A. G. Buckley[56], I. A. Budagov[78], M. K. Bugge[133], F. Bührer[51], O. Bulekov[111], D. Bullock[8], T. J. Burch[120], S. Burdin[89], C. D. Burgard[119], A. M. Burger[5], B. Burghgrave[120], K. Burka[83], S. Burke[143], I. Burmeister[46], J. T. P. Burr[134], V. Büscher[98], E. Buschmann[52], P. J. Bussey[56], J. M. Butler[25], C. M. Buttar[56], J. M. Butterworth[93], P. Butti[36], W. Buttinger[36], A. Buzatu[157], A. R. Buzykaev[121a,121b], G. Cabras[23a,23b], S. Cabrera Urbán[173], D. Caforio[141], H. Cai[172], V. M. M. Cairo[2], O. Cakir[4a], N. Calace[53], P. Calafiura[18], A. Calandri[100], G. Calderini[135], P. Calfayan[64], G. Callea[41a,41b], L. P. Caloba[79b], S. Calvente Lopez[97], D. Calvet[38], S. Calvet[38], T. P. Calvet[154], M. Calvetti[70a,70b], R. Camacho Toro[135], S. Camarda[36], D. Camarero Munoz[97], P. Camarri[72a,72b], D. Cameron[133], R. Caminal Armadans[101], C. Camincher[36], S. Campana[36], M. Campanelli[93], A. Camplani[40], A. Campoverde[150], V. Canale[68a,68b], M. Cano Bret[59c], J. Cantero[128], T. Cao[160], Y. Cao[172], M. D. M. Capeans Garrido[36], I. Caprini[27b], M. Caprini[27b], M. Capua[41a,41b], R. M. Carbone[39], R. Cardarelli[72a], F. C. Cardillo[148], I. Carli[142], T. Carli[36], G. Carlino[68a], B. T. Carlson[138], L. Carminati[67a,67b], R. M. D. Carney[44a,44b], S. Caron[118], E. Carquin[146b], S. Carrá[67a,67b], G. D. Carrillo-Montoya[36], D. Casadei[33b], M. P. Casado[14,f], A. F. Casha[166], D. W. Casper[170], R. Castelijn[119], F. L. Castillo[173], V. Castillo Gimenez[173], N. F. Castro[139a,139e], A. Catinaccio[36], J. R. Catmore[133], A. Cattai[36], J. Caudron[24], V. Cavaliere[29], E. Cavallaro[14], D. Cavalli[67a], M. Cavalli-Sforza[14], V. Cavasinni[70a,70b], E. Celebi[12b], F. Ceradini[73a,73b], L. Cerda Alberich[173], A. S. Cerqueira[79a], A. Cerri[155], L. Cerrito[72a,72b], F. Cerutti[18], A. Cervelli[23a,23b], S. A. Cetin[12b], A. Chafaq[35a], D. Chakraborty[120], S. K. Chan[58], W. S. Chan[119], Y. L. Chan[62a], J. D. Chapman[32], B. Chargeishvili[158b], D. G. Charlton[21], C. C. Chau[34], C. A. Chavez Barajas[155], S. Che[125], A. Chegwidden[105], S. Chekanov[6], S. V. Chekulaev[167a], G. A. Chelkov[78,ap], M. A. Chelstowska[36], C. Chen[59a], C. H. Chen[77], H. Chen[29], J. Chen[59a], J. Chen[39], S. Chen[136], S. J. Chen[15c], X. Chen[15b,ao], Y. Chen[81], Y-H. Chen[45], H. C. Cheng[104], H. J. Cheng[15a,15d], A. Cheplakov[78], E. Cheremushkina[122], R. Cherkaoui El Moursli[35e], E. Cheu[7], K. Cheung[63], L. Chevalier[144], V. Chiarella[50], G. Chiarelli[70a], G. Chiodini[66a], A. S. Chisholm[36,21], A. Chitan[27b], I. Chiu[162], Y. H. Chiu[175], M. V. Chizhov[78], K. Choi[64], A. R. Chomont[131], S. Chouridou[161], Y. S. Chow[119], V. Christodoulou[93], M. C. Chu[62a], J. Chudoba[140], A. J. Chuinard[102], J. J. Chwastowski[83], L. Chytka[129], D. Cinca[46], V. Cindro[90], I. A. Cioară[24], A. Ciocio[18], F. Cirotto[68a,68b], Z. H. Citron[179], M. Citterio[67a], A. Clark[53], M. R. Clark[39], P. J. Clark[49], C. Clement[44a,44b], Y. Coadou[100], M. Cobal[65a,65c], A. Coccaro[54b], J. Cochran[77], H. Cohen[160], A. E. C. Coimbra[179], L. Colasurdo[118], B. Cole[39], A. P. Colijn[119], J. Collot[57], P. Conde Muiño[139a], E. Coniavitis[51], S. H. Connell[33b], I. A. Connelly[99], S. Constantinescu[27b], F. Conventi[68a,as], A. M. Cooper-Sarkar[134], F. Cormier[174], K. J. R. Cormier[166], L. D. Corpe[93], M. Corradi[71a,71b], E. E. Corrigan[95], F. Corriveau[102,aa], A. Cortes-Gonzalez[36], M. J. Costa[173], F. Costanza[5], D. Costanzo[148], G. Cottin[32], G. Cowan[92], B. E. Cox[99], J. Crane[99], K. Cranmer[123], S. J. Crawley[56], R. A. Creager[136], G. Cree[34], S. Crépé-Renaudin[57], F. Crescioli[135], M. Cristinziani[24], V. Croft[123], G. Crosetti[41a,41b], A. Cueto[97], T. Cuhadar Donszelmann[148], A. R. Cukierman[152], S. Czekierda[83], P. Czodrowski[36], M. J. Da Cunha Sargedas De Sousa[59b], C. Da Via[99], W. Dabrowski[82a], T. Dado[28a,w], S. Dahbi[35e], T. Dai[104], F. Dallaire[108], C. Dallapiccola[101], M. Dam[40], G. D'amen[23a,23b], J. Damp[98], J. R. Dandoy[136], M. F. Daneri[30], N. P. Dang[180], N. D. Dann[99], M. Danninger[174],

V. Dao[36], G. Darbo[54b], S. Darmora[8], O. Dartsi[5], A. Dattagupta[130], T. Daubney[45], S. D'Auria[67a,67b], W. Davey[24], C. David[45], T. Davidek[142], D. R. Davis[48], E. Dawe[103], I. Dawson[148], K. De[8], R. De Asmundis[68a], A. De Benedetti[127], M. De Beurs[119], S. De Castro[23a,23b], S. De Cecco[71a,71b], N. De Groot[118], P. de Jong[119], H. De la Torre[105], F. De Lorenzi[77], A. De Maria[70a,70b], D. De Pedis[71a], A. De Salvo[71a], U. De Sanctis[72a,72b], M. De Santis[72a,72b], A. De Santo[155], K. De Vasconcelos Corga[100], J. B. De Vivie De Regie[131], C. Debenedetti[145], D. V. Dedovich[78], N. Dehghanian[3], A. M. Deiana[104], M. Del Gaudio[41a,41b], J. Del Peso[97], Y. Delabat Diaz[45], D. Delgove[131], F. Deliot[144], C. M. Delitzsch[7], M. Della Pietra[68a,68b], D. Della Volpe[53], A. Dell'Acqua[36], L. Dell'Asta[25], M. Delmastro[5], C. Delporte[131], P. A. Delsart[57], D. A. DeMarco[166], S. Demers[182], M. Demichev[78], S. P. Denisov[122], D. Denysiuk[119], L. D'Eramo[135], D. Derendarz[83], J. E. Derkaoui[35d], F. Derue[135], P. Dervan[89], K. Desch[24], C. Deterre[45], K. Dette[166], M. R. Devesa[30], P. O. Deviveiros[36], A. Dewhurst[143], S. Dhaliwal[26], F. A. Di Bello[53], A. Di Ciaccio[72a,72b], L. Di Ciaccio[5], W. K. Di Clemente[136], C. Di Donato[68a,68b], A. Di Girolamo[36], G. Di Gregorio[70a,70b], B. Di Micco[73a,73b], R. Di Nardo[101], K. F. Di Petrillo[58], R. Di Sipio[166], D. Di Valentino[34], C. Diaconu[100], M. Diamond[166], F. A. Dias[40], T. Dias Do Vale[139a], M. A. Diaz[146a], J. Dickinson[18], E. B. Diehl[104], J. Dietrich[19], S. Díez Cornell[45], A. Dimitrievska[18], J. Dingfelder[24], F. Dittus[36], F. Djama[100], T. Djobava[158b], J. I. Djuvsland[60a], M. A. B. Do Vale[79c], M. Dobre[27b], D. Dodsworth[26], C. Doglioni[95], J. Dolejsi[142], Z. Dolezal[142], M. Donadelli[79d], J. Donini[38], A. D'onofrio[91], M. D'Onofrio[89], J. Dopke[143], A. Doria[68a], M. T. Dova[87], A. T. Doyle[56], E. Drechsler[52], E. Dreyer[151], T. Dreyer[52], Y. Du[59b], F. Dubinin[109], M. Dubovsky[28a], A. Dubreuil[53], E. Duchovni[179], G. Duckeck[113], A. Ducourthial[135], O. A. Ducu[108,v], D. Duda[114], A. Dudarev[36], A. C. Dudder[98], E. M. Duffield[18], L. Duflot[131], M. Dührssen[36], C. Dülsen[181], M. Dumancic[179], A. E. Dumitriu[27b,d], A. K. Duncan[56], M. Dunford[60a], A. Duperrin[100], H. Duran Yildiz[4a], M. Düren[55], A. Durglishvili[158b], D. Duschinger[47], B. Dutta[45], D. Duvnjak[1], M. Dyndal[45], S. Dysch[99], B. S. Dziedzic[83], C. Eckardt[45], K. M. Ecker[114], R. C. Edgar[104], T. Eifert[36], G. Eigen[17], K. Einsweiler[18], T. Ekelof[171], M. El Kacimi[35c], R. El Kosseifi[100], V. Ellajosyula[100], M. Ellert[171], F. Ellinghaus[181], A. A. Elliot[91], N. Ellis[36], J. Elmsheuser[29], M. Elsing[36], D. Emeliyanov[143], A. Emerman[39], Y. Enari[162], J. S. Ennis[177], M. B. Epland[48], J. Erdmann[46], A. Ereditato[20], S. Errede[172], M. Escalier[131], C. Escobar[173], O. Estrada Pastor[173], A. I. Etienvre[144], E. Etzion[160], H. Evans[64], A. Ezhilov[137], M. Ezzi[35e], F. Fabbri[56], L. Fabbri[23a,23b], V. Fabiani[118], G. Facini[93], R. M. Faisca Rodrigues Pereira[139a], R. M. Fakhrutdinov[122], S. Falciano[71a], P. J. Falke[5], S. Falke[5], J. Faltova[142], Y. Fang[15a], M. Fanti[67a,67b], A. Farbin[8], A. Farilla[73a], E. M. Farina[69a,69b], T. Farooque[105], S. Farrell[18], S. M. Farrington[177], P. Farthouat[36], F. Fassi[35e], P. Fassnacht[36], D. Fassouliotis[9], M. Faucci Giannelli[49], A. Favareto[54a,54b], W. J. Fawcett[32], L. Fayard[131], O. L. Fedin[137,o], W. Fedorko[174], M. Feickert[42], S. Feigl[133], L. Feligioni[100], C. Feng[59b], E. J. Feng[36], M. Feng[48], M. J. Fenton[56], A. B. Fenyuk[122], L. Feremenga[8], J. Ferrando[45], A. Ferrari[171], P. Ferrari[119], R. Ferrari[69a], D. E. Ferreira de Lima[60b], A. Ferrer[173], D. Ferrere[53], C. Ferretti[104], F. Fiedler[98], A. Filipčič[90], F. Filthaut[118], K. D. Finelli[25], M. C. N. Fiolhais[139a,139c,a], L. Fiorini[173], C. Fischer[14], W. C. Fisher[105], N. Flaschel[45], I. Fleck[150], P. Fleischmann[104], R. R. M. Fletcher[136], T. Flick[181], B. M. Flierl[113], L. F. Flores[136], L. R. Flores Castillo[62a], F. M. Follega[74a,74b], N. Fomin[17], G. T. Forcolin[74a,74b], A. Formica[144], F. A. Förster[14], A. C. Forti[99], A. G. Foster[21], D. Fournier[131], H. Fox[88], S. Fracchia[148], P. Francavilla[70a,70b], M. Franchini[23a,23b], S. Franchino[60a], D. Francis[36], L. Franconi[145], M. Franklin[58], M. Frate[170], M. Fraternali[69a,69b], A. N. Fray[91], D. Freeborn[93], S. M. Fressard-Batraneanu[36], B. Freund[108], W. S. Freund[79b], E. M. Freundlich[46], D. C. Frizzell[127], D. Froidevaux[36], J. A. Frost[134], C. Fukunaga[163], E. Fullana Torregrosa[173], T. Fusayasu[115], J. Fuster[173], O. Gabizon[159], A. Gabrielli[23a,23b], A. Gabrielli[18], G. P. Gach[82a], S. Gadatsch[53], P. Gadow[114], G. Gagliardi[54a,54b], L. G. Gagnon[108], C. Galea[27b], B. Galhardo[139a,139c], E. J. Gallas[134], B. J. Gallop[143], P. Gallus[141], G. Galster[40], R. Gamboa Goni[91], K. K. Gan[125], S. Ganguly[179], J. Gao[59a], Y. Gao[89], Y. S. Gao[31,l], C. García[173], J. E. García Navarro[173], J. A. García Pascual[15a], M. Garcia-Sciveres[18], R. W. Gardner[37], N. Garelli[152], V. Garonne[133], K. Gasnikova[45], A. Gaudiello[54a,54b], G. Gaudio[69a], I. L. Gavrilenko[109], A. Gavrilyuk[110], C. Gay[174], G. Gaycken[24], E. N. Gazis[10], C. N. P. Gee[143], J. Geisen[52], M. Geisen[98], M. P. Geisler[60a], K. Gellerstedt[44a,44b], C. Gemme[54b], M. H. Genest[57], C. Geng[104], S. Gentile[71a,71b], S. George[92], D. Gerbaudo[14], G. Gessner[46], S. Ghasemi[150], M. Ghasemi Bostanabad[175], M. Ghneimat[24], B. Giacobbe[23b], S. Giagu[71a,71b], N. Giangiacomi[23a,23b], P. Giannetti[70a], A. Giannini[68a,68b], S. M. Gibson[92], M. Gignac[145], D. Gillberg[34], G. Gilles[181], D. M. Gingrich[3,aq], M. P. Giordani[65a,65c], F. M. Giorgi[23b], P. F. Giraud[144], P. Giromini[58], G. Giugliarelli[65a,65c], D. Giugni[67a], F. Giuli[134], M. Giulini[60b], S. Gkaitatzis[161], I. Gkialas[9,h], E. L. Gkougkousis[14], P. Gkountoumis[10], L. K. Gladilin[112], C. Glasman[97], J. Glatzer[14], P. C. F. Glaysher[45], A. Glazov[45], M. Goblirsch-Kolb[26], J. Godlewski[83], S. Goldfarb[103], T. Golling[53], D. Golubkov[122], A. Gomes[139a,139b], R. Goncalves Gama[79a], R. Gonçalo[139a], G. Gonella[51], L. Gonella[21], A. Gongadze[78], F. Gonnella[21], J. L. Gonski[58], S. González de la Hoz[173], S. Gonzalez-Sevilla[53], L. Goossens[36], P. A. Gorbounov[110], H. A. Gordon[29], B. Gorini[36], E. Gorini[66a,66b], A. Gorišek[90], A. T. Goshaw[48], C. Gössling[46], M. I. Gostkin[78], C. A. Gottardo[24], C. R. Goudet[131], D. Goujdami[35c], A. G. Goussiou[147], N. Govender[33b,b], C. Goy[5], E. Gozani[159], I. Grabowska-Bold[82a], P. O. J. Gradin[171], E. C. Graham[89], J. Gramling[170], E. Gramstad[133], S. Grancagnolo[19], V. Gratchev[137], P. M. Gravila[27f],

F. G. Gravili[66a,66b], C. Gray[56], H. M. Gray[18], Z. D. Greenwood[94], C. Grefe[24], K. Gregersen[95], I. M. Gregor[45], P. Grenier[152], K. Grevtsov[45], N. A. Grieser[127], J. Griffiths[8], A. A. Grillo[145], K. Grimm[31,k], S. Grinstein[14,x], Ph. Gris[38], J.-F. Grivaz[131], S. Groh[98], E. Gross[179], J. Grosse-Knetter[52], G. C. Grossi[94], Z. J. Grout[93], C. Grud[104], A. Grummer[117], L. Guan[104], W. Guan[180], J. Guenther[36], A. Guerguichon[131], F. Guescini[167a], D. Guest[170], R. Gugel[51], B. Gui[125], T. Guillemin[5], S. Guindon[36], U. Gul[56], C. Gumpert[36], J. Guo[59c], W. Guo[104], Y. Guo[59a,q], Z. Guo[100], R. Gupta[45], S. Gurbuz[12c], G. Gustavino[127], B. J. Gutelman[159], P. Gutierrez[127], C. Gutschow[93], C. Guyot[144], M. P. Guzik[82a], C. Gwenlan[134], C. B. Gwilliam[89], A. Haas[123], C. Haber[18], H. K. Hadavand[8], N. Haddad[35e], A. Hadef[59a], S. Hageböck[24], M. Hagihara[168], H. Hakobyan[183,*], M. Haleem[176], J. Haley[128], G. Halladjian[105], G. D. Hallewell[100], K. Hamacher[181], P. Hamal[129], K. Hamano[175], A. Hamilton[33a], G. N. Hamity[148], K. Han[59a,ae], L. Han[59a], S. Han[15a,15d], K. Hanagaki[80,t], M. Hance[145], D. M. Handl[113], B. Haney[136], R. Hankache[135], P. Hanke[60a], E. Hansen[95], J. B. Hansen[40], J. D. Hansen[40], M. C. Hansen[24], P. H. Hansen[40], E. C. Hanson[99], K. Hara[168], A. S. Hard[180], T. Harenberg[181], S. Harkusha[106], P. F. Harrison[177], N. M. Hartmann[113], Y. Hasegawa[149], A. Hasib[49], S. Hassani[144], S. Haug[20], R. Hauser[105], L. Hauswald[47], L. B. Havener[39], M. Havranek[141], C. M. Hawkes[21], R. J. Hawkings[36], D. Hayden[105], C. Hayes[154], C. P. Hays[134], J. M. Hays[91], H. S. Hayward[89], S. J. Haywood[143], M. P. Heath[49], V. Hedberg[95], L. Heelan[8], S. Heer[24], K. K. Heidegger[51], J. Heilman[34], S. Heim[45], T. Heim[18], B. Heinemann[45,al], J. J. Heinrich[113], L. Heinrich[123], C. Heinz[55], J. Hejbal[140], L. Helary[36], A. Held[174], S. Hellesund[133], S. Hellman[44a,44b], C. Helsens[36], R. C. W. Henderson[88], Y. Heng[180], S. Henkelmann[174], A. M. Henriques Correia[36], G. H. Herbert[19], H. Herde[26], V. Herget[176], Y. Hernández Jiménez[33c], H. Herr[98], M. G. Herrmann[113], T. Herrmann[47], G. Herten[51], R. Hertenberger[113], L. Hervas[36], T. C. Herwig[136], G. G. Hesketh[93], N. P. Hessey[167a], A. Higashida[162], S. Higashino[80], E. Higón-Rodriguez[173], K. Hildebrand[37], E. Hill[175], J. C. Hill[32], K. K. Hill[29], K. H. Hiller[45], S. J. Hillier[21], M. Hils[47], I. Hinchliffe[18], M. Hirose[132], D. Hirschbuehl[181], B. Hiti[90], O. Hladik[140], D. R. Hlaluku[33c], X. Hoad[49], J. Hobbs[154], N. Hod[167a], M. C. Hodgkinson[148], A. Hoecker[36], M. R. Hoeferkamp[117], F. Hoenig[113], D. Hohn[24], D. Hohov[131], T. R. Holmes[37], M. Holzbock[113], M. Homann[46], S. Honda[168], T. Honda[80], T. M. Hong[138], A. Hönle[114], B. H. Hooberman[172], W. H. Hopkins[130], Y. Horii[116], P. Horn[47], A. J. Horton[151], L. A. Horyn[37], J-Y. Hostachy[57], A. Hostiuc[147], S. Hou[157], A. Hoummada[35a], J. Howarth[99], J. Hoya[87], M. Hrabovsky[129], J. Hrdinka[36], I. Hristova[19], J. Hrivnac[131], A. Hrynevich[107], T. Hryn'ova[5], P. J. Hsu[63], S.-C. Hsu[147], Q. Hu[29], S. Hu[59c], Y. Huang[15a], Z. Hubacek[141], F. Hubaut[100], M. Huebner[24], F. Huegging[24], T. B. Huffman[134], M. Huhtinen[36], R. F. H. Hunter[34], P. Huo[154], A. M. Hupe[34], N. Huseynov[78,ac], J. Huston[105], J. Huth[58], R. Hyneman[104], G. Iacobucci[53], G. Iakovidis[29], I. Ibragimov[150], L. Iconomidou-Fayard[131], Z. Idrissi[35e], P. I. Iengo[36], R. Ignazzi[40], O. Igonkina[119,y], R. Iguchi[162], T. Iizawa[53], Y. Ikegami[80], M. Ikeno[80], D. Iliadis[161], N. Ilic[118], F. Iltzsche[47], G. Introzzi[69a,69b], M. Iodice[73a], K. Iordanidou[39], V. Ippolito[71a,71b], M. F. Isacson[171], N. Ishijima[132], M. Ishino[162], M. Ishitsuka[164], W. Islam[128], C. Issever[134], S. Istin[159], F. Ito[168], J. M. Iturbe Ponce[62a], R. Iuppa[74a,74b], A. Ivina[179], H. Iwasaki[80], J. M. Izen[43], V. Izzo[68a], P. Jacka[140], P. Jackson[1], R. M. Jacobs[24], V. Jain[2], G. Jäkel[181], K. B. Jakobi[98], K. Jakobs[51], S. Jakobsen[75], T. Jakoubek[140], D. O. Jamin[128], R. Jansky[53], J. Janssen[24], M. Janus[52], P. A. Janus[82a], G. Jarlskog[95], N. Javadov[78,ac], T. Javůrek[36], M. Javurkova[51], F. Jeanneau[144], L. Jeanty[18], J. Jejelava[158a,ad], A. Jelinskas[177], P. Jenni[51,c], J. Jeong[45], N. Jeong[45], S. Jézéquel[5], H. Ji[180], J. Jia[154], H. Jiang[77], Y. Jiang[59a], Z. Jiang[152], S. Jiggins[51], F. A. Jimenez Morales[38], J. Jimenez Pena[173], S. Jin[15c], A. Jinaru[27b], O. Jinnouchi[164], H. Jivan[33c], P. Johansson[148], K. A. Johns[7], C. A. Johnson[64], W. J. Johnson[147], K. Jon-And[44a,44b], R. W. L. Jones[88], S. D. Jones[155], S. Jones[7], T. J. Jones[89], J. Jongmanns[60a], P. M. Jorge[139a,139b], J. Jovicevic[167a], X. Ju[18], J. J. Junggeburth[114], A. Juste Rozas[14,x], A. Kaczmarska[83], M. Kado[131], H. Kagan[125], M. Kagan[152], T. Kaji[178], E. Kajomovitz[159], C. W. Kalderon[95], A. Kaluza[98], S. Kama[42], A. Kamenshchikov[122], L. Kanjir[90], Y. Kano[162], V. A. Kantserov[111], J. Kanzaki[80], B. Kaplan[123], L. S. Kaplan[180], D. Kar[33c], M. J. Kareem[167b], E. Karentzos[10], S. N. Karpov[78], Z. M. Karpova[78], V. Kartvelishvili[88], A. N. Karyukhin[122], L. Kashif[180], R. D. Kass[125], A. Kastanas[44a,44b], Y. Kataoka[162], C. Kato[59c,59d], J. Katzy[45], K. Kawade[81], K. Kawagoe[86], T. Kawamoto[162], G. Kawamura[52], E. F. Kay[89], V. F. Kazanin[121a,121b], R. Keeler[175], R. Kehoe[42], J. S. Keller[34], E. Kellermann[95], J. J. Kempster[21], J. Kendrick[21], O. Kepka[140], S. Kersten[181], B. P. Kerševan[90], S. Ketabchi Haghighat[166], R. A. Keyes[102], M. Khader[172], F. Khalil-Zada[13], A. Khanov[128], A. G. Kharlamov[121a,121b], T. Kharlamova[121a,121b], E. E. Khoda[174], A. Khodinov[165], T. J. Khoo[53], E. Khramov[78], J. Khubua[158b], S. Kido[81], M. Kiehn[53], C. R. Kilby[92], Y. K. Kim[37], N. Kimura[65a,65c], O. M. Kind[19], B. T. King[89,*], D. Kirchmeier[47], J. Kirk[143], A. E. Kiryunin[114], T. Kishimoto[162], D. Kisielewska[82a], V. Kitali[45], O. Kivernyk[5], E. Kladiva[28b,*], T. Klapdor-Kleingrothaus[51], M. H. Klein[104], M. Klein[89], U. Klein[89], K. Kleinknecht[98], P. Klimek[120], A. Klimentov[29], T. Klingl[24], T. Klioutchnikova[36], F. F. Klitzner[113], P. Kluit[119], S. Kluth[114], E. Kneringer[75], E. B. F. G. Knoops[100], A. Knue[51], A. Kobayashi[162], D. Kobayashi[86], T. Kobayashi[162], M. Kobel[47], M. Kocian[152], P. Kodys[142], P. T. Koenig[24], T. Koffas[34], E. Koffeman[119], N. M. Köhler[114], T. Koi[152], M. Kolb[60b], I. Koletsou[5], T. Kondo[80], N. Kondrashova[59c], K. Köneke[51], A. C. König[118], T. Kono[124], R. Konoplich[123,ah], V. Konstantinides[93], N. Konstantinidis[93], B. Konya[95], R. Kopeliansky[64], S. Koperny[82a], K. Korcyl[83],

K. Kordas[161], G. Koren[160], A. Korn[93], I. Korolkov[14], E. V. Korolkova[148], N. Korotkova[112], O. Kortner[114], S. Kortner[114], T. Kosek[142], V. V. Kostyukhin[24], A. Kotwal[48], A. Koulouris[10], A. Kourkoumeli-Charalampidi[69a,69b], C. Kourkoumelis[9], E. Kourlitis[148], V. Kouskoura[29], A. B. Kowalewska[83], R. Kowalewski[175], T. Z. Kowalski[82a], C. Kozakai[162], W. Kozanecki[144], A. S. Kozhin[122], V. A. Kramarenko[112], G. Kramberger[90], D. Krasnopevtsev[59a], M. W. Krasny[135], A. Krasznahorkay[36], D. Krauss[114], J. A. Kremer[82a], J. Kretzschmar[89], P. Krieger[166], K. Krizka[18], K. Kroeninger[46], H. Kroha[114], J. Kroll[140], J. Kroll[136], J. Krstic[16], U. Kruchonak[78], H. Krüger[24], N. Krumnack[77], M. C. Kruse[48], T. Kubota[103], S. Kuday[4b], J. T. Kuechler[181], S. Kuehn[36], A. Kugel[60a], F. Kuger[176], T. Kuhl[45], V. Kukhtin[78], R. Kukla[100], Y. Kulchitsky[106], S. Kuleshov[146b], Y. P. Kulinich[172], M. Kuna[57], T. Kunigo[84], A. Kupco[140], T. Kupfer[46], O. Kuprash[160], H. Kurashige[81], L. L. Kurchaninov[167a], Y. A. Kurochkin[106], A. Kurova[111], M. G. Kurth[15a,15d], E. S. Kuwertz[36], M. Kuze[164], J. Kvita[129], T. Kwan[102], A. La Rosa[114], J. L. La Rosa Navarro[79d], L. La Rotonda[41a,41b], F. La Ruffa[41a,41b], C. Lacasta[173], F. Lacava[71a,71b], J. Lacey[45], D. P. J. Lack[99], H. Lacker[19], D. Lacour[135], E. Ladygin[78], R. Lafaye[5], B. Laforge[135], T. Lagouri[33c], S. Lai[52], S. Lammers[64], W. Lampl[7], E. Lançon[29], U. Landgraf[51], M. P. J. Landon[91], M. C. Lanfermann[53], V. S. Lang[45], J. C. Lange[52], R. J. Langenberg[36], A. J. Lankford[170], F. Lanni[29], K. Lantzsch[24], A. Lanza[69a], A. Lapertosa[54a,54b], S. Laplace[135], J. F. Laporte[144], T. Lari[67a], F. Lasagni Manghi[23a,23b], M. Lassnig[36], T. S. Lau[62a], A. Laudrain[131], M. Lavorgna[68a,68b], M. Lazzaroni[67a,67b], B. Le[103], O. Le Dortz[135], E. Le Guirriec[100], E. P. Le Quilleuc[144], M. LeBlanc[7], T. LeCompte[6], F. Ledroit-Guillon[57], C. A. Lee[29], G. R. Lee[146a], L. Lee[58], S. C. Lee[157], B. Lefebvre[102], M. Lefebvre[175], F. Legger[113], C. Leggett[18], K. Lehmann[151], N. Lehmann[181], G. Lehmann Miotto[36], W. A. Leight[45], A. Leisos[161,u], M. A. L. Leite[79d], R. Leitner[142], D. Lellouch[179,*], K. J. C. Leney[93], T. Lenz[24], B. Lenzi[36], R. Leone[7], S. Leone[70a], C. Leonidopoulos[49], G. Lerner[155], C. Leroy[108], R. Les[166], A. A. J. Lesage[144], C. G. Lester[32], M. Levchenko[137], J. Levêque[5], D. Levin[104], L. J. Levinson[179], D. Lewis[91], B. Li[15b], B. Li[104], C-Q. Li[59a,ag], H. Li[59b], L. Li[59c], M. Li[15a], Q. Li[15a,15d], Q. Y. Li[59a], S. Li[59c,59d], X. Li[59c], Y. Li[150], Z. Liang[15a], B. Liberti[72a], A. Liblong[166], K. Lie[62c], S. Liem[119], A. Limosani[156], C. Y. Lin[32], K. Lin[105], T. H. Lin[98], R. A. Linck[64], J. H. Lindon[21], B. E. Lindquist[154], A. L. Lionti[53], E. Lipeles[136], A. Lipniacka[17], M. Lisovyi[60b], T. M. Liss[172,an], A. Lister[174], A. M. Litke[145], J. D. Little[8], B. Liu[77], B. L. Liu[6], H. B. Liu[29], H. Liu[104], J. B. Liu[59a], J. K. K. Liu[134], K. Liu[135], M. Liu[59a], P. Liu[18], Y. Liu[15a,15d], Y. L. Liu[59a], Y. W. Liu[59a], M. Livan[69a,69b], A. Lleres[57], J. Llorente Merino[15a], S. L. Lloyd[91], C. Y. Lo[62b], F. Lo Sterzo[42], E. M. Lobodzinska[45], P. Loch[7], T. Lohse[19], K. Lohwasser[148], M. Lokajicek[140], J. D. Long[172], R. E. Long[88], L. Longo[66a,66b], K. A. Looper[125], J. A. Lopez[146b], I. Lopez Paz[99], A. Lopez Solis[148], J. Lorenz[113], N. Lorenzo Martinez[5], M. Losada[22], P. J. Lösel[113], A. Lösle[51], X. Lou[45], X. Lou[15a], A. Lounis[131], J. Love[6], P. A. Love[88], J. J. Lozano Bahilo[173], H. Lu[62a], M. Lu[59a], N. Lu[104], Y. J. Lu[63], H. J. Lubatti[147], C. Luci[71a,71b], A. Lucotte[57], C. Luedtke[51], F. Luehring[64], I. Luise[135], L. Luminari[71a], B. Lund-Jensen[153], M. S. Lutz[101], P. M. Luzi[135], D. Lynn[29], R. Lysak[140], E. Lytken[95], F. Lyu[15a], V. Lyubushkin[78], T. Lyubushkina[78], H. Ma[29], L. L. Ma[59b], Y. Ma[59b], G. Maccarrone[50], A. Macchiolo[114], C. M. Macdonald[148], J. Machado Miguens[136,139b], D. Madaffari[173], R. Madar[38], W. F. Mader[47], A. Madsen[45], N. Madysa[47], J. Maeda[81], K. Maekawa[162], S. Maeland[17], T. Maeno[29], M. Maerker[47], A. S. Maevskiy[112], V. Magerl[51], D. J. Mahon[39], C. Maidantchik[79b], T. Maier[113], A. Maio[139a,139b,139d], O. Majersky[28a], S. Majewski[130], Y. Makida[80], N. Makovec[131], B. Malaescu[135], Pa. Malecki[83], V. P. Maleev[137], F. Malek[57], U. Mallik[76], D. Malon[6], C. Malone[32], S. Maltezos[10], S. Malyukov[36], J. Mamuzic[173], G. Mancini[50], I. Mandić[90], J. Maneira[139a], L. Manhaes de Andrade Filho[79a], J. Manjarres Ramos[47], K. H. Mankinen[95], A. Mann[113], A. Manousos[75], B. Mansoulie[144], J. D. Mansour[15a], M. Mantoani[52], S. Manzoni[67a,67b], A. Marantis[161], G. Marceca[30], L. March[53], L. Marchese[134], G. Marchiori[135], M. Marcisovsky[140], C. A. Marin Tobon[36], M. Marjanovic[38], D. E. Marley[104], F. Marroquim[79b], Z. Marshall[18], M.U.F Martensson[171], S. Marti-Garcia[173], C. B. Martin[125], T. A. Martin[177], V. J. Martin[49], B. Martin dit Latour[17], M. Martinez[14,x], V. I. Martinez Outschoorn[101], S. Martin-Haugh[143], V. S. Martoiu[27b], A. C. Martyniuk[93], A. Marzin[36], L. Masetti[98], T. Mashimo[162], R. Mashinistov[109], J. Masik[99], A. L. Maslennikov[121a,121b], L. H. Mason[103], L. Massa[72a,72b], P. Massarotti[68a,68b], P. Mastrandrea[5], A. Mastroberardino[41a,41b], T. Masubuchi[162], P. Mättig[181], J. Maurer[27b], B. Maček[90], S. J. Maxfield[89], D. A. Maximov[121a,121b], R. Mazini[157], I. Maznas[161], S. M. Mazza[145], G. Mc Goldrick[166], S. P. Mc Kee[104], T. G. McCarthy[114], L. I. McClymont[93], E. F. McDonald[103], J. A. Mcfayden[36], M. A. McKay[42], K. D. McLean[175], S. J. McMahon[143], P. C. McNamara[103], C. J. McNicol[177], R. A. McPherson[175,aa], J. E. Mdhluli[33c], Z. A. Meadows[101], S. Meehan[147], T. Megy[51], S. Mehlhase[113], A. Mehta[89], T. Meideck[57], B. Meirose[43], D. Melini[173,ar], B. R. Mellado Garcia[33c], J. D. Mellenthin[52], M. Melo[28a], F. Meloni[45], A. Melzer[24], S. B. Menary[99], E. D. Mendes Gouveia[139a], L. Meng[89], X. T. Meng[104], A. Mengarelli[23a,23b], S. Menke[114], E. Meoni[41a,41b], S. Mergelmeyer[19], S. A. M. Merkt[138], C. Merlassino[20], P. Mermod[53], L. Merola[68a,68b], C. Meroni[67a], F. S. Merritt[37], A. Messina[71a,71b], J. Metcalfe[6], A. S. Mete[170], C. Meyer[136], J. Meyer[159], J-P. Meyer[144], H. Meyer Zu Theenhausen[60a], F. Miano[155], R. P. Middleton[143], L. Mijović[49], G. Mikenberg[179], M. Mikestikova[140], M. Mikuž[90], M. Milesi[103], A. Milic[166], D. A. Millar[91], D. W. Miller[37], A. Milov[179], D. A. Milstead[44a,44b],

A. A. Minaenko[122], M. Miñano Moya[173], I. A. Minashvili[158b], A. I. Mincer[123], B. Mindur[82a], M. Mineev[78], Y. Minegishi[162], Y. Ming[180], L. M. Mir[14], A. Mirto[66a,66b], K. P. Mistry[136], T. Mitani[178], J. Mitrevski[113], V. A. Mitsou[173], M. Mittal[59c], A. Miucci[20], P. S. Miyagawa[148], A. Mizukami[80], J. U. Mjörnmark[95], T. Mkrtchyan[183], M. Mlynarikova[142], T. Moa[44a,44b], K. Mochizuki[108], P. Mogg[51], S. Mohapatra[39], S. Molander[44a,44b], R. Moles-Valls[24], M. C. Mondragon[105], K. Mönig[45], J. Monk[40], E. Monnier[100], A. Montalbano[151], J. Montejo Berlingen[36], F. Monticelli[87], S. Monzani[67a], N. Morange[131], D. Moreno[22], M. Moreno Llácer[36], P. Morettini[54b], M. Morgenstern[119], S. Morgenstern[47], D. Mori[151], M. Morii[58], M. Morinaga[178], V. Morisbak[133], A. K. Morley[36], G. Mornacchi[36], A. P. Morris[93], J. D. Morris[91], L. Morvaj[154], P. Moschovakos[10], M. Mosidze[158b], H. J. Moss[148], J. Moss[31,m], K. Motohashi[164], R. Mount[152], E. Mountricha[36], E. J. W. Moyse[101], S. Muanza[100], F. Mueller[114], J. Mueller[138], R. S. P. Mueller[113], D. Muenstermann[88], G. A. Mullier[95], F. J. Munoz Sanchez[99], P. Murin[28b], W. J. Murray[177,143], A. Murrone[67a,67b], M. Muškinja[90], C. Mwewa[33a], A. G. Myagkov[122,ai], J. Myers[130], M. Myska[141], B. P. Nachman[18], O. Nackenhorst[46], K. Nagai[134], K. Nagano[80], Y. Nagasaka[61], M. Nagel[51], E. Nagy[100], A. M. Nairz[36], Y. Nakahama[116], K. Nakamura[80], T. Nakamura[162], I. Nakano[126], H. Nanjo[132], F. Napolitano[60a], R. F. Naranjo Garcia[45], R. Narayan[11], D. I. Narrias Villar[60a], I. Naryshkin[137], T. Naumann[45], G. Navarro[22], R. Nayyar[7], H. A. Neal[104,*], P. Y. Nechaeva[109], T. J. Neep[144], A. Negri[69a,69b], M. Negrini[23b], S. Nektarijevic[118], C. Nellist[52], M. E. Nelson[134], S. Nemecek[140], P. Nemethy[123], M. Nessi[36,e], M. S. Neubauer[172], M. Neumann[181], P. R. Newman[21], T. Y. Ng[62c], Y. S. Ng[19], H. D. N. Nguyen[100], T. Nguyen Manh[108], E. Nibigira[38], R. B. Nickerson[134], R. Nicolaidou[144], D. S. Nielsen[40], J. Nielsen[145], N. Nikiforou[11], V. Nikolaenko[122,ai], I. Nikolic-Audit[135], K. Nikolopoulos[21], P. Nilsson[29], Y. Ninomiya[80], A. Nisati[71a], N. Nishu[59c], R. Nisius[114], I. Nitsche[46], T. Nitta[178], T. Nobe[162], Y. Noguchi[84], M. Nomachi[132], I. Nomidis[135], M. A. Nomura[29], T. Nooney[91], M. Nordberg[36], N. Norjoharuddeen[134], T. Novak[90], O. Novgorodova[47], R. Novotny[141], L. Nozka[129], K. Ntekas[170], E. Nurse[93], F. Nuti[103], F. G. Oakham[34,aq], H. Oberlack[114], J. Ocariz[135], A. Ochi[81], I. Ochoa[39], J. P. Ochoa-Ricoux[146a], K. O'Connor[26], S. Oda[86], S. Odaka[80], S. Oerdek[52], A. Oh[99], S. H. Oh[48], C. C. Ohm[153], H. Oide[54a,54b], M. L. Ojeda[166], H. Okawa[168], Y. Okazaki[84], Y. Okumura[162], T. Okuyama[80], A. Olariu[27b], L. F. Oleiro Seabra[139a], S. A. Olivares Pino[146a], D. Oliveira Damazio[29], J. L. Oliver[1], M. J. R. Olsson[37], A. Olszewski[83], J. Olszowska[83], D. C. O'Neil[151], A. Onofre[139a,139e], K. Onogi[116], P. U. E. Onyisi[11], H. Oppen[133], M. J. Oreglia[37], G. E. Orellana[87], Y. Oren[160], D. Orestano[73a,73b], N. Orlando[62b], A. A. O'Rourke[45], R. S. Orr[166], B. Osculati[54a,54b,*], V. O'Shea[56], R. Ospanov[59a], G. Otero y Garzon[30], H. Otono[86], M. Ouchrif[35d], F. Ould-Saada[133], A. Ouraou[144], Q. Ouyang[15a], M. Owen[56], R. E. Owen[21], V. E. Ozcan[12c], N. Ozturk[8], J. Pacalt[129], H. A. Pacey[32], K. Pachal[151], A. Pacheco Pages[14], L. Pacheco Rodriguez[144], C. Padilla Aranda[14], S. Pagan Griso[18], M. Paganini[182], G. Palacino[64], S. Palazzo[49], S. Palestini[36], M. Palka[82b], D. Pallin[38], I. Panagoulias[10], C. E. Pandini[36], J. G. Panduro Vazquez[92], P. Pani[36], G. Panizzo[65a,65c], L. Paolozzi[53], T. D. Papadopoulou[10], K. Papageorgiou[9,h], A. Paramonov[6], D. Paredes Hernandez[62b], S. R. Paredes Saenz[134], B. Parida[165], T. H. Park[34], A. J. Parker[88], K. A. Parker[45], M. A. Parker[32], F. Parodi[54a,54b], J. A. Parsons[39], U. Parzefall[51], V. R. Pascuzzi[166], J. M. P. Pasner[145], E. Pasqualucci[71a], S. Passaggio[54b], F. Pastore[92], P. Pasuwan[44a,44b], S. Pataraia[98], J. R. Pater[99], A. Pathak[180], T. Pauly[36], B. Pearson[114], M. Pedersen[133], L. Pedraza Diaz[118], R. Pedro[139a,139b], S. V. Peleganchuk[121a,121b], O. Penc[140], C. Peng[15a], H. Peng[59a], B. S. Peralva[79a], M. M. Perego[131], A. P. Pereira Peixoto[139a], D. V. Perepelitsa[29], F. Peri[19], L. Perini[67a,67b], H. Pernegger[36], S. Perrella[68a,68b], V. D. Peshekhonov[78,*], K. Peters[45], R. F. Y. Peters[99], B. A. Petersen[36], T. C. Petersen[40], E. Petit[57], A. Petridis[1], C. Petridou[161], P. Petroff[131], M. Petrov[134], F. Petrucci[73a,73b], M. Pettee[182], N. E. Pettersson[101], A. Peyaud[144], R. Pezoa[146b], T. Pham[103], F. H. Phillips[105], P. W. Phillips[143], M. W. Phipps[172], G. Piacquadio[154], E. Pianori[18], A. Picazio[101], M. A. Pickering[134], R. H. Pickles[99], R. Piegaia[30], J. E. Pilcher[37], A. D. Pilkington[99], M. Pinamonti[72a,72b], J. L. Pinfold[3], M. Pitt[179], L. Pizzimento[72a,72b], M.-A. Pleier[29], V. Pleskot[142], E. Plotnikova[78], D. Pluth[77], P. Podberezko[121a,121b], R. Poettgen[95], R. Poggi[53], L. Poggioli[131], I. Pogrebnyak[105], D. Pohl[24], I. Pokharel[52], G. Polesello[69a], A. Poley[18], A. Policicchio[71a,71b], R. Polifka[36], A. Polini[23b], C. S. Pollard[45], V. Polychronakos[29], D. Ponomarenko[111], L. Pontecorvo[36], G. A. Popeneciu[27d], D. M. Portillo Quintero[135], S. Pospisil[141], K. Potamianos[45], I. N. Potrap[78], C. J. Potter[32], H. Potti[11], T. Poulsen[95], J. Poveda[36], T. D. Powell[148], M. E. Pozo Astigarraga[36], P. Pralavorio[100], S. Prell[77], D. Price[99], M. Primavera[66a], S. Prince[102], N. Proklova[111], K. Prokofiev[62c], F. Prokoshin[146b], S. Protopopescu[29], J. Proudfoot[6], M. Przybycien[82a], A. Puri[172], P. Puzo[131], J. Qian[104], Y. Qin[99], A. Quadt[52], M. Queitsch-Maitland[45], A. Qureshi[1], P. Rados[103], F. Ragusa[67a,67b], G. Rahal[96], J. A. Raine[53], S. Rajagopalan[29], A. Ramirez Morales[91], T. Rashid[131], S. Raspopov[5], M. G. Ratti[67a,67b], D. M. Rauch[45], F. Rauscher[113], S. Rave[98], B. Ravina[148], I. Ravinovich[179], J. H. Rawling[99], M. Raymond[36], A. L. Read[133], N. P. Readioff[57], M. Reale[66a,66b], D. M. Rebuzzi[69a,69b], A. Redelbach[176], G. Redlinger[29], R. Reece[145], R. G. Reed[33c], K. Reeves[43], L. Rehnisch[19], J. Reichert[136], D. Reikher[160], A. Reiss[98], C. Rembser[36], H. Ren[15a], M. Rescigno[71a], S. Resconi[67a], E. D. Resseguie[136], S. Rettie[174], E. Reynolds[21], O. L. Rezanova[121a,121b], P. Reznicek[142], E. Ricci[74a,74b], R. Richter[114], S. Richter[45], E. Richter-Was[82b], O. Ricken[24], M. Ridel[135], P. Rieck[114], C. J. Riegel[181], O. Rifki[45],

M. Rijssenbeek[154], A. Rimoldi[69a,69b], M. Rimoldi[20], L. Rinaldi[23b], G. Ripellino[153], B. Ristić[88], E. Ritsch[36], I. Riu[14], J. C. Rivera Vergara[146a], F. Rizatdinova[128], E. Rizvi[91], C. Rizzi[14], R. T. Roberts[99], S. H. Robertson[102,aa], D. Robinson[32], J. E. M. Robinson[45], A. Robson[56], E. Rocco[98], C. Roda[70a,70b], Y. Rodina[100], S. Rodriguez Bosca[173], A. Rodriguez Perez[14], D. Rodriguez Rodriguez[173], A. M. Rodríguez Vera[167b], S. Roe[36], C. S. Rogan[58], O. Røhne[133], R. Röhrig[114], C. P. A. Roland[64], J. Roloff[58], A. Romaniouk[111], M. Romano[23a,23b], N. Rompotis[89], M. Ronzani[123], L. Roos[135], S. Rosati[71a], K. Rosbach[51], N-A. Rosien[52], B. J. Rosser[136], E. Rossi[45], E. Rossi[73a,73b], E. Rossi[68a,68b], L. P. Rossi[54b], L. Rossini[67a,67b], J. H. N. Rosten[32], R. Rosten[14], M. Rotaru[27b], J. Rothberg[147], D. Rousseau[131], D. Roy[33c], A. Rozanov[100], Y. Rozen[159], X. Ruan[33c], F. Rubbo[152], F. Rühr[51], A. Ruiz-Martinez[173], Z. Rurikova[51], N. A. Rusakovich[78], H. L. Russell[102], J. P. Rutherfoord[7], E. M. Rüttinger[45,j], Y. F. Ryabov[137], M. Rybar[172], G. Rybkin[131], S. Ryu[6], A. Ryzhov[122], G. F. Rzehorz[52], P. Sabatini[52], G. Sabato[119], S. Sacerdoti[131], H.F-W. Sadrozinski[145], R. Sadykov[78], F. Safai Tehrani[71a], P. Saha[120], M. Sahinsoy[60a], A. Sahu[181], M. Saimpert[45], M. Saito[162], T. Saito[162], H. Sakamoto[162], A. Sakharov[123,ah], D. Salamani[53], G. Salamanna[73a,73b], J. E. Salazar Loyola[146b], P. H. Sales De Bruin[171], D. Salihagic[114,*], A. Salnikov[152], J. Salt[173], D. Salvatore[41a,41b], F. Salvatore[155], A. Salvucci[62a,62b,62c], A. Salzburger[36], J. Samarati[36], D. Sammel[51], D. Sampsonidis[161], D. Sampsonidou[161], J. Sánchez[173], A. Sanchez Pineda[65a,65c], H. Sandaker[133], C. O. Sander[45], M. Sandhoff[181], C. Sandoval[22], D. P. C. Sankey[143], M. Sannino[54a,54b], Y. Sano[116], A. Sansoni[50], C. Santoni[38], H. Santos[139a], I. Santoyo Castillo[155], A. Santra[173], A. Sapronov[78], J. G. Saraiva[139a,139d], O. Sasaki[80], K. Sato[168], E. Sauvan[5], P. Savard[166,aq], N. Savic[114], R. Sawada[162], C. Sawyer[143], L. Sawyer[94,af], C. Sbarra[23b], A. Sbrizzi[23a], T. Scanlon[93], J. Schaarschmidt[147], P. Schacht[114], B. M. Schachtner[113], D. Schaefer[37], L. Schaefer[136], J. Schaeffer[98], S. Schaepe[36], U. Schäfer[98], A. C. Schaffer[131], D. Schaile[113], R. D. Schamberger[154], N. Scharmberg[99], V. A. Schegelsky[137], D. Scheirich[142], F. Schenck[19], M. Schernau[170], C. Schiavi[54a,54b], S. Schier[145], L. K. Schildgen[24], Z. M. Schillaci[26], E. J. Schioppa[36], M. Schioppa[41a,41b], K. E. Schleicher[51], S. Schlenker[36], K. R. Schmidt-Sommerfeld[114], K. Schmieden[36], C. Schmitt[98], S. Schmitt[45], S. Schmitz[98], J. C. Schmoeckel[45], U. Schnoor[51], L. Schoeffel[144], A. Schoening[60b], E. Schopf[134], M. Schott[98], J. F. P. Schouwenberg[118], J. Schovancova[36], S. Schramm[53], A. Schulte[98], H-C. Schultz-Coulon[60a], M. Schumacher[51], B. A. Schumm[145], Ph. Schune[144], A. Schwartzman[152], T. A. Schwarz[104], Ph. Schwemling[144], R. Schwienhorst[105], A. Sciandra[24], G. Sciolla[26], M. Scornajenghi[41a,41b], F. Scuri[70a], F. Scutti[103], L. M. Scyboz[114], C. D. Sebastiani[71a,71b], P. Seema[19], S. C. Seidel[117], A. Seiden[145], T. Seiss[37], J. M. Seixas[79b], G. Sekhniaidze[68a], K. Sekhon[104], S. J. Sekula[42], N. Semprini-Cesari[23a,23b], S. Sen[48], S. Senkin[38], C. Serfon[133], L. Serin[131], L. Serkin[65a,65b], M. Sessa[59a], H. Severini[127], F. Sforza[169], A. Sfyrla[53], E. Shabalina[52], J. D. Shahinian[145], N. W. Shaikh[44a,44b], L. Y. Shan[15a], R. Shang[172], J. T. Shank[25], M. Shapiro[18], A. Sharma[134], A. S. Sharma[1], P. B. Shatalov[110], K. Shaw[155], S. M. Shaw[99], A. Shcherbakova[137], Y. Shen[127], N. Sherafati[34], A. D. Sherman[25], P. Sherwood[93], L. Shi[157,am], S. Shimizu[80], C. O. Shimmin[182], Y. Shimogama[178], M. Shimojima[115], I. P. J. Shipsey[134], S. Shirabe[86], M. Shiyakova[78], J. Shlomi[179], A. Shmeleva[109], D. Shoaleh Saadi[108], M. J. Shochet[37], S. Shojaii[103], D. R. Shope[127], S. Shrestha[125], E. Shulga[111], P. Sicho[140], A. M. Sickles[172], P. E. Sidebo[153], E. Sideras Haddad[33c], O. Sidiropoulou[36], A. Sidoti[23a,23b], F. Siegert[47], Dj. Sijacki[16], J. Silva[139a], M. Silva Jr.[180], M. V. Silva Oliveira[79a], S. B. Silverstein[44a], S. Simion[131], E. Simioni[98], M. Simon[98], R. Simoniello[98], P. Sinervo[166], N. B. Sinev[130], M. Sioli[23a,23b], G. Siragusa[176], I. Siral[104], S. Yu. Sivoklokov[112], J. Sjölin[44a,44b], P. Skubic[127], M. Slater[21], T. Slavicek[141], M. Slawinska[83], K. Sliwa[169], R. Slovak[142], V. Smakhtin[179], B. H. Smart[5], J. Smiesko[28a], N. Smirnov[111], S. Yu. Smirnov[111], Y. Smirnov[111], L. N. Smirnova[112,r], O. Smirnova[95], J. W. Smith[52], M. Smizanska[88], K. Smolek[141], A. Smykiewicz[83], A. A. Snesarev[109], I. M. Snyder[130], S. Snyder[29], R. Sobie[175,aa], A. M. Soffa[170], A. Soffer[160], A. Søgaard[49], D. A. Soh[157], G. Sokhrannyi[90], C. A. Solans Sanchez[36], M. Solar[141], E. Yu. Soldatov[111], U. Soldevila[173], A. A. Solodkov[122], A. Soloshenko[78], O. V. Solovyanov[122], V. Solovyev[137], P. Sommer[148], H. Son[169], W. Song[143], W. Y. Song[167b], A. Sopczak[141], F. Sopkova[28b], C. L. Sotiropoulou[70a,70b], S. Sottocornola[69a,69b], R. Soualah[65a,65c,g], A. M. Soukharev[121a,121b], D. South[45], B. C. Sowden[92], S. Spagnolo[66a,66b], M. Spalla[114], M. Spangenberg[177], F. Spanò[92], D. Sperlich[19], T. M. Spieker[60a], R. Spighi[23b], G. Spigo[36], L. A. Spiller[103], D. P. Spiteri[56], M. Spousta[142], A. Stabile[67a,67b], R. Stamen[60a], S. Stamm[19], E. Stanecka[83], R. W. Stanek[6], C. Stanescu[73a], B. Stanislaus[134], M. M. Stanitzki[45], B. Stapf[119], S. Stapnes[133], E. A. Starchenko[122], G. H. Stark[37], J. Stark[57], S. H. Stark[40], P. Staroba[140], P. Starovoitov[60a], S. Stärz[36], R. Staszewski[83], M. Stegler[45], P. Steinberg[29], B. Stelzer[151], H. J. Stelzer[36], O. Stelzer-Chilton[167a], H. Stenzel[55], T. J. Stevenson[155], G. A. Stewart[36], M. C. Stockton[36], G. Stoicea[27b], P. Stolte[52], S. Stonjek[114], A. Straessner[47], J. Strandberg[153], S. Strandberg[44a,44b], M. Strauss[127], P. Strizenec[28b], R. Ströhmer[176], D. M. Strom[130], R. Stroynowski[42], A. Strubig[49], S. A. Stucci[29], B. Stugu[17], J. Stupak[127], N. A. Styles[45], D. Su[152], J. Su[138], S. Suchek[60a], Y. Sugaya[132], M. Suk[141], V. V. Sulin[109], M. J. Sullivan[89], D. M. S. Sultan[53], S. Sultansoy[4c], T. Sumida[84], S. Sun[104], X. Sun[3], K. Suruliz[155], C. J. E. Suster[156], M. R. Sutton[155], S. Suzuki[80], M. Svatos[140], M. Swiatlowski[37], S. P. Swift[2], A. Sydorenko[98], I. Sykora[28a], T. Sykora[142], D. Ta[98], K. Tackmann[45], J. Taenzer[160], A. Taffard[170], R. Tafirout[167a], E. Tahirovic[91], N. Taiblum[160], H. Takai[29], R. Takashima[85], E. H. Takasugi[114], K. Takeda[81],

T. Takeshita[149], Y. Takubo[80], M. Talby[100], A. A. Talyshev[121a,121b], J. Tanaka[162], M. Tanaka[164], R. Tanaka[131], B. B. Tannenwald[125], S. Tapia Araya[146b], S. Tapprogge[98], A. Tarek Abouelfadl Mohamed[135], S. Tarem[159], G. Tarna[27b,d], G. F. Tartarelli[67a], P. Tas[142], M. Tasevsky[140], T. Tashiro[84], E. Tassi[41a,41b], A. Tavares Delgado[139a,139b], Y. Tayalati[35e], A. C. Taylor[117], A. J. Taylor[49], G. N. Taylor[103], P. T. E. Taylor[103], W. Taylor[167b], A. S. Tee[88], P. Teixeira-Dias[92], H. Ten Kate[36], J. J. Teoh[119], S. Terada[80], K. Terashi[162], J. Terron[97], S. Terzo[14], M. Testa[50], R. J. Teuscher[166,aa], S. J. Thais[182], T. Theveneaux-Pelzer[45], F. Thiele[40], D. W. Thomas[92], J. P. Thomas[21], A. S. Thompson[56], P. D. Thompson[21], L. A. Thomsen[182], E. Thomson[136], Y. Tian[39], R. E. Ticse Torres[52], V. O. Tikhomirov[109,aj], Yu. A. Tikhonov[121a,121b], S. Timoshenko[111], P. Tipton[182], S. Tisserant[100], K. Todome[164], S. Todorova-Nova[5], S. Todt[47], J. Tojo[86], S. Tokár[28a], K. Tokushuku[80], E. Tolley[125], K. G. Tomiwa[33c], M. Tomoto[116], L. Tompkins[152], K. Toms[117], B. Tong[58], P. Tornambe[51], E. Torrence[130], H. Torres[47], E. Torró Pastor[147], C. Tosciri[134], J. Toth[100,z], F. Touchard[100], D. R. Tovey[148], C. J. Treado[123], T. Trefzger[176], F. Tresoldi[155], A. Tricoli[29], I. M. Trigger[167a], S. Trincaz-Duvoid[135], M. F. Tripiana[14], W. Trischuk[166], B. Trocmé[57], A. Trofymov[131], C. Troncon[67a], M. Trovatelli[175], F. Trovato[155], L. Truong[33b], M. Trzebinski[83], A. Trzupek[83], F. Tsai[45], J.C-L. Tseng[134], P. V. Tsiareshka[106], A. Tsirigotis[161], N. Tsirintanis[9], V. Tsiskaridze[154], E. G. Tskhadadze[158a], I. I. Tsukerman[110], V. Tsulaia[18], S. Tsuno[80], D. Tsybychev[154], Y. Tu[62b], A. Tudorache[27b], V. Tudorache[27b], T. T. Tulbure[27a], A. N. Tuna[58], S. Turchikhin[78], D. Turgeman[179], I. Turk Cakir[4b,s], R. T. Turra[67a], P. M. Tuts[39], E. Tzovara[98], G. Ucchielli[23a,23b], I. Ueda[80], M. Ughetto[44a,44b], F. Ukegawa[168], G. Unal[36], A. Undrus[29], G. Unel[170], F. C. Ungaro[103], Y. Unno[80], K. Uno[162], J. Urban[28b], P. Urquijo[103], P. Urrejola[98], G. Usai[8], J. Usui[80], L. Vacavant[100], V. Vacek[141], B. Vachon[102], K. O. H. Vadla[133], A. Vaidya[93], C. Valderanis[113], E. Valdes Santurio[44a,44b], M. Valente[53], S. Valentinetti[23a,23b], A. Valero[173], L. Valéry[45], R. A. Vallance[21], A. Vallier[5], J. A. Valls Ferrer[173], T. R. Van Daalen[14], H. Van der Graaf[119], P. Van Gemmeren[6], J. Van Nieuwkoop[151], I. Van Vulpen[119], M. Vanadia[72a,72b], W. Vandelli[36], A. Vaniachine[165], P. Vankov[119], R. Vari[71a], E. W. Varnes[7], C. Varni[54a,54b], T. Varol[42], D. Varouchas[131], K. E. Varvell[156], G. A. Vasquez[146b], J. G. Vasquez[182], F. Vazeille[38], D. Vazquez Furelos[14], T. Vazquez Schroeder[36], J. Veatch[52], V. Vecchio[73a,73b], L. M. Veloce[166], F. Veloso[139a,139c], S. Veneziano[71a], A. Ventura[66a,66b], M. Venturi[175], N. Venturi[36], V. Vercesi[69a], M. Verducci[73a,73b], C. M. Vergel Infante[77], C. Vergis[24], W. Verkerke[119], A. T. Vermeulen[119], J. C. Vermeulen[119], M. C. Vetterli[151,aq], N. Viaux Maira[146b], M. Vicente Barreto Pinto[53], I. Vichou[172,*], T. Vickey[148], O. E. Vickey Boeriu[148], G. H. A. Viehhauser[134], S. Viel[18], L. Vigani[134], M. Villa[23a,23b], M. Villaplana Perez[67a,67b], E. Vilucchi[50], M. G. Vincter[34], V. B. Vinogradov[78], A. Vishwakarma[45], C. Vittori[23a,23b], I. Vivarelli[155], S. Vlachos[10], M. Vogel[181], P. Vokac[141], G. Volpi[14], S. E. von Buddenbrock[33c], E. Von Toerne[24], V. Vorobel[142], K. Vorobev[111], M. Vos[173], J. H. Vossebeld[89], N. Vranjes[16], M. Vranjes Milosavljevic[16], V. Vrba[141], M. Vreeswijk[119], T. Šfiligoj[90], R. Vuillermet[36], I. Vukotic[37], T. Ženiš[28a], L. Živković[16], P. Wagner[24], W. Wagner[181], J. Wagner-Kuhr[113], H. Wahlberg[87], S. Wahrmund[47], K. Wakamiya[81], V. M. Walbrecht[114], J. Walder[88], R. Walker[113], S. D. Walker[92], W. Walkowiak[150], V. Wallangen[44a,44b], A. M. Wang[58], C. Wang[59b,d], F. Wang[180], H. Wang[18], H. Wang[3], J. Wang[156], J. Wang[60b], P. Wang[42], Q. Wang[127], R.-J. Wang[135], R. Wang[59a], R. Wang[6], S. M. Wang[157], W. T. Wang[59a], W. Wang[15c,ab], W. X. Wang[59a,ab], Y. Wang[59a,ag], Z. Wang[59c], C. Wanotayaroj[45], A. Warburton[102], C. P. Ward[32], D. R. Wardrope[93], A. Washbrook[49], P. M. Watkins[21], A. T. Watson[21], M. F. Watson[21], G. Watts[147], S. Watts[99], B. M. Waugh[93], A. F. Webb[11], S. Webb[98], C. Weber[182], M. S. Weber[20], S. A. Weber[34], S. M. Weber[60a], A. R. Weidberg[134], B. Weinert[64], J. Weingarten[46], M. Weirich[98], C. Weiser[51], P. S. Wells[36], T. Wenaus[29], T. Wengler[36], S. Wenig[36], N. Wermes[24], M. D. Werner[77], P. Werner[36], M. Wessels[60a], T. D. Weston[20], K. Whalen[130], N. L. Whallon[147], A. M. Wharton[88], A. S. White[104], A. White[8], M. J. White[1], R. White[146b], D. Whiteson[170], B. W. Whitmore[88], F. J. Wickens[143], W. Wiedenmann[180], M. Wielers[143], C. Wiglesworth[40], L. A. M. Wiik-Fuchs[51], F. Wilk[99], H. G. Wilkens[36], L. J. Wilkins[92], H. H. Williams[136], S. Williams[32], C. Willis[105], S. Willocq[101], J. A. Wilson[21], I. Wingerter-Seez[5], E. Winkels[155], F. Winklmeier[130], O. J. Winston[155], B. T. Winter[51], M. Wittgen[152], M. Wobisch[94], A. Wolf[98], T. M. H. Wolf[119], R. Wolff[100], M. W. Wolter[83], H. Wolters[139a,139c], V. W. S. Wong[174], N. L. Woods[145], S. D. Worm[21], B. K. Wosiek[83], K. W. Woźniak[83], K. Wraight[56], M. Wu[37], S. L. Wu[180], X. Wu[53], Y. Wu[59a], T. R. Wyatt[99], B. M. Wynne[49], S. Xella[40], Z. Xi[104], L. Xia[177], D. Xu[15a], H. Xu[59a,d], L. Xu[29], T. Xu[144], W. Xu[104], B. Yabsley[156], S. Yacoob[33a], K. Yajima[132], D. P. Yallup[93], D. Yamaguchi[164], Y. Yamaguchi[164], A. Yamamoto[80], T. Yamanaka[162], F. Yamane[81], M. Yamatani[162], T. Yamazaki[162], Y. Yamazaki[81], Z. Yan[25], H. J. Yang[59c,59d], H. T. Yang[18], S. Yang[76], Y. Yang[162], Z. Yang[17], W-M. Yao[18], Y. C. Yap[45], Y. Yasu[80], E. Yatsenko[59c,59d], J. Ye[42], S. Ye[29], I. Yeletskikh[78], E. Yigitbasi[25], E. Yildirim[98], K. Yorita[178], K. Yoshihara[136], C. J. S. Young[36], C. Young[152], J. Yu[77], J. Yu[8], X. Yue[60a], S. P. Y. Yuen[24], B. Zabinski[83], G. Zacharis[10], E. Zaffaroni[53], R. Zaidan[14], A. M. Zaitsev[122,ai], T. Zakareishvili[158b], N. Zakharchuk[34], J. Zalieckas[17], S. Zambito[58], D. Zanzi[36], D. R. Zaripovas[56], S. V. Zeißner[46], C. Zeitnitz[181], G. Zemaityte[134], J. C. Zeng[172], Q. Zeng[152], O. Zenin[122], D. Zerwas[131], M. Zgubič[134], D. F. Zhang[59b], D. Zhang[104], F. Zhang[180], G. Zhang[59a], G. Zhang[15b], H. Zhang[15c], J. Zhang[6], L. Zhang[15c], L. Zhang[59a], M. Zhang[172], P. Zhang[15c], R. Zhang[59a], R. Zhang[24], X. Zhang[59b], Y. Zhang[15a,15d], Z. Zhang[131], P. Zhao[48],

Y. Zhao[59b,131,ae], Z. Zhao[59a], A. Zhemchugov[78], Z. Zheng[104], D. Zhong[172], B. Zhou[104], C. Zhou[180], L. Zhou[42], M. S. Zhou[15a,15d], M. Zhou[154], N. Zhou[59c], Y. Zhou[7], C. G. Zhu[59b], H. L. Zhu[59a], H. Zhu[15a], J. Zhu[104], Y. Zhu[59a], X. Zhuang[15a], K. Zhukov[109], V. Zhulanov[121a,121b], A. Zibell[176], D. Zieminska[64], N. I. Zimine[78], S. Zimmermann[51], Z. Zinonos[114], M. Zinser[98], M. Ziolkowski[150], G. Zobernig[180], A. Zoccoli[23a,23b], K. Zoch[52], T. G. Zorbas[148], R. Zou[37], M. Zur Nedden[19], L. Zwalinski[36]

[1] Department of Physics, University of Adelaide, Adelaide, Australia
[2] Physics Department, SUNY Albany, Albany, NY, USA
[3] Department of Physics, University of Alberta, Edmonton, AB, Canada
[4] [(a)]Department of Physics, Ankara University, Ankara, Turkey; [(b)]Istanbul Aydin University, Istanbul, Turkey; [(c)]Division of Physics, TOBB University of Economics and Technology, Ankara, Turkey
[5] LAPP, Université Grenoble Alpes, Université Savoie Mont Blanc, CNRS/IN2P3, Annecy, France
[6] High Energy Physics Division, Argonne National Laboratory, Argonne, IL, USA
[7] Department of Physics, University of Arizona, Tucson, AZ, USA
[8] Department of Physics, University of Texas at Arlington, Arlington, TX, USA
[9] Physics Department, National and Kapodistrian University of Athens, Athens, Greece
[10] Physics Department, National Technical University of Athens, Zografou, Greece
[11] Department of Physics, University of Texas at Austin, Austin, TX, USA
[12] [(a)]Faculty of Engineering and Natural Sciences, Bahcesehir University, Istanbul, Turkey; [(b)]Faculty of Engineering and Natural Sciences, Istanbul Bilgi University, Istanbul, Turkey; [(c)]Department of Physics, Bogazici University, Istanbul, Turkey; [(d)]Department of Physics Engineering, Gaziantep University, Gaziantep, Turkey
[13] Institute of Physics, Azerbaijan Academy of Sciences, Baku, Azerbaijan
[14] Institut de Física d'Altes Energies (IFAE), Barcelona Institute of Science and Technology, Barcelona, Spain
[15] [(a)]Institute of High Energy Physics, Chinese Academy of Sciences, Beijing, China; [(b)]Physics Department, Tsinghua University, Beijing, China; [(c)]Department of Physics, Nanjing University, Nanjing, China; [(d)]University of Chinese Academy of Science (UCAS), Beijing, China
[16] Institute of Physics, University of Belgrade, Belgrade, Serbia
[17] Department for Physics and Technology, University of Bergen, Bergen, Norway
[18] Physics Division, Lawrence Berkeley National Laboratory and University of California, Berkeley, CA, USA
[19] Institut für Physik, Humboldt Universität zu Berlin, Berlin, Germany
[20] Albert Einstein Center for Fundamental Physics and Laboratory for High Energy Physics, University of Bern, Bern, Switzerland
[21] School of Physics and Astronomy, University of Birmingham, Birmingham, UK
[22] Facultad de Ciencias y Centro de Investigaciónes, Universidad Antonio Nariño, Bogota, Colombia
[23] [(a)]Dipartimento di Fisica, INFN Bologna and Universita' di Bologna, Bologna, Italy; [(b)]INFN Sezione di Bologna, Bologna, Italy
[24] Physikalisches Institut, Universität Bonn, Bonn, Germany
[25] Department of Physics, Boston University, Boston, MA, USA
[26] Department of Physics, Brandeis University, Waltham, MA, USA
[27] [(a)]Transilvania University of Brasov, Brasov, Romania; [(b)]Horia Hulubei National Institute of Physics and Nuclear Engineering, Bucharest, Romania; [(c)]Department of Physics, Alexandru Ioan Cuza University of Iasi, Iasi, Romania; [(d)]Physics Department, National Institute for Research and Development of Isotopic and Molecular Technologies, Cluj-Napoca, Romania; [(e)]University Politehnica Bucharest, Bucharest, Romania; [(f)]West University in Timisoara, Timisoara, Romania
[28] [(a)]Faculty of Mathematics, Physics and Informatics, Comenius University, Bratislava, Slovak Republic; [(b)]Department of Subnuclear Physics, Institute of Experimental Physics of the Slovak Academy of Sciences, Kosice, Slovak Republic
[29] Physics Department, Brookhaven National Laboratory, Upton, NY, USA
[30] Departamento de Física, Universidad de Buenos Aires, Buenos Aires, Argentina
[31] California State University, San Diego, CA, USA
[32] Cavendish Laboratory, University of Cambridge, Cambridge, UK
[33] [(a)]Department of Physics, University of Cape Town, Cape Town, South Africa; [(b)]Department of Mechanical Engineering Science, University of Johannesburg, Johannesburg, South Africa; [(c)]School of Physics, University of the Witwatersrand, Johannesburg, South Africa

[34] Department of Physics, Carleton University, Ottawa, ON, Canada
[35] [(a)]Faculté des Sciences Ain Chock, Réseau Universitaire de Physique des Hautes Energies-Université Hassan II, Casablanca, Morocco; [(b)]Faculté des Sciences, Université Ibn-Tofail, Kénitra, Morocco; [(c)]Faculté des Sciences Semlalia, Université Cadi Ayyad, LPHEA-Marrakech, Marrakech, Morocco; [(d)]Faculté des Sciences, Université Mohamed Premier and LPTPM, Oujda, Morocco; [(e)]Faculté des sciences, Université Mohammed V, Rabat, Morocco
[36] CERN, Geneva, Switzerland
[37] Enrico Fermi Institute, University of Chicago, Chicago, IL, USA
[38] LPC, Université Clermont Auvergne, CNRS/IN2P3, Clermont-Ferrand, France
[39] Nevis Laboratory, Columbia University, Irvington, NY, USA
[40] Niels Bohr Institute, University of Copenhagen, Copenhagen, Denmark
[41] [(a)]Dipartimento di Fisica, Università della Calabria, Rende, Italy; [(b)]Laboratori Nazionali di Frascati, INFN Gruppo Collegato di Cosenza, Rende, Italy
[42] Physics Department, Southern Methodist University, Dallas, TX, USA
[43] Physics Department, University of Texas at Dallas, Richardson, TX, USA
[44] [(a)]Department of Physics, Stockholm University, Stockholm, Sweden; [(b)]Oskar Klein Centre, Stockholm, Sweden
[45] Deutsches Elektronen-Synchrotron DESY, Hamburg and Zeuthen, Germany
[46] Lehrstuhl für Experimentelle Physik IV, Technische Universität Dortmund, Dortmund, Germany
[47] Institut für Kern- und Teilchenphysik, Technische Universität Dresden, Dresden, Germany
[48] Department of Physics, Duke University, Durham, NC, USA
[49] SUPA-School of Physics and Astronomy, University of Edinburgh, Edinburgh, UK
[50] INFN e Laboratori Nazionali di Frascati, Frascati, Italy
[51] Physikalisches Institut, Albert-Ludwigs-Universität Freiburg, Freiburg, Germany
[52] II. Physikalisches Institut, Georg-August-Universität Göttingen, Göttingen, Germany
[53] Département de Physique Nucléaire et Corpusculaire, Université de Genève, Geneva, Switzerland
[54] [(a)]Dipartimento di Fisica, Università di Genova, Genoa, Italy; [(b)]INFN Sezione di Genova, Genoa, Italy
[55] II. Physikalisches Institut, Justus-Liebig-Universität Giessen, Giessen, Germany
[56] SUPA-School of Physics and Astronomy, University of Glasgow, Glasgow, UK
[57] LPSC, Université Grenoble Alpes, CNRS/IN2P3, Grenoble INP, Grenoble, France
[58] Laboratory for Particle Physics and Cosmology, Harvard University, Cambridge, MA, USA
[59] [(a)]Department of Modern Physics and State Key Laboratory of Particle Detection and Electronics, University of Science and Technology of China, Hefei, China; [(b)]Institute of Frontier and Interdisciplinary Science and Key Laboratory of Particle Physics and Particle Irradiation (MOE), Shandong University, Qingdao, China; [(c)]School of Physics and Astronomy, Shanghai Jiao Tong University, KLPPAC-MoE, SKLPPC, Shanghai, China; [(d)]Tsung-Dao Lee Institute, Shanghai, China
[60] [(a)]Kirchhoff-Institut für Physik, Ruprecht-Karls-Universität Heidelberg, Heidelberg, Germany; [(b)]Physikalisches Institut, Ruprecht-Karls-Universität Heidelberg, Heidelberg, Germany
[61] Faculty of Applied Information Science, Hiroshima Institute of Technology, Hiroshima, Japan
[62] [(a)]Department of Physics, Chinese University of Hong Kong, Shatin, N.T., Hong Kong, China; [(b)]Department of Physics, University of Hong Kong, Hong Kong, China; [(c)]Department of Physics and Institute for Advanced Study, Hong Kong University of Science and Technology, Clear Water Bay, Kowloon, Hong Kong, China
[63] Department of Physics, National Tsing Hua University, Hsinchu, Taiwan
[64] Department of Physics, Indiana University, Bloomington, IN, USA
[65] [(a)]INFN Gruppo Collegato di Udine, Sezione di Trieste, Udine, Italy; [(b)]ICTP, Trieste, Italy; [(c)]Dipartimento Politecnico di Ingegneria e Architettura, Università di Udine, Udine, Italy
[66] [(a)]INFN Sezione di Lecce, Zona Monte, Italy; [(b)]Dipartimento di Matematica e Fisica, Università del Salento, Lecce, Italy
[67] [(a)]INFN Sezione di Milano, Milan, Italy; [(b)]Dipartimento di Fisica, Università di Milano, Milan, Italy
[68] [(a)]INFN Sezione di Napoli, Naples, Italy; [(b)]Dipartimento di Fisica, Università di Napoli, Naples, Italy
[69] [(a)]INFN Sezione di Pavia, Pavia, Italy; [(b)]Dipartimento di Fisica, Università di Pavia, Pavia, Italy
[70] [(a)]INFN Sezione di Pisa, Pisa, Italy; [(b)]Dipartimento di Fisica E. Fermi, Università di Pisa, Pisa, Italy
[71] [(a)]INFN Sezione di Roma, Rome, Italy; [(b)]Dipartimento di Fisica, Sapienza Università di Roma, Rome, Italy
[72] [(a)]INFN Sezione di Roma Tor Vergata, Rome, Italy; [(b)]Dipartimento di Fisica, Università di Roma Tor Vergata, Rome, Italy

[73] [(a)]INFN Sezione di Roma Tre, Rome, Italy; [(b)]Dipartimento di Matematica e Fisica, Università Roma Tre, Rome, Italy
[74] [(a)]INFN-TIFPA, Povo, Italy; [(b)]Università degli Studi di Trento, Trento, Italy
[75] Institut für Astro- und Teilchenphysik, Leopold-Franzens-Universität, Innsbruck, Austria
[76] University of Iowa, Iowa City, IA, USA
[77] Department of Physics and Astronomy, Iowa State University, Ames, IA, USA
[78] Joint Institute for Nuclear Research, Dubna, Russia
[79] [(a)]Departamento de Engenharia Elétrica, Universidade Federal de Juiz de Fora (UFJF), Juiz de Fora, Brazil; [(b)]Universidade Federal do Rio De Janeiro COPPE/EE/IF, Rio de Janeiro, Brazil; [(c)]Universidade Federal de São João del Rei (UFSJ), São João del Rei, Brazil; [(d)]Instituto de Física, Universidade de São Paulo, São Paulo, Brazil
[80] KEK, High Energy Accelerator Research Organization, Tsukuba, Japan
[81] Graduate School of Science, Kobe University, Kobe, Japan
[82] [(a)]AGH University of Science and Technology, Faculty of Physics and Applied Computer Science, Kraków, Poland; [(b)]Marian Smoluchowski Institute of Physics, Jagiellonian University, Kraków, Poland
[83] Institute of Nuclear Physics Polish Academy of Sciences, Kraków, Poland
[84] Faculty of Science, Kyoto University, Kyoto, Japan
[85] Kyoto University of Education, Kyoto, Japan
[86] Research Center for Advanced Particle Physics and Department of Physics, Kyushu University, Fukuoka, Japan
[87] Instituto de Física La Plata, Universidad Nacional de La Plata and CONICET, La Plata, Argentina
[88] Physics Department, Lancaster University, Lancaster, UK
[89] Oliver Lodge Laboratory, University of Liverpool, Liverpool, UK
[90] Department of Experimental Particle Physics, Jožef Stefan Institute and Department of Physics, University of Ljubljana, Ljubljana, Slovenia
[91] School of Physics and Astronomy, Queen Mary University of London, London, UK
[92] Department of Physics, Royal Holloway University of London, Egham, UK
[93] Department of Physics and Astronomy, University College London, London, UK
[94] Louisiana Tech University, Ruston, LA, USA
[95] Fysiska institutionen, Lunds universitet, Lund, Sweden
[96] Centre de Calcul de l'Institut National de Physique Nucléaire et de Physique des Particules (IN2P3), Villeurbanne, France
[97] Departamento de Física Teorica C-15 and CIAFF, Universidad Autónoma de Madrid, Madrid, Spain
[98] Institut für Physik, Universität Mainz, Mainz, Germany
[99] School of Physics and Astronomy, University of Manchester, Manchester, UK
[100] CPPM, Aix-Marseille Université, CNRS/IN2P3, Marseille, France
[101] Department of Physics, University of Massachusetts, Amherst, MA, USA
[102] Department of Physics, McGill University, Montreal, QC, Canada
[103] School of Physics, University of Melbourne, Victoria, Australia
[104] Department of Physics, University of Michigan, Ann Arbor, MI, USA
[105] Department of Physics and Astronomy, Michigan State University, East Lansing, MI, USA
[106] B.I. Stepanov Institute of Physics, National Academy of Sciences of Belarus, Minsk, Belarus
[107] Research Institute for Nuclear Problems of Byelorussian State University, Minsk, Belarus
[108] Group of Particle Physics, University of Montreal, Montreal, QC, Canada
[109] P.N. Lebedev Physical Institute of the Russian Academy of Sciences, Moscow, Russia
[110] Institute for Theoretical and Experimental Physics of the National Research Centre Kurchatov Institute, Moscow, Russia
[111] National Research Nuclear University MEPhI, Moscow, Russia
[112] D.V. Skobeltsyn Institute of Nuclear Physics, M.V. Lomonosov Moscow State University, Moscow, Russia
[113] Fakultät für Physik, Ludwig-Maximilians-Universität München, Munich, Germany
[114] Max-Planck-Institut für Physik (Werner-Heisenberg-Institut), Munich, Germany
[115] Nagasaki Institute of Applied Science, Nagasaki, Japan
[116] Graduate School of Science and Kobayashi-Maskawa Institute, Nagoya University, Nagoya, Japan
[117] Department of Physics and Astronomy, University of New Mexico, Albuquerque, NM, USA
[118] Institute for Mathematics, Astrophysics and Particle Physics, Radboud University Nijmegen/Nikhef, Nijmegen, The Netherlands
[119] Nikhef National Institute for Subatomic Physics and University of Amsterdam, Amsterdam, The Netherlands

[120] Department of Physics, Northern Illinois University, DeKalb, IL, USA
[121] [(a)]Budker Institute of Nuclear Physics and NSU, SB RAS, Novosibirsk, Russia; [(b)]Novosibirsk State University Novosibirsk, Novosibirsk, Russia
[122] Institute for High Energy Physics of the National Research Centre Kurchatov Institute, Protvino, Russia
[123] Department of Physics, New York University, New York, NY, USA
[124] Ochanomizu University, Otsuka, Bunkyo-ku, Tokyo, Japan
[125] Ohio State University, Columbus, OH, USA
[126] Faculty of Science, Okayama University, Okayama, Japan
[127] Homer L. Dodge Department of Physics and Astronomy, University of Oklahoma, Norman, OK, USA
[128] Department of Physics, Oklahoma State University, Stillwater, OK, USA
[129] Palacký University, RCPTM, Joint Laboratory of Optics, Olomouc, Czech Republic
[130] Center for High Energy Physics, University of Oregon, Eugene, OR, USA
[131] LAL, Université Paris-Sud, CNRS/IN2P3, Université Paris-Saclay, Orsay, France
[132] Graduate School of Science, Osaka University, Osaka, Japan
[133] Department of Physics, University of Oslo, Oslo, Norway
[134] Department of Physics, Oxford University, Oxford, UK
[135] LPNHE, Sorbonne Université, Paris Diderot Sorbonne Paris Cité, CNRS/IN2P3, Paris, France
[136] Department of Physics, University of Pennsylvania, Philadelphia, PA, USA
[137] Konstantinov Nuclear Physics Institute of National Research Centre "Kurchatov Institute", PNPI, St. Petersburg, Russia
[138] Department of Physics and Astronomy, University of Pittsburgh, Pittsburgh, PA, USA
[139] [(a)]Laboratório de Instrumentação e Física Experimental de Partículas-LIP, Lisbon, Portugal; [(b)]Departamento de Física, Faculdade de Ciências, Universidade de Lisboa, Lisbon, Portugal; [(c)]Departamento de Física, Universidade de Coimbra, Coimbra, Portugal; [(d)]Centro de Física Nuclear da Universidade de Lisboa, Lisbon, Portugal; [(e)]Departamento de Física, Universidade do Minho, Braga, Portugal; [(f)]Universidad de Granada, Granada, Spain; [(g)]Dep Física and CEFITEC of Faculdade de Ciências e Tecnologia, Universidade Nova de Lisboa, Caparica, Portugal
[140] Institute of Physics of the Czech Academy of Sciences, Prague, Czech Republic
[141] Czech Technical University in Prague, Prague, Czech Republic
[142] Faculty of Mathematics and Physics, Charles University, Prague, Czech Republic
[143] Particle Physics Department, Rutherford Appleton Laboratory, Didcot, UK
[144] IRFU, CEA, Université Paris-Saclay, Gif-sur-Yvette, France
[145] Santa Cruz Institute for Particle Physics, University of California Santa Cruz, Santa Cruz, CA, USA
[146] [(a)]Departamento de Física, Pontificia Universidad Católica de Chile, Santiago, Chile; [(b)]Departamento de Física, Universidad Técnica Federico Santa María, Valparaiso, Chile
[147] Department of Physics, University of Washington, Seattle, WA, USA
[148] Department of Physics and Astronomy, University of Sheffield, Sheffield, UK
[149] Department of Physics, Shinshu University, Nagano, Japan
[150] Department Physik, Universität Siegen, Siegen, Germany
[151] Department of Physics, Simon Fraser University, Burnaby, BC, Canada
[152] SLAC National Accelerator Laboratory, Stanford, CA, USA
[153] Physics Department, Royal Institute of Technology, Stockholm, Sweden
[154] Departments of Physics and Astronomy, Stony Brook University, Stony Brook, NY, USA
[155] Department of Physics and Astronomy, University of Sussex, Brighton, UK
[156] School of Physics, University of Sydney, Sydney, Australia
[157] Institute of Physics, Academia Sinica, Taipei, Taiwan
[158] [(a)]E. Andronikashvili Institute of Physics, Iv. Javakhishvili Tbilisi State University, Tbilisi, Georgia; [(b)]High Energy Physics Institute, Tbilisi State University, Tbilisi, Georgia
[159] Department of Physics, Technion, Israel Institute of Technology, Haifa, Israel
[160] Raymond and Beverly Sackler School of Physics and Astronomy, Tel Aviv University, Tel Aviv, Israel
[161] Department of Physics, Aristotle University of Thessaloniki, Thessaloníki, Greece
[162] International Center for Elementary Particle Physics and Department of Physics, University of Tokyo, Tokyo, Japan
[163] Graduate School of Science and Technology, Tokyo Metropolitan University, Tokyo, Japan
[164] Department of Physics, Tokyo Institute of Technology, Tokyo, Japan
[165] Tomsk State University, Tomsk, Russia

[166] Department of Physics, University of Toronto, Toronto, ON, Canada
[167] [(a)]TRIUMF, Vancouver, BC, Canada; [(b)]Department of Physics and Astronomy, York University, Toronto, ON, Canada
[168] Division of Physics and Tomonaga Center for the History of the Universe, Faculty of Pure and Applied Sciences, University of Tsukuba, Tsukuba, Japan
[169] Department of Physics and Astronomy, Tufts University, Medford, MA, USA
[170] Department of Physics and Astronomy, University of California Irvine, Irvine, CA, USA
[171] Department of Physics and Astronomy, University of Uppsala, Uppsala, Sweden
[172] Department of Physics, University of Illinois, Urbana, IL, USA
[173] Instituto de Física Corpuscular (IFIC), Centro Mixto Universidad de Valencia - CSIC, Valencia, Spain
[174] Department of Physics, University of British Columbia, Vancouver, BC, Canada
[175] Department of Physics and Astronomy, University of Victoria, Victoria, BC, Canada
[176] Fakultät für Physik und Astronomie, Julius-Maximilians-Universität Würzburg, Würzburg, Germany
[177] Department of Physics, University of Warwick, Coventry, UK
[178] Waseda University, Tokyo, Japan
[179] Department of Particle Physics, Weizmann Institute of Science, Rehovot, Israel
[180] Department of Physics, University of Wisconsin, Madison, WI, USA
[181] Fakultät für Mathematik und Naturwissenschaften, Fachgruppe Physik, Bergische Universität Wuppertal, Wuppertal, Germany
[182] Department of Physics, Yale University, New Haven, CT, USA
[183] Yerevan Physics Institute, Yerevan, Armenia

[a] Also at Borough of Manhattan Community College, City University of New York, New York NY, USA.
[b] Also at Centre for High Performance Computing, CSIR Campus, Rosebank, Cape Town, South Africa.
[c] Also at CERN, Geneva, Switzerland.
[d] Also at CPPM, Aix-Marseille Université, CNRS/IN2P3, Marseille, France.
[e] Also at Département de Physique Nucléaire et Corpusculaire, Université de Genève, Genève, Switzerland.
[f] Also at Departament de Fisica de la Universitat Autonoma de Barcelona, Barcelona, Spain.
[g] Also at Department of Applied Physics and Astronomy, University of Sharjah, Sharjah, UAE.
[h] Also at Department of Financial and Management Engineering, University of the Aegean, Chios, Greece.
[i] Also at Department of Physics and Astronomy, University of Louisville, Louisville, KY, USA.
[j] Also at Department of Physics and Astronomy, University of Sheffield, Sheffield, UK.
[k] Also at Department of Physics, California State University, East Bay, USA.
[l] Also at Department of Physics, California State University, Fresno, USA.
[m] Also at Department of Physics, California State University, Sacramento, USA.
[n] Also at Department of Physics, King's College London, London, UK.
[o] Also at Department of Physics, St. Petersburg State Polytechnical University, St. Petersburg, Russia.
[p] Also at Department of Physics, University of Fribourg, Fribourg, Switzerland.
[q] Also at Department of Physics, University of Michigan, Ann Arbor, MI, USA.
[r] Also at Faculty of Physics, M.V. Lomonosov Moscow State University, Moscow, Russia.
[s] Also at Giresun University, Faculty of Engineering, Giresun, Turkey.
[t] Also at Graduate School of Science, Osaka University, Osaka, Japan.
[u] Also at Hellenic Open University, Patras, Greece.
[v] Also at Horia Hulubei National Institute of Physics and Nuclear Engineering, Bucharest, Romania.
[w] Also at II. Physikalisches Institut, Georg-August-Universität Göttingen, Göttingen, Germany.
[x] Also at Institucio Catalana de Recerca i Estudis Avancats, ICREA, Barcelona, Spain.
[y] Also at Institute for Mathematics, Astrophysics and Particle Physics, Radboud University Nijmegen/Nikhef, Nijmegen, Netherlands.
[z] Also at Institute for Particle and Nuclear Physics, Wigner Research Centre for Physics, Budapest, Hungary.
[aa] Also at Institute of Particle Physics (IPP), Canada.
[ab] Also at Institute of Physics, Academia Sinica, Taipei, Taiwan.
[ac] Also at Institute of Physics, Azerbaijan Academy of Sciences, Baku, Azerbaijan.
[ad] Also at Institute of Theoretical Physics, Ilia State University, Tbilisi, Georgia.
[ae] Also at LAL, Université Paris-Sud, CNRS/IN2P3, Université Paris-Saclay, Orsay, France.

[af] Also at Louisiana Tech University, Ruston, LA, USA.
[ag] Also at LPNHE, Sorbonne Université, Paris Diderot Sorbonne Paris Cité, CNRS/IN2P3, Paris, France.
[ah] Also at Manhattan College, New York, NY, USA.
[ai] Also at Moscow Institute of Physics and Technology State University, Dolgoprudny, Russia.
[aj] Also at National Research Nuclear University MEPhI, Moscow, Russia.
[ak] Also at Physics Department, An-Najah National University, Nablus, Palestine.
[al] Also at Physikalisches Institut, Albert-Ludwigs-Universität Freiburg, Freiburg, Germany.
[am] Also at School of Physics, Sun Yat-sen University, Guangzhou, China.
[an] Also at The City College of New York, New York, NY, USA.
[ao] Also at The Collaborative Innovation Center of Quantum Matter (CICQM), Beijing, China.
[ap] Also at Tomsk State University, Tomsk, and Moscow Institute of Physics and Technology State University, Dolgoprudny, Russia.
[aq] Also at TRIUMF, Vancouver, BC, Canada.
[ar] Also at Universidad de Granada, Granada, Spain.
[as] Also at Universita di Napoli Parthenope, Naples, Italy.
* Deceased